Sede Amministrativa: Università degli Studi di Padova

Dipartimento di Scienze Chimiche

SCUOLA DI DOTTORATO DI RICERCA IN SCIENZE MOLECOLARI

INDIRIZZO: SCIENZE CHIMICHE

CICLO XXII

OXYGEN TRANSFER CATALYSIS BY d_0 METAL COMPLEXES: ACTIVATION / DEACTIVATION BY LEWIS BASE CO-LIGANDS

Direttore della Scuola : Ch.mo Prof. Maurizio Casarin

Coordinatore d'indirizzo : Ch.mo Prof. Maurizio Casarin

Supervisore : Ch.mo Prof. Giulia Marina Licini

**Dottoranda** : Silvia Lovat

Contents

Chapter 1

General introduction

1.1 Introduction

Enzymes are nature's catalysts that are designed to accelerate specific reactions taking place in the cell and its immediate surroundings. Recent advances in understanding enzyme catalysis, particularly the availability of detailed structural information coupled with mechanistic information, have enabled the design and synthesis of sophisticated target structures as enzyme analogues. As in enzymes, which are usually composed of an active site surrounded by high molecular weight proteins, also in artificial systems the proper control of the ligand environment surrounding the active site is of main importance. The key of the successful development of homogeneous catalysts has undoubtedly been the exploitation of the effects that ligands exert on the properties of metals: by tuning the electronic and steric properties of a catalytically active complex, selectivities and rates can be dramatically altered. For these reasons catalysis has been ruled by the development of effective ligands.

When addition of ligand gives rise to a more reactive catalyst relative to the parent catalyst, then ligand-accelerated catalysis occurs. As defined by Berrisford, Bolm and Sharpless *"In ligand-accelerated catalysis (LAC) the addition of a ligand increases the reaction rate of an already existing catalytic transformation. Both the ligand-accelerated and the basic catalytic process operate simultaneously and in competition with each other."* (Scheme 1) [1]

$$A + B \xrightarrow[k_0]{\text{catalyst}} \text{product} \xleftarrow[k_1]{\text{catalyst/ }\textbf{ligand}} A + B \qquad k_1 > k_0$$
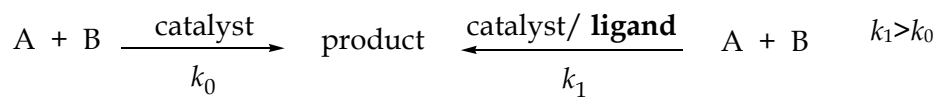
Scheme 1. Ligand acceleration. The ligand can be optically active.

When a ligand is bound to a metal centre, the rate of product formation can either be slowed down ($\upsilon_{ML} < \upsilon_M$, where υ_{ML} is the overall rate of product formation in the presence of the ligand, and υ_M is the rate of the reference reaction in the absence of the ligand in question), remain the same ($\upsilon_{ML} = \upsilon_M$), or be increased ($\upsilon_{ML} > \upsilon_M$). The latter, the accelerated process, offers a powerful approach to increasing reaction efficiency.[2]

Particularly attractive possibilities are offered when the accelerating ligand also affects the stereochemical outcome of the process.[3] Thus, use of chiral ligands[4] open the possibility towards stereoselective catalysis.[5] In this case, if the reaction rate is increased upon ligand binding, the stereoselective pathway can dominate over the nonselective one. For the majority of stereoselective processes, however, no significant reactivity enhancement is observed; that is, $\upsilon_{ML} \leq \upsilon_M$. The creation of an effective chiral environment often results in extra steric crowding around the binding/catalytic site, which leads to rate deceleration.

[1] Berrisford, D. J.; Bolm, C.; Sharpless, K. B. *Angew. Chem. Int. Ed.* **1995**, 34, 1059-1070.

[2] The activation of a stoichiometric reagent by a ligand is considered as "ligand acceleration". To be a ligand-accelerated catalysis (LAC) a catalyticlly active species (other than the ligand) must be present.

[3] For a very well studied example of a ligand-accelerated stereoselective reaction, see W. Klute, R. Dress, R. W. Hoffmann, *J. Am. Chem. Soc. Perkin Trans 2*, **1993**, 1409.

[4] a) Brunner, H.; Zettlmeier,W. *Handbook of Enantioselective Catalysis*, 2 Vols., VCH, Weinheim, **1994**; b) Brunner, H. *Top. Stereochem.* **1988**, 18, 129.

[5] a) Noyori, R. *Chem. Soc. Rev.* **1989**, 18, 187; b) Brunner, H. *Pure Appl. Chem.* **1990**, 62, 589; c) Noyori, R. *Science*, **1990**, 248, 1194 ; d) Brunner, H. *Synthesis* **1988**, 645 ; e) Evans, D. A. *Science* **1988**, 240, 420 ; f) Brown, J. M.; Davies, S. G. *Nature (London)* **1989**, 342, 631; g) Ojima, I.; Clos, N.; Bastos, C. *Tetrahedron* **1989**, 45, 6901.

Useful levels of stereoselectivity then require high ligand concentrations, a situation not conducive to efficient catalysis. For these reasons LAC is a rare phenomenon while, the ligand-decelerated catalysis is the rule. The fact that additives can dramatically enhance the reaction rate and in some cases increase the enantiomeric excess of the products makes the subject exciting. However the discovery and understanding of new ligand accelerated processes are almost always difficult.

The first and best-known example of ligand acceleration is found in Criegee's paper published in the thirties.[6] He observed that pyridine accelerates the osmium-catalyzed dihydroxylation of olefines. Later, Criegee's ligand-acceleration effect was the direct inspiration for the discovery by Sharpless of the stoichiometric version of the asymmetric osmium-catalyzed dihydroxylation.[7] In the same years Katsuki and Sharpless discovered the titanium-catalyzed asymmetric epoxidation of allylic alcohols.[8] Asymmetric dihydroxylation and asymmetric epoxidation are both manifestations, and owe their success to LAC.

In this chapter examples of ligand-acceleration effects, in early and late transition metal-catalyzed reactions, will be presented. For practical reasons these examples are divided into two classes named classical LAC and CO-LAC (Figure 1).
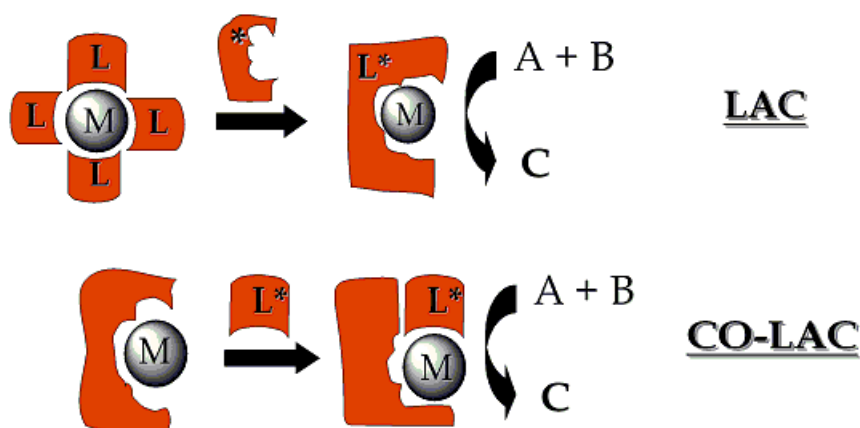
Figure 1. Schematic representation of classical LAC and CO-LAC.

In classical LAC the addition of a polydentate chiral ligand induces the generation, towards ligand exchange, of a new chiral metallic complex characterized by an increased reactivity. In CO-LAC the addition of a chiral or achiral monodentate ligand allows the modification of the reactivity of the original metal complex without the occurrency of a ligand exchange.

Among the well-known reviewed examples of classical LAC already reported by Sharpless, Bolm and Berrisford in 1995, a list of more recent examples, expecially in the field of the oxidations, will be presented. In the classical LAC the ligands, generally alkoxides or chlorides, initially bound to a metal have a little influence in the outcome of the reaction. Indeed, a dynamic ligand exchange between these labile monodentate ligands and an added

---

[6] a) Criegee, R. *Angew. Chem.* **1937**, 50, 153. b) Criegee, R. *Angew. Chem.* **1938**, 51, 519. c)Criegge, R. *Angew. Chem.* **1938**, 51, 519. d) Criegge, R.; Marchand, B.; Wannowias, H. *Justus Liebigs Ann. Chem.* **1942**, 550, 99, and references therein.

[7] Hentges, S. G.; Sharpless, K. B. *J. Am. Chem. Soc.* **1980**, 102, 4263.

[8] Katsuki, T.; Sharpless, K. B. *J. Am. Chem. Soc.* **1980**, 102, 5974.

polydentate one generates a mixture of metal-ligand species in which only a few complexes are significantly active. However, there are several examples in which the starting ligand is polydentate and it remains coordinated to the metal centre, while an external co-ligand (co-catalyst hence the term CO-LAC), generally a monodentate ligand is varying the reactivity of the catalytic system. In this case the addition of a suitable chiral or achiral additive to a catalytic system, enhances the yield, the reactivity and in many cases also the enantioselectivity very efficiently. A number of literature examples of how addition of nitrogen bases, alcohols, phosphane, phosphane oxides, pyridine *N*-oxides, halides, or acid can positively effect the performance of starting polydentate metal complexes will be discussed. In some examples, however, the presence of a co-catalyst are able to reduce or completely inhibit the reactivity of a complex. Some examples about this phenomenon will also be presented to understand the general effects induced by additives in the field of catalytic processes.

Since the original work of Sharpless, LAC has found main application on oxygen transfer processes. For this reason our attention will be focalized on this class of reactions. The present chapter will mainly deal, in its first part, on LAC processes in the field of oxidations. The second part will be dedicated to CO-LAC examples, divided into two classes namely oxo and peroxo reactivity.

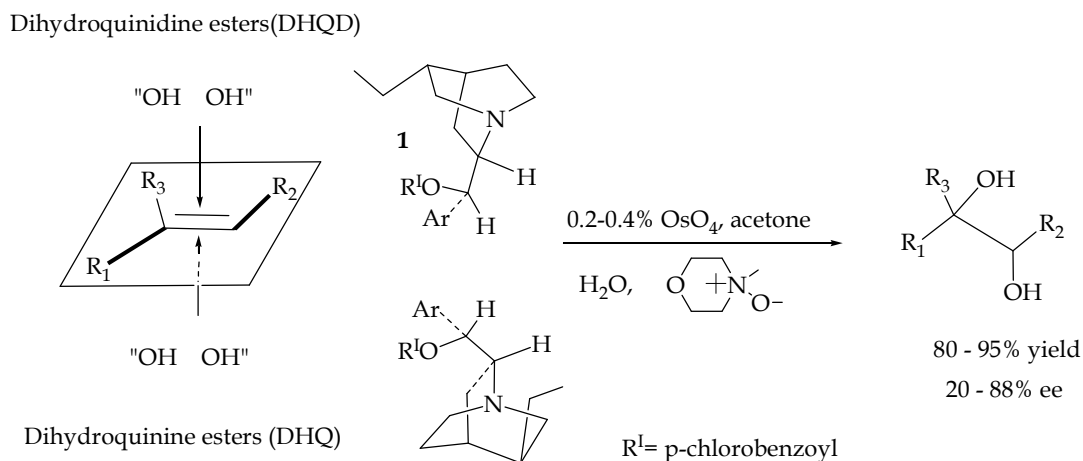### 1.2 Classical-LAC.

1.2.1 Asymmetric Oxidations

Historically, the first documented example of a ligand-accelerated reaction emerged from the pioneering study by Criegee in which the stoichiometric reaction of OsO_4 with olefins was found to be considerably accelerated in the presence of pyridine.[6] Later, efforts by Sharpless and Hentges to obtain stereoselectivity in the osmylation with chiral pyridine derivatives failed due to the low affinity of these ligands for OsO_4.[9] It was found that the binding constant of the ligand is extremely sensitive to the steric hindrance near the reacting centre. Consequently, quinuclidine derivatives were used for further investigations due to their intrinsically higher affinity for OsO_4.[10] This logic proved to be correct, and in 1979 it allowed Hentges to obtain diols with moderate to good enantiomeric excesses using acetate esters of cinchona alkaloids as chiral ligands.[9] Initially, the asymmetric dihydroxylation (AD) using derivatives of cinchona alkaloids was performed under stoichiometric conditions, but in 1987 Markó and Sharpless found that the process can become catalytic using *N*-methylmorpholine *N*-oxide as co-oxidant (Scheme 2).[11]

From this study emerged that alkaloid **1** binds strongly enough to OsO_4 to accelerate addition to olefins, but it doesn't bind so tightly to the osmate esters to interfere with the subsequent catalyst's hydrolysis/reoxidation steps. In this way the catalyst turnover is not inhibited.

[9] Henteges, S. G.; Sharpless, K. B. *J. Am. Chem. Soc.* **1980**, 102, 4263.
[10] a) Cleare, M. J.; Hydes, P. C.; Griffith, W. P.; Wright, M. J. *J. Chem. Soc., Dalton Trans.* **1977**, 941. b) Griffith, W. P.; Skapski, A. C.; Woode, K. A.; Wright, M. *J. Inorg. Chim. Acta* **1978**, 31, 413.
[11] Jacobsen, E. N.; Markó, I.; Mungall, W. S.; Schröder, G.; Sharpless, K. B. *J. Am. Chem. Soc.* **1988**, 110, 1968.

Dihydroquinidine esters(DHQD)

1

"OH   OH"

R_3 R_2

R_1

"OH   OH"

R^IO

Ar   H

H

0.2-0.4% OsO$_4$, acetone

H_2O,

Ar   H

R^IO H

N

Dihydroquinine esters (DHQ)

R^I= p-chlorobenzoyl

R_3 OH

R_1 R_2

OH

80 - 95% yield

20 - 88% ee

Scheme 2. Asymmetric catalytic dihydroxylation (AD) in the presence of Dihydroquinidine (R=H) DHQD and Dihydroquinine (R=H) DHQ.

In the course of ligand optimization studies, more than 300 cinchona alkaloid derivatives were prepared and tested.[13] These ligand structure-activity studies have shed light on the origin of the stereoselectivity in the AD reaction and demonstrated that the cinchona alkaloid backbone is ideally suited for providing high ligand acceleration as well as high enantioselectivity. A summary of these studies is shown in Figure 2.
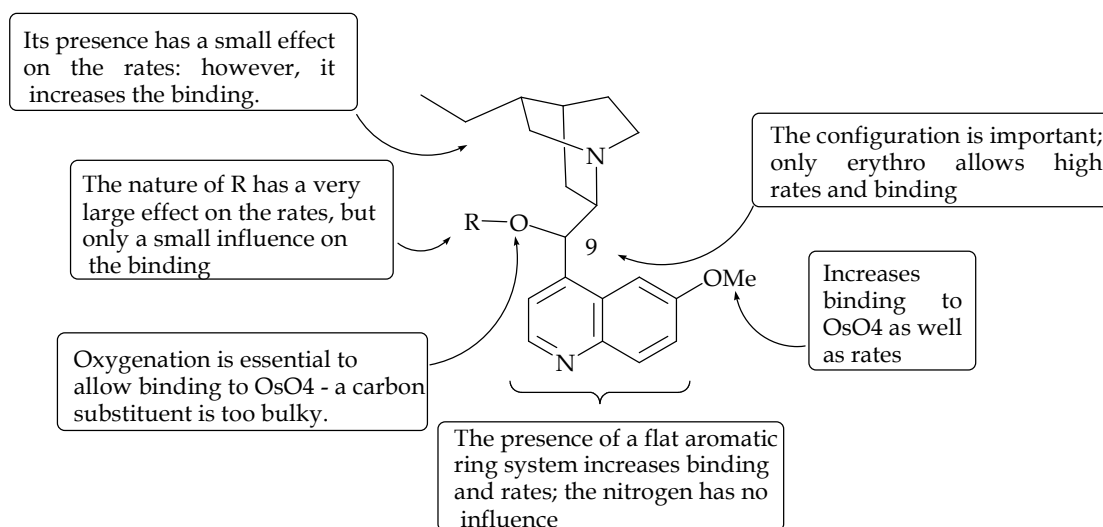
Its presence has a small effect on the rates: however, it increases the binding.

The nature of R has a very large effect on the rates, but only a small influence on the binding

Oxygenation is essential to allow binding to OsO4 - a carbon substituent is too bulky.

The configuration is important; only erythro allows high rates and binding

Increases binding to OsO4 as well as rates

R—O

9

OMe

N

The presence of a flat aromatic ring system increases binding and rates; the nitrogen has no influence

Figure 2. Relationship between ligand structure and binding and ceiling rate constants.[12] The alkaloid core is ideally set up to ensure high rates, binding, and solubility. The rates and enantioselectivities are influenced considerably by the nature of the substituent in position 9, while the binding to OsO$_4$ is almost independent.[13]

Another example of LAC in oxidation reactions is the titanium-catalyzed asymmetric epoxidation (AE) of olefins described by Katsuki and Sharpless in 1980. This is one of the most significant example of ligand accelerated catalysis. The AE of allylic alcohols proceeds using titanium tetra-isopropoxide Ti(OiPr)$_4$, a chiral ligand (diethyl tartrate, DET), and t-butyl hydroperoxide (TBHP) as oxidant (Scheme 3).[8] This procedure converts allylic alcohols

---

[12] Kolb, H. C.; Andersson, P. G.; Sharpless, K. B. *J. Am. Chem. Soc.* **1994**, 116, 1278.

[13] Kolb, H. C.; VanNieuwenhze, M. S.; Sharpless, K. B. *Chem. Rev.* **1994**, 94, 2483-2547.

into the corresponding epoxy-alcohols in good yields and with excellent enantiomeric excess. For these reasons the AE is one of the most important reaction discovered in the last 30 years. This importance has been recognised by the award of the 2001 Nobel Prize in Chemistry to Professor Berry Sharpless. AE of allylic alcohol, as AD, crucially depends on the ligand acceleration effect, which ensures that the reaction is funnelled through a pathway involving the chiral catalyst. The mechanism of the Sharpless epoxidation is quite complicated. Co-ordination of the chiral ligand DET, and the oxidant TBHP to the metal centre forms the catalytically active specie. It is generally believed that this specie is present as dimer in which the two metal centres are bridged via two oxygen bridges giving the overall shape of two edge-fused octahedra (Table 1, Ti_2L_2). The tartrate skeleton imposes a dissymmetric environment of pseudo-C_2 symmetry on each metal centre of Ti_2L_2. In order for the epoxidation reaction to proceed, the olefin and peroxide moieties must be coordinated to the metal center and oriented in a particular fashion with respect to one another. It is the superposition of the stereoelectronic requirements of the epoxidation transition state and the steric environment of the reaction template that provides high enantioselectivity.[14]
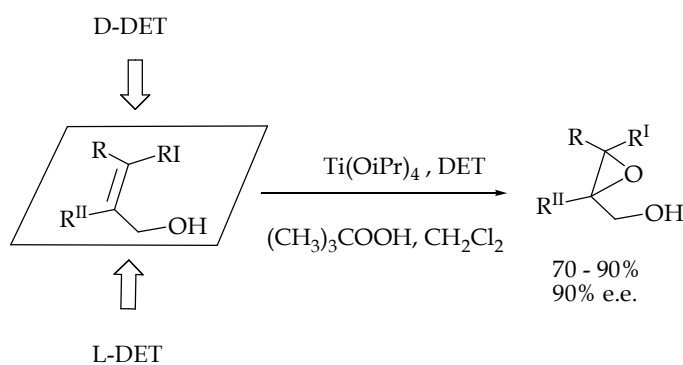
Scheme 3. Catalytic asymmetric epoxidation (AE) of allylic alcohols with *D*-(-)- and *L*-(+)- diethyltartrate (*D*- and *L*- DET).

As defined by Sharpless "*the Ti-tartrate catalyst can be regarded as a reactivity and stability spike in a complicated mixture of equilibrating complexes*".[14] In fact, in the asymmetric epoxidation catalyzed by such a complex, dynamic ligand exchange generates several species that makes the reaction mixture difficult to characterize. In equimolar amounts of titanium tetraalkoxides and dialkyltartrates more than one complex is present in solution, and individual oligomeric complex may have nonequivalent amounts of metal and tartrate ligand. Many of these are potential epoxidation catalysts, each of which would be expected to operate with a different profile with respect to rate and enantioselectivity.[1] This is the reason why the discovery of this catalytic system was serendipitous. In fact it was impossible to anticipate that a single species would dominate the Ti-tartrate equilibrium mixture and that this species would be the kinetically active. Kinetic experiments using different ratios of [Ti(O*i*Pr)₄]/(+)-diisopropyltartrate [(+)-DIPET] revealed that the major specie present in solution is a dimeric complex and this is the catalyst that dominates the epoxidation.[1] One minor component identified as a 2:1 Ti:tartrate specie, as well as other oligomeric species with higher Ti(IV)/tartrate ratio proved to be sluggish epoxidation catalysts. Thus, a comparison of the epoxidation rates of different titanium alkoxides (Table 1) showed that

---

[14] Finn, M. G.; Sharpless, K. B. *J. Am. Chem. Soc.* **1991**, 113, 113-126.

the reaction rate with a mixture of [Ti(OiPr)$_4$] and 50 mol% tartrate (forming the [Ti$_2$(DIPT)(OiPr)$_6$] complex as the major species) was significantly lower than that of free [Ti(OiPr)$_4$] alone – an example of ligand deceleration. In contrast, substantial rate acceleration was observed for the 1:1 [Ti(OiPr)$_4$]: tartrate ratio known to favour the formation of the most active dimeric complex, [Ti(DIPT)(OiPr)$_2$]$_2$.
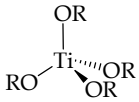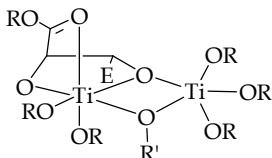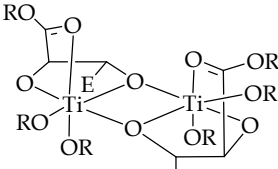
	Ti$_1$L$_0$	Ti$_2$L$_1$	Ti$_2$L$_2$
fraction in solution [%]	ca. 10	ca. 10	ca. 80
relative epoxidation rate	1.4	1.0	3.6
enantioselectivity	none	low	high

Table 1. Estimated fractions of the main epoxidation catalysts present in a 1:1 mixture of [Ti(OiPr)$_4$] and DIPT (R= iPr, E= CO$_2$$i$Pr), their approximate relative epoxidation rates, and the enantioselectivity of the epoxidation of (E)-2-hexen-1-ol in CH$_2$Cl$_2$.[1]

It has been since then found, in experiments involving pairing approximately 50 tartrate analogues with titanium and other neighbouring transition metal alkoxide epoxidation catalysts,[15] that tartrate and titanium are perfectly matched. Slight deviations in ligand structure and/or change in the metal catalyst severely reduce the rate and/or enantioselectivity.[16] Ligand deceleration catalysis seems to be the dominant phenomenon. Fortunately, in the titanium/tartrate-catalyzed epoxidation of allylic alcohols, the major specie present in solution is not only the most reactive but probably also the most enantioselective. The in situ self-selection of a highly reactive and enantioselective catalyst from a variety of titanium-containing species is also important in sulfide oxidations. Kagan et al. discovered a water modified titanium reagent consisting of [Ti(OiPr)$_4$], diethyltartrate (DET), and water in a 1:2:1 ratio.[17] With TBHP as oxidant, sulfoxides with high enantiomeric excess were obtained by asymmetric oxidation. The titanium-mediated pathway is almost 200 times faster than the uncatalyzed oxidation with TBHP. Use of cumene hydroperoxide allowed the development of a catalytic process.[18] Catalyst loading can be reduced to 20 mol% while retaining good enantioselectivity. In the absence of water a large excess of DET with respect to [Ti(OiPr)$_4$] has a beneficial effect on enantioselectivity.[19] This system has been developed here in Padova. Uemura et al. studied a similar sulfoxidation system prepared from [Ti(OiPr)$_4$] and binaphthol (BINOL).[20] Again, added water is essential for high

[15] Sharpless, K. B. *Tetrahedron* **1994**, 50, 4235.
[16] a) Pfenninger, A. *Synthesis*, **1986**, 89. b) Gao, Y.; Hanson, R. M.; Klunder, J. M.; Ko, S. Y.; Masamune, H.; Sharpless, K. B. *J. Am. Chem. Soc.* **1987**, 109, 5765. c) Ko, S. Y.; Masamune, H.; Sharpless, K. B. *J. Org. Chem.* **1987**, 52, 667.
[17] a) Kagan, H. B.; Rebière, F. *Synlett.* **1990**, 643. b) Pitchen, P.; Dunach, E.; Deshmukh, M. N.; Kagan, H. B. *J. Am. Chem. Soc.* **1984**, 106, 8188.
[18] a) Zhao, S. H.; Samuel, O.; Kagan, H. B. *Tetrahedron*, **1987**, 43, 5135. b) Zhao, S.; Samuel, O.; Kagan, H. B. *Org. Synth.* **1989**, 68, 49.
[19] Di Furia, F.; Modena, G.; Seraglia, R. *Synthesis*, **1984**, 325.
[20] Komatsu, N.; Hashizume, M.; Sugita, T.; Uemura, S. *J. Org. Chem.* **1993**, 58, 4529, 7624.

enantioselectivity. With 2.5 mol% of the titanium complex, acqueous TBHP as oxidant, and an excess of water, about 50% e.e. was achieved in the oxidation of aryl methyl sulfides to the corresponding sulfoxides. Cooperative kinetic resolution following the stereoselective sulfoxidation provides chiral sulfoxides with e.e.'s over 90%.

Several other examples on classical LAC have been presented in the literature after the work of Sharpless. In 1995 Bolm and Bienewald reported a method for the stereoselective oxidation of sulfides catalyzed by VO(acac)$_2$ (acac = acetylacetonate) and hydrogen peroxide in the presence of the very simple ligands readily available from salicylaldehydes and amino alcohols of type **4** (Scheme 4).[21]
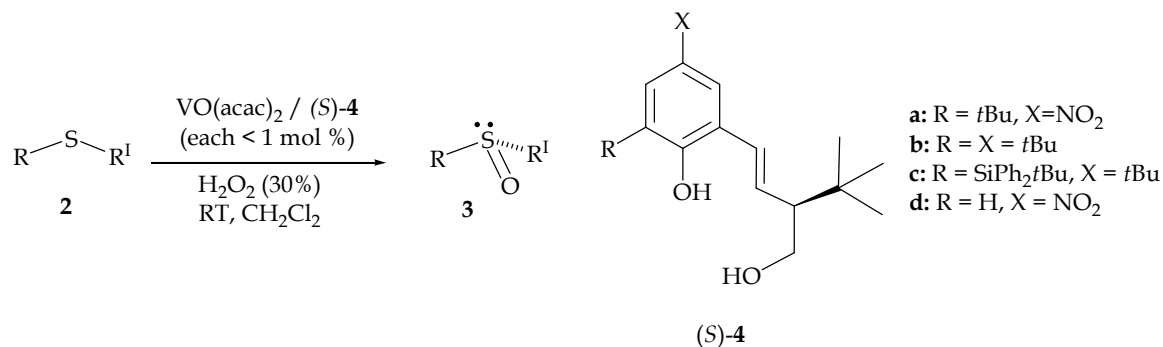

Figure 6. Enantioselective catalytic oxidation of aryl alkyl sulfides with H$_2$O$_2$ as oxidant, in the presence of VO(acac)$_2$ and various chiral ligands (**4 a-d**).

The catalytic system proved to be extremely efficient catalyzing the sulfoxide formation in concentrations of 1.0 mol % of the complex. The e.e. values range from 53 to 85%, depend on the substrate and on the chiral ligand. Furthermore, the reaction was found to be ligand accelerated, and thus the enantioselectivity was not, or only slightly, affected by the presence of the achiral vanadium precursor [VO(acac)$_2$].[22]

In 1998, Ellmann and co-workers described the catalytic asymmetric oxidation of *tert*-butyl disulfide **5** using H$_2$O$_2$ as stoichiometric oxidant and a similar catalysts VO(acac)$_2$ and a chiral Shiff base ligand **4 b)** (Scheme 5).[23]
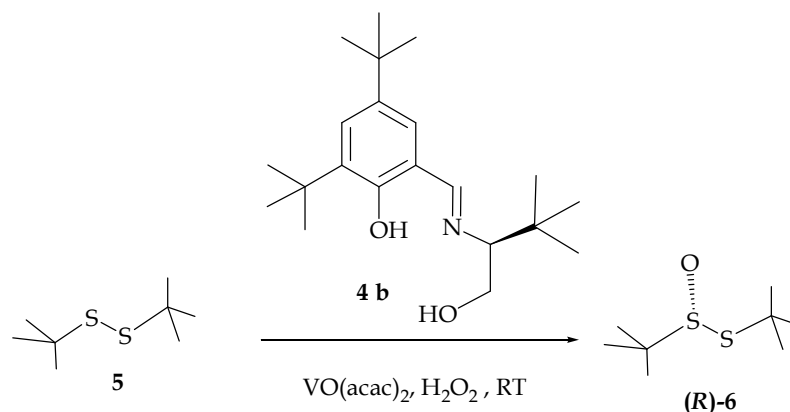
Scheme 5. First example of the catalytic asymmetric oxidation of *tert*-butyl disulfide with H$_2$O$_2$ as oxidant in the presence of VO(acac)$_2$ (0.25 mol %) and a chiral ligand **4 b** (0.26 mol %).

[21] Bolm, C.; Bienewald, F. *Angew. Chem. Int. Ed.* **1995**, 34, 2640-2642.
[22] Bolm, C.; Schlingloff, C.; Bienewald, F. *J. Mol. Catal. A* **1997**, 117, 347.
[23] Cogan, D. A.; Liu, G.; Kim, K.; Backes, B.; Ellmann, J. *J. Am. Chem. Soc.* **1998**, 120, 8011-8019.

The product, *tert*-butyl *tert*-butanethiosulfinate **6**, an excellent precursor to chiral *tert*-butanesulfinyl compounds, was obtained with 91 % enantiomeric excess in high yields on molar scale.[23] As in the case of sulfoxidation cited above, VO(acac)$_2$ alone did not catalyze the oxidation of **5**. Use of 2 equiv of VO(acac)$_2$ with respect to ligand **4 b** had no effect on either the rate of oxidation or the enantioselection. In fact, the ligand acceleration eliminates the impact of vanadium species not complexed with the chiral ligand and precludes the need for ligand excess.

Another example, of oxidation which display LAC is the palladium catalyzed oxidations of alcohols to aldehydes and ketones by molecular oxygen developed in the group of Uemura.[24] In 1998 Uemura *et al.* found that Pd(OAc)$_2$ was a good catalyst to promote the oxidation of benzyl alcohol in the presence of base under O$_2$ atmosphere. Among the organic bases examined, pyridine revealed to be the most effective (Table 2).[25]
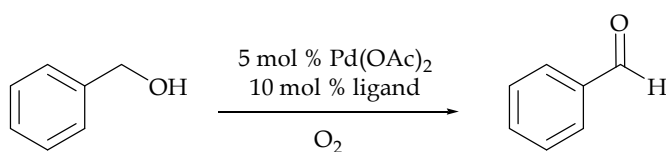
Ligand	Conversion (2h)
none	5 %
pyridine	86 %
2,6-lutidine	82 %
triethylamine	78 %
2,2^l-bipyridine	5 %
pyrididne with 3Å ms	quantitative

Table 2. Ligand screening for the palladum-catalyzed oxidation of alcohols to aldehydes.

Later, he found that the reaction rate shows a marked dependence on ligand concentration with a maximum of catalytic activity achieved in the presence of at least 4 equivalent of pyridine in respect to Pd(OAc)$_2$.[26] Although the role of pyridine is unknown, it is supposed that pyridine coordinates with Pd(II) and stabilizes the Pd(II)-hydride specie formed during the catalytic cycle, preventing thus reductive elimination.

1.2.2 LAC in other processes.

LAC has not only been observed and pursued in oxidation reactions. In another important class of reactions, like hydrogenation of multiple bonds to create stereo-defined tertiary carbon centres, particular attention has been focused in the possibility to have LAC. However, the field of catalytic hydrogenation is ruled by the use of bidentate phosphine ligands which are strongly bound to the metal. As mentioned before, ligand-accelerated processes require the in situ selection of a catalyst from many possible interconverting

[24] a) Nishimura, T.; Ohe, K.; Uemura, S. *J. Org. Chem.* **2001**, 66, 4, 1455-1465. b) Nischimura, T.; Maeda, Y.; Kakiuchi, N.; Uemura, S. *J. Chem. Soc. Perk. Trans. 1* **2000**, 24, 4301-4305.

[25] Nishimura, T.; Ohe, K.; Uemura, S. *Tetrhedron Lett.* **1998**, 39,6011.

[26] Nishimura, T.; Ohe, K.; Uemura, S. *J. Org. Chem* **1999**, 64,6750.

structures, and in this case in situ selection becomes irrelevant. Indeed, these ligands have uniformly high binding constants for the transition metal which translates into the incompatibility for ligand-acceleration to be involved. Despite this, a striking example of LAC has been discovered in an important heterogeneous hydrogenation process. Heterogeneous stereoselective hydrogenation of α-keto esters was reported by Orito *et al*[27] in 1980 (Scheme 6). In this transformation the Pt/Al$_2$O$_3$ catalyst, modified with cinchona alkaloids, is able to give the desired products with e.e.'s approaching 90%. Interestingly, it was noticed by Blaser that modifications of the catalyst lead to a marked increase in reaction rate.[28] In particular, modified catalysts are up to 100 times more active than the original ones without cinchona alkaloids, suggesting a ligand-accelerated catalysis mode of action.
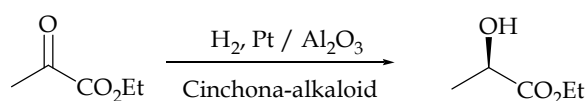
Scheme 6. Heterogeneous asymmetric hydrogenation of ethyl pyruvate.

Blaser *et al.*[29] have tried to draw a general picture on the mechanism of the enantioselection by cinchona-modified Pt catalysts to understand the origin of LAC. A successful chiral ligand needs two structural elements: first, an (extended) aromatic system, which is able to form a strong adsorption complex with the Pt surface; second a suitable amino function able to interact with the keto group of the adsorbed ethyl pyruvate (etpy) or its half-hydrogenated intermediate via a hydrogen bridge. This activated complex is thought to be responsible both for enantiocontrol and for rate acceleration (Figure 3).
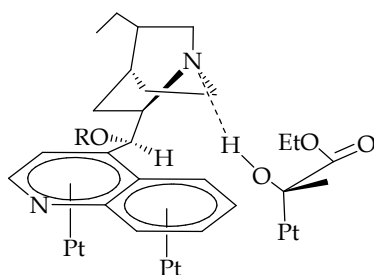
Figure 3. Structure of proposed adsorbed adduct complexes between modifier and ethyl pyruvate on a Pt catalyst surface.

LAC has also been observed in the transfer hydrogenation of aryl alkyl ketones with ruthenium complexes with chiral (phosphinoferrocenyl)oxazolines using 2-propanol as a source of hydrogen. This procedure, originally developed by Backvall and Chowdhury using RuCl$_2$(PPh$_3$)$_3$,[30] has been further developed in an stereoselective processes which utilizes Ru chiral catalysts.[31] In particular, Sammakia and Stangeland described a method for the preparation of chiral (phosphinoferrocenyl)oxazolines **7** and their use as ligands in conjunction with RuCl$_2$(PPh$_3$)$_3$ in the enantioselective transfer hydrogenation of aryl-alkyl

[27] Orito, Y.; Imai, S.; Niwa, S. J. *Chem. Soc. Jpn.* **1980**, 670.
[28] Blaser, H. U.; Jalett, H. P.; Monti, D. M.; Reber, J. F.; Wehrli, J. T. *Stud. Surf. Sci. Catal.* **1988**, 41, 153.
[29] Blaser, H. U.; Jalett, H. P.; Lottenbach, W.; Studer, M. *J. Am. Chem. Soc.* **2000**, 122, 12675-12682.
[30] Chowdhuri, R. L.; Backvall, J.-E. *J. Chem. Soc., Chem. Commun.* **1991**, 1063.
[31] a) Zassinovich, G.; Mestroni, G.; Gladiali, S. *Chem. Rev.* **1992**, 92, 1051. b) Jiang, Y.; Jiang, Q.; Zhu, G.; Zhang, X. *Tetrahedron. Lett.* **1997**, 38, 215.

ketones. They observed that the Ru catalysts became significantly more reactive and provide high enantioselectivity in the presence of various ferrocene ligands (Table 3).[32] Mechanistic studies indicate that the phosphine ligand is bound to the Ru center during the stereochemistry-determining step.
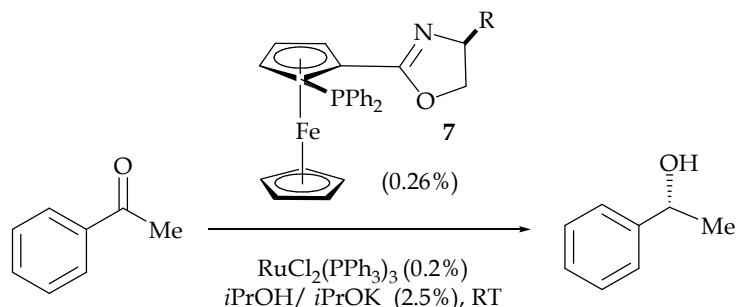
entry	R	time (h)	% conversion	% e.e.
1	Me	8	92	92
2	Bn	6	93	90
3	*i*-Pr	3	93	92
4	Ph	6	93	94
5	*t*-Bu	6	51	94
6	No ligand	20	5	_

Table 3. Hydrogenation of ketones in the presence of $RuCl_2(PPh_3)_3$ catalyst and various ferrocene ligands.

1.3 Co-Ligand Accelerated Catalysis

In the examples shown since now the metal source has a small influence in the course of the reaction. This is because the metal rapidly exchanges with the ligands present in solution, usually polydentate, and, being the resulting species also the more active, the new formed catalysts promote the reaction. However, this is not the methodology followed by biological systems. Most of the time, in these systems, the metal is already complexed in a polydentated ligand and the catalysis starts when an external co-ligand enhances the activity of the complex. We suggest for this activation the term of Co-Ligand Accelerated Catalysis (CO-LAC) due to the similarity with the examples shown before in term of activation of a metal complex, but, distinguishing from them because in this activation phenomena the starting ligand has an important role in the reaction.

Indeed, CO-LAC effect can be found in many biological systems. As example, in nature some classes of enzymes are accompanied by axial ligands coordinated to the active sites that are able to influence their catalytic properties.[33] For instance, the active species of

---

[32] Sammakia, T.; Strangeland, E. L. *J. Org. Chem.* **1997**, 62, 6104.
[33] a) Wang, R.; Visser, S. P. *Inorg. Biochem.* **2007**, 101, 1464-1472. b) Choi, M.; Sukumar, N. ; Liu, A. M. ; Davidson, V. L. *Biochem.* **2009**, 48, 9174-9184. c) Jamaat, P. R. ; Safari, N. ; Ghiasi, M. ; Naghavi, S. S. A. D.; Zamedi, M. *J. of Biol. Inorg, Chem.* **2008**, 13, 121-132. d) Tanaka, A.; Takahashi, H.; Shimizu, T. *J. of Biol. Chem.* **2007**, 282, 21301-21307. e) Oba, T.; Tamiaki, H. *Bioorg. & Med. Chem.* **2005**, 13, 5733-5739.

cytochromes P450 enzymes is an oxoiron heme group that is linked to the protein via a sulfur bridge of a cysteinate residue.[34] The cysteinate ligand entices a push effect on the oxoiron group[35] that enables the system catalytic properties. Studies on biomimetic and synthetic catalysts confirmed that the axial ligand plays an important role in reactivity of the catalysis through pushing electrons.[36] Other enzymes containing a central heme group are peroxidases and catalases. Peroxidases generally have a histidine as axial ligand, while catalases have a tyrosinate one.[37] Thus, heme enzymes come in many varieties and have different functions. For instance, the cytocromes P450 are enzymes that typically catalyze C-H hydroxylation and C=C epoxidation reactions, instead peroxidases and catalases bind hydrogen peroxide and convert it into an oxoiron species and water.[38] It has been proposed that the key factor that distinguishes catalase, peroxidase and P450 enzymes is the nature of the axial ligand.[34] Cobalamines are another important class of enzymes that present an axial ligand coordinated to the catalytic site.[39]

Cobalamines are important cofactors for many enzymatic processes.[40] They are able to produce a highly reactive alkyl radical through homolytic cleavage of a covalent Co-C bond. This radical mechanism is the usual operation mode of coenzyme B_{12}, and has also been proposed recently to operate in some biological methylation reactions carried out by methylcobalamines.[41] The X-ray diffraction analysis of coenzyme B_{12} showed that in its active centre the cobalt atom is in an octahedral environment with an axial position occupied by a derivative of the benzimidazole.[31] It was proposed that a conformational rearrangement induced by the axial benzimidazole is able to pushing the alkyl group away from the Co centre weakening the Co-C bond.[42] The possible electronic effect of the axial base has also been analyzed. In an extensive study on the Co-C thermolysis in cobalamin derivatives with a variety of different axial bases, Finke and co-workers have found that an increase in the basicity of the axial base does indeed enhance the rate of Co-C bond homolysis but has an even stronger effect on the competing heterolysis.[43] In another recent study by Grabowski and co-workers it is found that the axial base has a effect on the kinetic of the reaction, stabilizing the transition state of the Co-C bond homolysis.[44]

The axial-ligand effect can be also found in many synthetic model compounds of enzymes and in many synthetic catalytic systems. In this section a number of examples from the recent literature will be presented. For our purposes the synthetic examples have been divided in

---

[34] a) Schlichting, J.; Berendzen, K.; Chu, A. M.; Stock, S. A.; Maves, D. E.; Benson, R. M.; Sweet, D.; Ringe, D.; Petsko, G. A.; Sligar, S. G. *Science* **2000**, 287, 1615-1622. b) Denisov, I. G.; Makris, T. M.; Sligar, S. G.; Schlichting, I. *Chem. Rev.* **2005**, 105, 2253-2277.

[35] a) Dawson, J. H.; Holm, R. H.; Trudell, J. R.; Barth, G.; Linder, R. F.; Bunnenberg, E.; Djerassi, C.; Tang, S. C. *J. Am. Chem. Soc.* **1976**, 98, 3707-3709. b) Poulos, T. L.; Biol, J. *Inorg. Chem.* **1996**, 1, 356-359.

[36] a) Gross, Z.; Biol, J. *Inorg. Chem.* **1996**, 1, 368-371. b) Nam, W.; Lim, M. H.; Oh, S. Y.; Lee, J. H.; Lee, H. J.; Woo, S. K.; Kim, C.; Shin, W. *Angew. Chem. Int. Ed.* **2000**, 39, 3646-3649.

[37] a) Nicholls, P.; Fita, I.; Loewen, P. C. *Adv. Inorg. Chem.* **2000**, 51, 51-106. b) Veitch, N. G.; Smith, A. T. *Adv. Inorg. Chem.* **2000**, 51, 107-162.

[38] Sono, M.; Roach, M. P.; Coulter, E. D.; Dawson, J. H. *Chem. Rev.* **1996**, 96, 2841-2887.

[39] Lenhert, P. G. *Proc. R. Soc. London, Ser. A* **1968**, 303, 45.

[40] Strayer, L. *Biochemistry*, Freeman: New York, **1996**.

[41] Mosimann, H.; Kräutler, B. *Angew. Chem. Int. Ed. Engl.* **2000**, 39, 393.

[42] Hill, H. A. O.; Pratt, J. M.; Williams, R. J. P. *Chem. Ber.* **1969**, 5, 156.

[43] Garr, C. D.; Sirovatka, J. M.; Finke, R. G. *J. Am. Chem. Soc.* **1996**, 118, 11142.

[44] Hung, R. R.; Grabwosky, J. J. *J. Am. Chem. Soc.* **1999**, 121, 1359.

three sections. The first two regard the reactivity in oxidation reactions (variation of the reactivity of oxo and of the peroxo species). The third section displays some examples of other classes of reactions.

1.3.1 Change of reactivity of oxo species

In the mid-1980s Kochi and co-workers reported that Cr(salen) complexes were capable of catalyze the epoxidation of unfunctionalized alkenes using iodosylbenzene (PhIO) as the stoichiometric oxidant.[45] Good yields were obtained for many alkenes, and from the outset it was noted that addition of oxygen-donor ligands such as pyridine *N*-oxide (PyO) and triphenylphosphine oxide (Ph₃PO) increased reaction rates. For these complexes the active epoxidizing specie is believed to be a chromium(V)-oxo specie as demonstrated from the X-ray analysis of various O=Cr(salen)⁺ complexes reported by Kochi.[45,46] Crystals suitable for X-ray analysis of a 1:1 association complex of O=Cr(salen)⁺ specie with PyO were also isolated (Figure 4). The donor ligand was shown to occupy the vacant apical position in O=Cr(salen)⁺, filling the octahedral coordination about Cr.
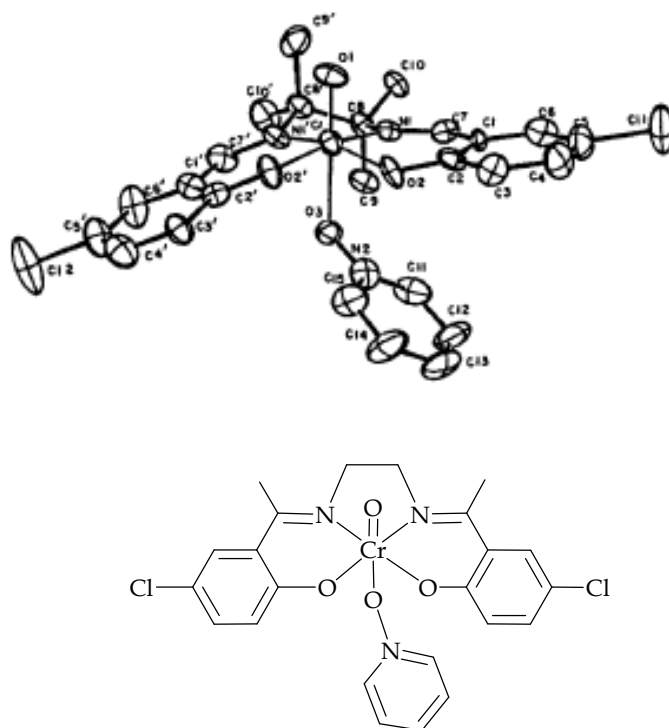
Figure 4. ORTEP diagram of the adduct of the oxo-chromium (V) cation triflate with PyO.[32]

IR studies indicated that the formation of a complex between the donor ligand and the O=Cr-(salen) weakens the oxo-chromium bond for the crystallized adduct complex (ca. 0.2 kcal for PyO) even though the Cr=O bond length was shortened by only 0.01 Å. It was noted that the chromium atom was pulled back toward the plane of the ligand oxygen and nitrogen atoms by 0.27 Å and that the Cr-O single bonds lengthened by 0.03-0.04 Å. The latter change resulted in an increase in the distance between the two salen oxygen atoms,

---

[45] a) Samsel, E. G.; Srinivasan, K.; Kochi, J. K. J. *J. Am. Chem. Soc.* **1985**, 107, 7606. b) Siddall, T. S.; Miyaura, N.; Huffman, J. C.; Kochi, J. K. J.; *J. Chem. Soc.; Chem. Commun.* **1983**, 1185.
[46] Srinivasan, K.; Kochi, J. K. J. *Inorg. Chem.* **1985**, 24, 4671.

i.e., the bite angle of the ligand widened. The pyridine ring was oriented away from the axial methylene substituent of the diamine backbone, suggesting a steric clash.

As mentioned before, addition of donor ligands led to increased reaction rates and yields in the stoichiometric epoxidations. The increase in yield was in part attributable to suppressed side product formation. The effect of donor ligands on rates showed a saturation effect which was explained by reversible binding of the ligand with the O=Cr-(salen) complex.

Thus, addition of 0.5-1 equiv. of PyO led to increased reaction rates, but addition of more than 1 equivalent led to deceleration. This was explained by the formation of the $(PyO)_2Cr^{III}$(Salen) specie which is inactive to PhIO. Even if in this case the process is stoichiometric and not catalytic, it represents a typical example of co-ligand effects on a metal-mediated process. The co-ligand is structurally and electronically modifying the structure of the starting metal complex and, consequently its reactivity performances. Moreover, this seminary work has been the base for the development of some of the best known artificial catalysts.

Indeed, following the work on Cr(salen)-catalyzed epoxidations, Kochi and co-workers reported that Mn(salen) complexes also catalyzed the epoxidation of alkenes with PhIO as terminal oxidant.[47] They noted that the reaction was faster than with Cr(salen) complexes and had a much broader substrate scope. For this catalyst it was proposed an O=Mn^V(salen)$^+$ specie as the reactive intermediate responsible for epoxidation and a µ-oxo-Mn^{IV}(salen) specie as the detectable transient specie (Scheme 7).
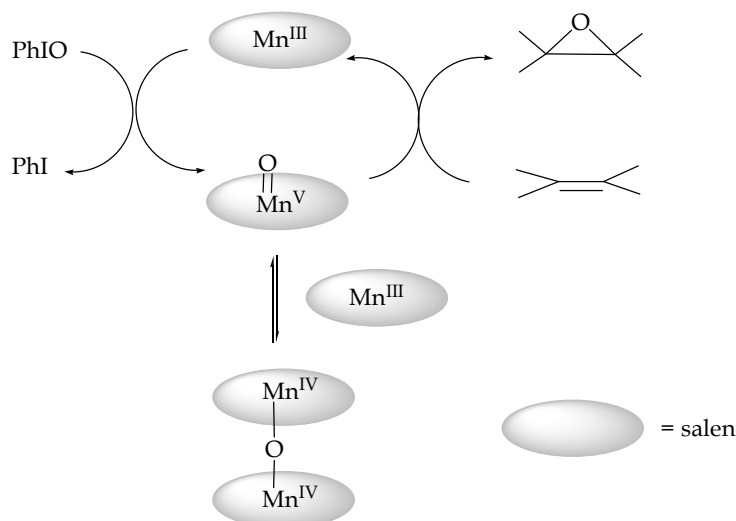
Scheme 7. Catalytic cycle for the epoxidation of alkenes catalyzed by Mn(salen) complexes proposed by Kochi and co-workers.[52]

As for the Cr analogues, the addition of pyridine or PyO (5-10 equiv. with respect to catalyst) to Mn(salen) complex led to increased yields with cyclooctene but had little or no effect on the yields of electron-rich alkenes such as (*Z*)-stilbene or (*Z*)-β-methylstyrene.[47] Skarzewski *et al.* reported their results on the effects of additional ligands on Mn(salen) catalysts in 1995.[48] They found that the σ-donating power, and the lipophilicity of the

---

[47] Srinivasan, K.; Michaud, P.; Kochi, J. K. J. *J. Am. Chem. Soc.* **1986**, 108, 2309.
[48] Skarzewski, J.; Gupta, A.; Vogt, A. *J. Mol. Catal. A* **1995**, 103, L63.

ligand, both contributed to the catalytic performance of the Mn(salen) catalysts. Their UV studies indicated that added *N*-oxides were bound to the Mn^{III}(salen) complex. Increased amounts of *N*-oxides decreased the production of carbonyl side products in the epoxidation of styrene and changed the ratio of *cis/trans*-epoxide produced from (*Z*)-stilbene (Table 4).
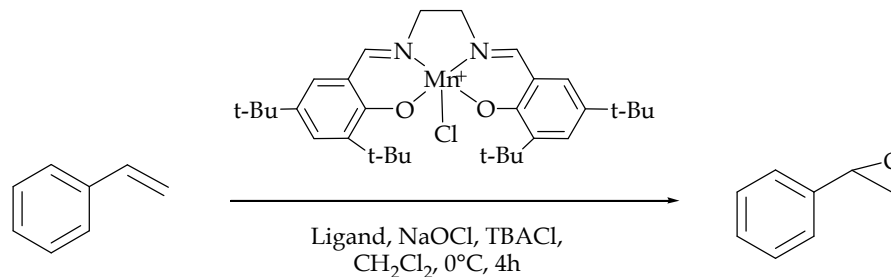
entry	Additional ligand	Recovered substrate %	Epoxide %	Carbonyl product[a] %
1	None	84	8.3	3
2	Pyridine 1-oxide	82.5	9.5	4
3	4-ethoxypyridine 1-oxide	63.5	19	7
4	4-benzylpyridine 1-oxide	19	45	5
5	4-*tert*-butylpyridine 1-oxide	2.6	85.5	6
6	4-phenylpyridine 1-oxide	No	85.5	7

a) In the oxidation a mixture of phenylacetaldehyde and acetophenone was found as by-product.

Table 4. Epoxidation of styrene with sodium hypochlorite catalyzed by salen(Mn^{III}) complex (1 mol%) and additional ligands (4 mol%).

Later, both Katsuki and Jacobsen recognized the potential to develop an asymmetric version of the Kochi catalysts. These systems have the particularly attractive feature that the metal-ligand complex is not formed reversibly, as in the case of the Sharpless AE and AD systems. Thus, there is no background ligand-free reaction catalyzed by the metal, and the number of different metal complexes that can exist in solution is greatly reduced. Thus, the rate acceleration for any particular metal-ligand complex that is selective does not need to be so great in order to obtain reasonable enantioselectivities. In 1990 Jacobsen and Katsuki, independently, reported on the Mn(salen)-catalyzed AEs of unfunctionalized alkenes using iodosylarenes (ArIO) as stoichiometric oxidants.[49] From the outset it was clear that the addition of nitrogen- and oxygen-donor ligands (especially pyridine *N*-oxide and imidazole derivatives) was significantly affecting the outcome of Mn(salen)-catalyzed AE. The rates, yields, and stereoselectivities of the reaction can all be influenced as the catalyst stability as well (and thus TON). Depending on the terminal oxidant used, the

---

[49] a) Zhang, W.; Loebach, J. L.; Wilson, S. R.; Jacobsen, E. N. *J. Am. Chem. Soc.* **1990**, 112, 2801.b) Irie, R.; Noda, K.; Ito, Y.; Matsumoto, N.; Katsuki, T. *Tetrahedron. Lett.* **1990**, 31, 7345.

donor ligand adopts different roles, but in all cases the effect of the coordination by the donor ligand to the active Mn centre is significant. Over the past decade a variety of effects have been reported and a number of different explanations have been proposed.[50] In the following only some examples concerning the effect on the rate of the reaction are described. Jacobsen and co-workers noted that in the AE of cyclic 1,3-dienes catalyzed by **8** (Figure 5), donor ligands were able to increase reaction rates and yields.[51]
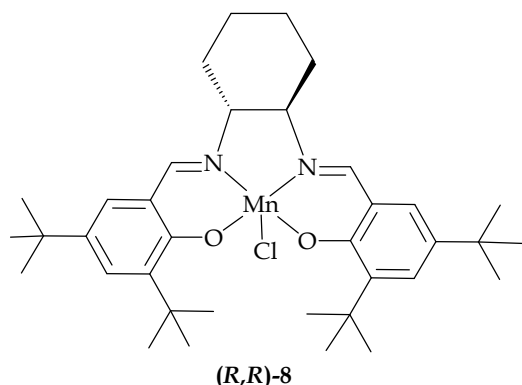

(R,R)-8

Figure 5. The most used and active asymmetric Mn(salen) catalyst (known as Jacobsen's catalyst).

In a screening of a wide range of potential donor ligands only the derivatives of pyridine *N*-oxides showed beneficial effects on AE reactions catalyzed by Mn(salen) complexes. The effects were more pronounced for relatively unreactive substrates. Jacobsen noted that the hypothesis that pyridine *N*-oxides act as axial ligands, as was the case in the Cr(salen)⁺ systems investigated by Kochi, was not consistent with the fact that the additives had little effect on either enantioselectivity of AE or *cis/trans* epoxide ratios (Table 5).

additive	Turnover rate (min⁻¹)[a]	Turnover[b]	Epoxide yield (%)	ee %	Cis epoxide/trans epoxide
None	2.3	13	67	93	4-5:1
H₃C—⟨N⁺—OH⟩ (0.25 equiv.)	3.3	20	82	92	4-5:1
Ph—⟨N⁺—O⁻⟩ (0.25 equiv.)	4.0	48	96	93	4-5:1
Ph—⟨N⁺—O⁻⟩ (1 equiv.)	7.6	43	98	93	4-5:1

[a] initial rate. [b] Total moles of reacted olefin per mole of catalyst at reaction completion measured using 1 mol % cat.

Table 5. Additive effects on epoxidation of *cis*-Ethyl Cinnamate.

[50] a) Robert, A.; Tsapara, A.; Meunier, B. *J. Mol. Catal.* **1993**, 85, 13. b) Collman, J. P. ; Zeng, L. ; Brauman, J. I. *Inorg. Chem.* **2004**, 43, 2672. c) Hashihayata, T.; Ito, Y.; Katsuki, T. *Synlett.* **1996**, 1079. d)Deng, L.; Jacobsen, E. N. *J. Org. Chem.* **1992**, 57, 4320.
[51] Chang, S.; Heid, R. M.; Jacobsen, E. N. *Tetrahedron. Lett.* **1994**, 35, 669.

The effect on rate, yield, and catalyst lifetime were ascribed to the effect of PyO derivatives on the manganese μ-oxo dimers disproportionation of and on the stability of manganese species (Table 5).[52]

Researchers at Merck also examined the effects of *N*-oxide donor ligands on the AE of indene catalyzed by Jacobsen's catalyst **8**.[53] In agreement with work by Skarzewski et al.[48] lipophilic *N*-oxide donor ligands provided reaction rate enhancements. They found that 4-(3-Phenylpropyl)pyridine-*N*-oxide (P₃NO, Scheme 8) suppressed catalyst decomposition and increased the reaction rates. In addition, it was found that P₃NO plays a role in transporting HOCl into the organic layer, where it acted as the major oxidant of Mn^{III}species (Figure 18). The turnover-limiting step for the epoxidation is the oxidation of the Mn(salen) complex and so the rate acceleration observed with P₃NO is due to increased HOCl concentration in the organic layer.
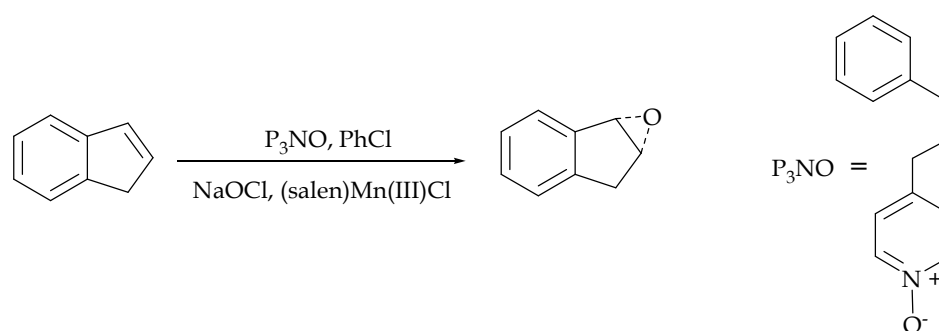
Scheme 8. The standard epoxidation of indene is carried out in a two-phase system that includes the (salen)Mn^{III}Cl catalyst, 4-(3-Phenylpropyl)pyridine-*N*-oxide (P₃NO), indene, and chlorobenzene as the organic components and 1.5 M aqueous sodium hypochlorite as the terminal oxidant.

While in the metal salen ligand is not clear if the external ligand has an effect on the electronic characteristics of the metal, a marked effect has been found on the study of corrolazine complexes. In 2006 Goldberg and co-workers described the reactivity of a manganese(III) corrolazine complex toward H_2O_2 and cumene hydroperoxide (CHP).[54] Corrolazines, which are ring-contracted porphyrinoid ligands, have been shown to stabilize high oxidation states of transition metals.[55] For example, treatment of **9** with the oxidants PhIO or *meta*-chloroperoxybenzoic acid (*m*CPBA) gives a stable Mn^{V}-oxo complex which can be isolated at room temperature (Scheme 9).[56] Surprisingly, the same reaction doesn't occur in the presence of H_2O_2 if an external axial ligand is not present in the complex. As an example, cloride ions, which are tightly coordinated to the metal in solution, led to the rapid formation of the Mn^{V}-oxo complex.

[52] Jacobsen, E. N.; Deng, L.; Furukawa, Y.; Martínez, L. E. *Tetrahedron* **1994**, 50, 4323.

[53] Hughes, D. L.; Smith, G. B.; Liu, J.; Dezeny, G. C.; Senanayake, C. H.; Larsen, R. D.; Verhoeven, T. R. Reider, P. J. *J. Org. Chem.* **1997**, 62, 2222.

[54] Lansky, D. E.; Narducci Sarjeant, A.; Goldberg, P.P. *Angew. Chem. Int. Ed.* **2006**, 45, 8214-8217.

[55] Kerber, W. D.; Goldberg, D. P. *J. Inorg. Biochem.* **2006**, 100, 838-857.

[56] a) Mandimutsira, B. S.; Ramdhanie, B.; Todd, R. C.; Wang, H. L.; Zareba, A. A.; Czernuszewicz, R. S.; Goldberg, D. P. *J. Am. Chem. Soc.* **2002**, 124, 15170-15171. b) Wang, S. H.; Mandimutsira, B. S.; Todd, R.; Ramdhanie, B.; Fox, J. P.; Goldberg, D. P. *J. Am. Chem. Soc.* **2004**, 126, 18-19. c) Lansky, D. E.; Mandimutsira, B.; Ramdhanie, B.; Clausén, M.; Penner-Hahn, J.; Zvyagin, S. A.; Telser, J.; Krzystek, J.; Zhan, R. Q.; Ou, Z. P.; Kadish, K. M.; Zakharov, L.; Rheingold, A. L.; Goldberg, D. P. *Inorg. Chem.* **2005**, 44, 4485-4498.
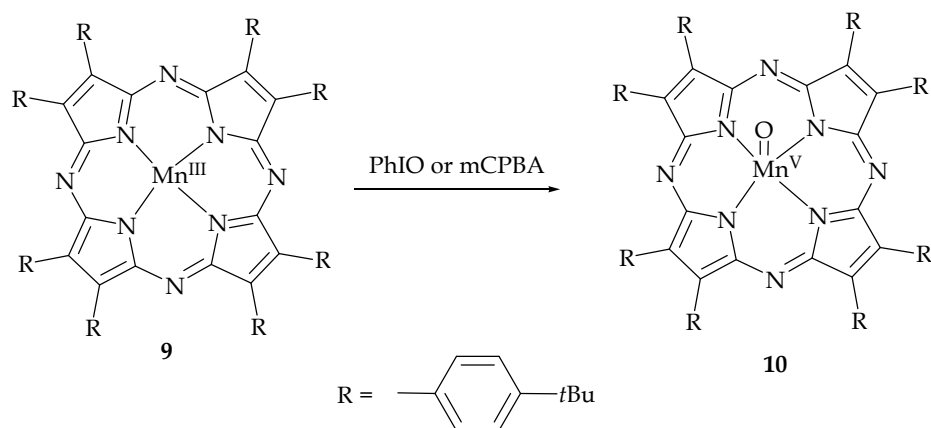
Scheme 9. Synthesis of the stable $Mn^V=O$ corrolazine complex 10.

The proposed mechanism for the formation of 10 involves the coordination of H_2O_2 followed by heterolytic O-O bond cleavage and two electron oxidation at the metal center (Scheme 10). It was proposed that the step influenced by the presence of the donor ligands (L) is the O-O bond cleavage because it is unlikely that the coordination of the $H_2O_2$ would be strongly enhanced by the formation of [9-L]⁻, a negatively charged complex. Addition of a series of *para*-substituted arylthiolate ligands (p-X-$C_6H_4S^-Na^+$, where X = H, OMe, CH_3, Cl, or NO_2) had the same influence as Cl⁻ on the reactivity of 9 toward H_2O_2. A kinetic analysis of these reactions revealed significant differences in the activity of the axial ligands examined. In particular the rate of the H_2O_2 reaction increases with an increase in the electron-withdrawing nature of the arilthiolate ligand. This trend is opposite from what has been observed for porphyrine/heme systems in which the more electron-donating axial ligand increases the rate of O-O bond cleavage for both electrolitic and homolitic pathway. Moreover, Goldberg estabilished that the electronic properties of anionic axial ligands bound to a manganese(III) corrolazine have a strong influence also on the mechanism of O-O-bond cleavage. A dramatic increase in heterolytic cleavage occurs with F⁻, which is significantly more electronegative than Cl⁻ or Br⁻. Similarily, heterolitic cleavage increases with the electron-withdrawing nature of the *para* substituent of arylthiolate donors. These observation proved to be very useful in understanding the mechanism of O-O-bond cleavage in porphyrinoid systems of both synthetic and biological origin. Moreover, the insights gained regarding the activation of oxidants such as hydrogen peroxide may led to the design of practical corrolazine-based catalysts that can utilize the highly desirable terminal oxidant H_2O_2 or perhaps even O_2 itself.
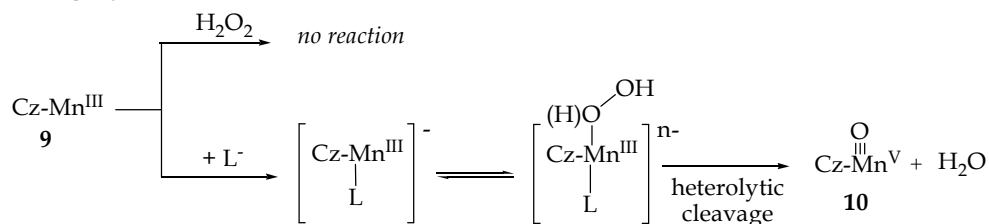
Scheme 10. Activation of H_2O_2 by axially legated manganese(III) corrolazine (Cz=corrolazine).

Almost at the same time, Chang and co-workers demonstrated that the reactivity of oxomanganese (V) 5,10,15-*tris*(pentafluorophenyl)corrole [(tpfc)Mn^VO] towards alkenes

could be strongly enhanced by the presence of axial ligands.[57] In particular, they showed that the 1:1 complex formed between (tpfc)Mn^{III} and imidazole significantly increases the stability of the (tpfc)Mn^VO complex (Scheme 11).
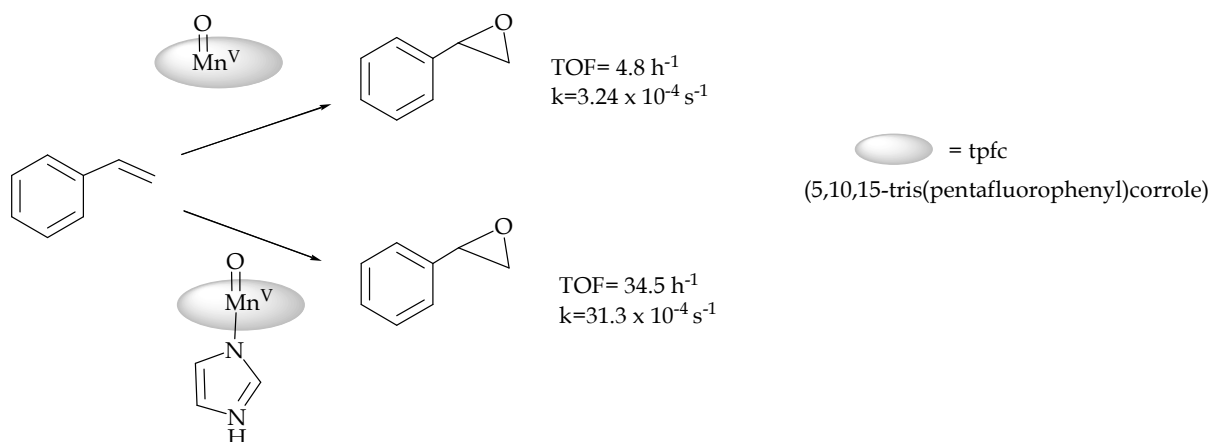
Scheme 11. The presence of imidazole ligand increases the rate and stability of the catalyst in styrene epoxidation.

Moreover, the presence of imidazole in catalytic oxidation of styrene by (tpfc)Mn^{III} and PhIO as terminal oxidant remarkably enhances the oxygen transfer rates. An explanation comes, from theoretical calculations. The axial coordination interaction weaks the Mn-oxo bond, raising the energy of HOMO and LUMO, as well as altering the HOMO distribution of (tpfc)Mn^VO significantly.

Nam and co-workers recently investigated the reactivity of mononuclear non-heme iron(IV)-oxo complexes bearing different axial ligands, $[Fe^{IV}(O)(TMC)(X)]^{n+}$ **11** [where TMC is 1,4,8,11-tetramethyl-1,2,8,11-tertaazacyclotetradecane and X is $NCCH_3$ (**11**-$NCCH_3$), CF_3COO^- (**11**-$OOCF_3$), or N_3^- (**11**-N_3)], and $[Fe^{IV}(O)(TMCS)]^+$ (**11'**-SR) (where TMCS is 1-mercaptoethyl-4,8,11-trimethyl-1,4,8,11-tetraazacyclotetradecane) (see structures in Figure 6), towards oxo transfer to PPh_3, hydrogen atom abstraction from phenol or alkylaromatic C-H bonds.[58]

These reactivities were significantly affected by the nature of the axial ligands, but the reactivity trends differed significantly. In the oxidation of PPh_3, the reactivity order of **11**-$NCCH_3$>**11**-$OOCCF_3$>**11**-N_3>**11'**-SR was observed, reflecting a decrease in the electrophilicity of iron(IV)-oxo unit upon replacement of CH_3CN with anionic axial ligand.[59] Surprisingly, the reactivity order was inverted in the oxidation of alkylaromatic C-H and phenol O-H bonds (**11'**-SR >**11**-N_3 >**11**-$OOCCF_3$ > **11**-$NCCH_3$).

[57] Liu, H.-Y.; Zhou, H.; Liu, L.-Y. ; Ying, X. ; Jiang, H.-F.; Chang, C.-K. *Chem. Lett.* **2007**, 36, 274-275.

[58] Sastri, C. V.; Lee, J.; Oh, K.; Lee, Y. J.; Lee, J.; Jackson, T. A.; Ray, K.; Hirao, H.; Shin, W.; Halfen, J. A.; Kim, J.; Que, L.; Shaik, S.; Nam, W. *PNAS*, **2007**, 104, 19181-19186.

[59] a) Sastri, C. V.; Park, M. J.; Ohta, T.; Jackson, T. A.; Stubna, A.; Seo, M. S.; Lee, J.; Kim, J.; Kitagawa, T.; Münck, E.; Que, L.; Nam, W. *J. Am. Chem. Soc.* **2005**, 127, 12494. b) Rohde, J. U.; Que, L. *Angew. Chem. Int. Ed.* **2005**, 44, 2255. c) Bukowski, M. R.; Koehntop, K. D.; Stubna, A.; Bominaar, E. L.; Halfen, J. A.; Münck, E.; Nam, W.; Que, L. *Science* **2005**, 310, 1000.
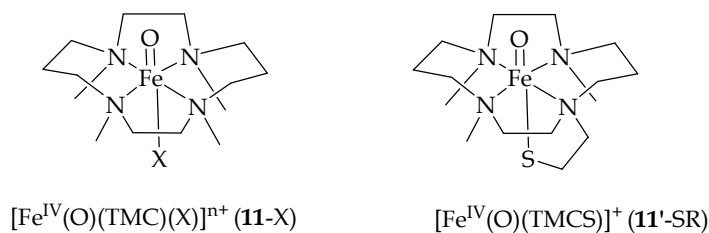
[Fe^IV(O)(TMC)(X)]^{n+} (**11**-X)   [Fe^IV(O)(TMCS)]^+ (**11'**-SR)

Figure 6. Schematic structures of [Fe^IV(O)(TMC)(X)]^{n+} (**11**-X) and [Fe^IV(O)(TMCS)]^+ (**11'**-SR).

Catalyst	substrate	K_2, M$^{-1 \cdot}$ s^{-1}
11-NCCH$_3$	PPh$_3$	5.9
	DHA	0.14
11-OOCCF$_3$	PPh$_3$	2.9
	DHA	1.3
11-N$_3$	PPh$_3$	0.61
	DHA	2.4
11'-SR	PPh$_3$	0.016
	DHA	7.5

Table 6. Second-order rate constants determined in substrate oxidations by [Fe^IV(O)(TMC)(X)]^{n+} (**11**-X) and [Fe^IV(O)(TMCS)]^+ (**11'**-SR). DHA= 9,10-Dihydroanthracene.

Furthermore, a good correlation was observed between the reactivities of iron(IV)-oxo species in H atom abstraction reactions and their reduction potentials, with the most reactive **11'**-SR complex exhibiting the lowest potential. In other words, the more electron-donating the axial ligand is, the more reactive the iron(IV)-oxo specie became in H abstraction. Quantum mechanical calculations show that a two-state reactivity model applies to the serie of complexes, in which a triplet ground state and a nearby quintet excited-state both contribute to the reactivity of the complexes. The inverted reactivity order in H atom abstraction can be rationalized by a decreased triplet-quintet gap with the more electron-donating axial ligand, which increases the contribution of the much more reactive quintet state and enhances the overall reactivity.

1.3.2   Change of reactivity of peroxo species

As described since now, axial ligands play a key roles in electrophilic oxidation reactions catalyzed by various metal oxo complexes. Similarly, the co-ligand effect has been investigated in oxidative reactions of metal peroxo complexes. The oxidation chemistry of transition metal peroxo complexes is a matter of general interest ranging from biological processes to industrial applications. A key point for the understanding of the oxidative mechanism is to establish the electronic nature of the oxidant. In this respect, the selectivity of the two-step sulfide/sulfoxide oxidation, i.e., the k_s/k_{so} ratio, provides a useful probe (Figure 12). This is based on the assumption that electrophilic oxidants oxidize sulfide to sulfoxides and these to sulfones with $k_s/k_{so} > 1$[4] while nucleophilic ones oxidize exclusively sulfoxides ($k_s = 0$). Peroxo complexes of d^0 transition metals such as Ti(IV), V(V), Mo(VI),

and W(VI) are strong electrophiles exhibiting a remarkably high selectivity in the oxidation of dialkyl and aryl alkyl sulfides; ratios of $k_s/k_{so} > 100$ are ususaly found, the sulfoxide being the only observed product.
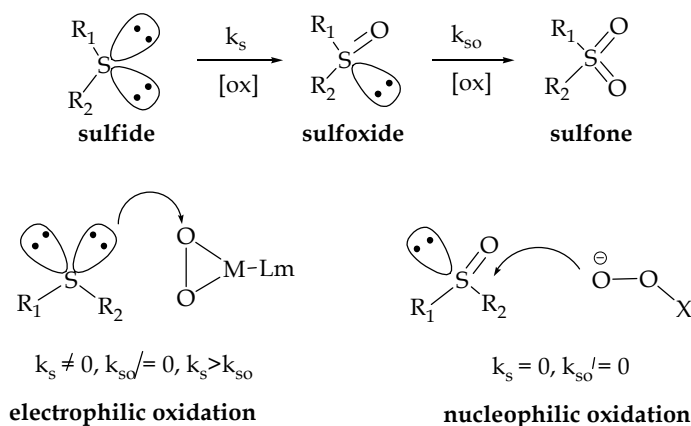
Scheme 12. The study of the selectivity (k_s/k_{so}) of the oxidation of thioethers (sulfide) and of sulfoxides constitutes a mechanistic probe of the electronic character of the oxidants, based on the assumption that electrophilic oxidants preferentially oxidize sulfides while nucleophilic ones oxidize sulfoxides.

The studies on the k_s/k_{so} ratio in sulfoxidation are in general accompanied by the investigation on the effects that the presence of co-ligands, such as HMPT, induce in the corresponding reactive metal peroxo complexes. In fact, HMPT coordinates to the metal without being oxidized and for this reason is frequently used to study the mechanism of the oxidation of sulfides and olefins and to establish the electronic nature of the oxidant. In 1983, Mimoun and co-workers[60] studied the reactivity of V(V) peroxo complexes and found that it is very different from the one of Mo(VI) analogues especially when equatorial anionic ligands adjacent to the peroxo moiety are present. In particular, while Mo(VI) peroxo complexes such as $MoO(O_2)Cl(Pic)$-HMPT,[61] $MoO(O_2)(Dipic)$-HMPT and $Mo(O_2)(OOH)(Pic)$,[62] are completely inactive in epoxidation reactions, vanadium complexes $VO(OOH)(Pic)_2L$ (L=H_2O, HMPT) are powerful epoxidizing and hydroxylating agents. This effect was explained in term of inhibition of substrate coordination by the HMPT in the case of molybdenum complexes. However, Di Furia and co-workers observed that the complexation of HMPT to molybdenum oxide diperoxide $Mo(O_5)$ complex (Scheme 13a) did not affect the selectivity of oxidation products of thiantrene-5-oxide, so they concluded that the oxidation reaction proceed by an electrophilic process taking place via a simple bimolecular mechanism not involving the coordination of the substrate to the metal.[63] Furthermore they observed that the rate of oxidation decreases by increasing the HMPT concentration. In fact, at large excesses of HMPT over the oxidant, the reaction rate tends to a plateau. The inhibitory effect of added HMPT was simply rationalized on the basis of the formation of $MoO_5(HMPT)_2$ specie which is a weaker electrophilic oxidant than the corresponding monocoordinate complex (Scheme 13b).

[60] Mimoun, H.; Saussine, L.; Daire, E.; Postel, M.; Ficher, J.; Weiss, R. *J. Am. Chem. Soc.* **1983**, 105, 3101.

[61] Chaumette, P.; Mimoun, H.; Saussine, L.; Fischer, J.; Mitschler, A. *J. Organomet. Chem.* **193**, *250,* 291.

[62] Jacobsen, S. E.; Tang, R.; Mares, F. *Inorg. Chem.* **1978**, 17, 3055-3063.

[63] Bonchio, M.; Conte, V.; De Cunciliis, M. A.; Di Furia, F.; Ballistreri, F. P.; Tomaselli, G. A.; Toscano, R. M. *J. Org. Chem.* **1995**, 60, 4475-4480.
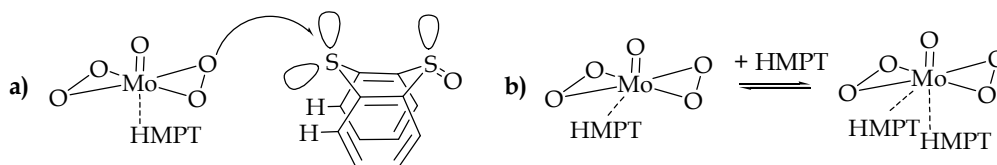
Scheme 13. a) The mechanism of the oxygen transfer processes to thiantrene-5-oxide in the presence of $MoO_5(HMPT)$ and b) the formation of $MoO_5(HMPT)_2$ in the presence of excess of HMPT.

A different behaviour was observed by Licini et al. in the oxidation of methyl *p*-tolyl sulfide by the titanium(IV) trialkanolamine complex **12** occurring in the presence of HMPT.[64] In this case the oxidation using cumyl hydroperoxide as oxidant yields both the sulfoxide and the sulfone with comparable reaction rates (ks/kso= 3.2) (Scheme 14).
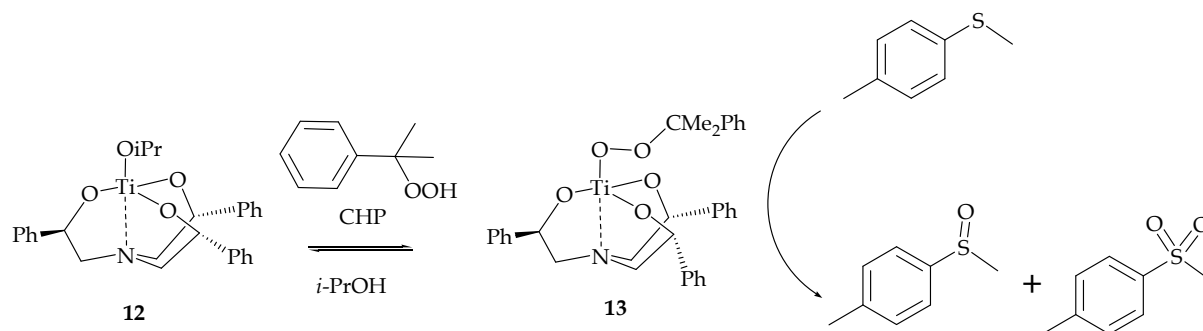
Scheme 14. Oxidation of metyl p-tolyl sulfide by the titanium(IV) trialkanolamine complex **1** in the presence of cumyl hydroperoxide (CHP) as oxidant.
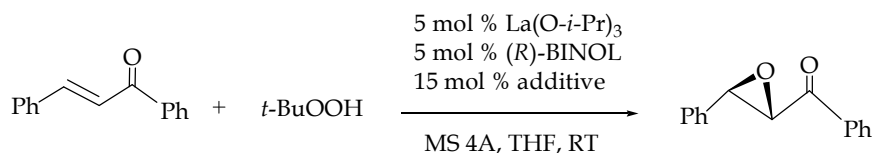
Such a low difference in reactivity hardly fits within the generally accepted mechanistic schemes involving two consecutive electrophilic oxygen transfer steps to the sulfur atom. The presence of an excess of HMPT reduced the reaction rate to the extent of 50% and at the same time a change in the selectivity of the product appeared. From these pieces of observation it was proposed that the peroxo titanium complex has a biphilic nature, behaving as an electrophilic oxidant toward sulfides while a nucleophilic pathway dominates the oxidation of sulfoxides. This mechanistic modification of the reactivity is triggered by coordination of the sulfoxide to the metal center, which promotes an unprecedented switch of the electronic character of the oxygen transfer step from electrophilic to nucleophilic. The addition of HMPT, which competes with the sulfoxide for the coordination to the Ti(IV) center, drive the oxidation toward the external electrophilic pathway by depressing the intramolecular one. In this way the abnormal selectivity found can be explained.

A pronounced ligand effect on the enantioselectivity and rate acceleration in the chiral lanthanum complex catalyzed asymmetric epoxidation of enones was found by Inanaga and co-workers.[65] In particular, they examined a variety of additives for the La-(*R*)-BINOL complex-catalyzed asymmetric epoxidation of chalcone with TBHP (Table 7).[66] Among the additives tested, triphenylphosphine oxide gave the best result, affording 96% e.e. and showing a notable ligand-acceleration of the reaction rate.

[64] Bonchio, M.; Calloni, S.; Di Furia, F.; Licini, G.; Modena, G.; Moro, S.; Nugent, W. *J. Am. Chem. Soc.* **1997**, 119, 6935-6936.

[65] Inanaga, J.; Furuno, H.; Hayano, T. *Catalysis Surveys from Japan* **2001**, 5, 37-42.

[66] Daika, K,; Kamamura, M.; Inanaga, J. *Tetrahedron. Lett.* **1998**, *39*, 7321.

Ph ⌣ Ph + t-BuOOH →[5 mol % La(O-i-Pr)$_3$ / 5 mol % (R)-BINOL / 15 mol % additive / MS 4A, THF, RT] Ph ⌣ Ph

Entry	Additive	Time (h)	Yield (%)	ee (%)
1	None	3.0	86	73
2	2,6-lutidine N-oxide	3.0	96	74
3	O=P(NMe$_2$)$_3$	1.5	99	86
4	O=P(c-Hex)$_3$	1.5	97	83
5	O=PPh$_3$	0.5	99	96
6	O=P(p-tolyl)$_3$	1.0	95	94
7	O=P(o-tolyl)$_3$	1.5	96	73

Table 7. Effects of achiral additives on the enantioselectivities, rates and yields of the chalcone epoxidation in the presence of TBHP as oxidant and La-(R)-BINOL catalyst.

The addition of triphenylphosphine oxide caused the spontaneous formation of a thermodynamically very stable complex as the active catalyst. The relationship between the enantiomeric purity of the chiral ligand and that of the product was also checked by Inanaga in order to provide insight into the mechanism of the enantioselective epoxidation. It results that using the ligand with only 40% e.e., in the presence of triphenylphosphine oxide products with e.e.'s =99% are obtained. This result strongly suggests that the active catalyst may not be monomeric and may have a particular structure that hardly changes during the reaction because of its thermodynamic stability. A homochiral dimeric complex like a binuclear μ-oxo complex, composed of La/(R)-BINOL/ O=PPh$_3$/ROOH= 1:1:1:1 (Figure 7), has been tentatively proposed as active catalytic species for the reaction. One of the lanthanum ions may work as Lewis acid to activate the substrate, the other lanthanum ion might be involved in the activation of the peroxide.

Figure 7. Speculated structure of the catalyst.
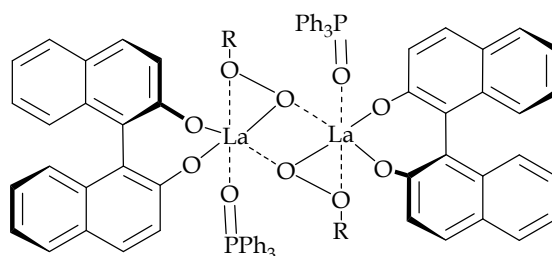
More recently an improved version of this catalyst bearing fluorinated phosphine oxide has shown improved affording excellent stereoselectivities (e.e. up to > 99%) and good to excellent yields.[67] A similar catalytic system has been used by Shibasaki to test the

---

[67] Kino, R.; Daikai, K.; Kawanami, T.; Furuno, H.; Inanaga, J. *Org. Biomol. Chem.* **2004**, *2*, 1822.

reactivity of a series of rare-earth metals.[68] The best catalytic system for the epoxidation of α,β-unsaturated esters was found to be composed of $Y(OiPr)_3$-biphenyldiol ligand and triphenylarsine oxide. Later the same system was used for the asymmetric epoxidation of α,β-unsaturated phosphane oxides.[69]

All of the examples shown since now, regarding the reactivity of peroxo complexes, are related to d_0 metals. In these metal complexes the oxidation state does not vary along the reaction and the activation is given only in function of their Lewis acid character. However, there are also two examples of peroxo reactivity involving non d_0 metals.

The first example of co-ligand effect on peroxo systems of non d_0 metals has been shown by Valentine et al. This study relates to the capability of an additional axial ligand to act as a switch to turn on nucleophilic epoxidation reaction catalyzed by electron-deficient ferric porphyrin peroxo complexes. The authors proposed that axial ligands, such as a solvent molecule (e. g., DMSO) push the side-on-binding peroxo group opening, making the peroxo ligand more nucleophilic (Scheme 15).[70] However, the observed effect was small and it was detectable in the presence of a large amount of DMSO (20% by vol.).
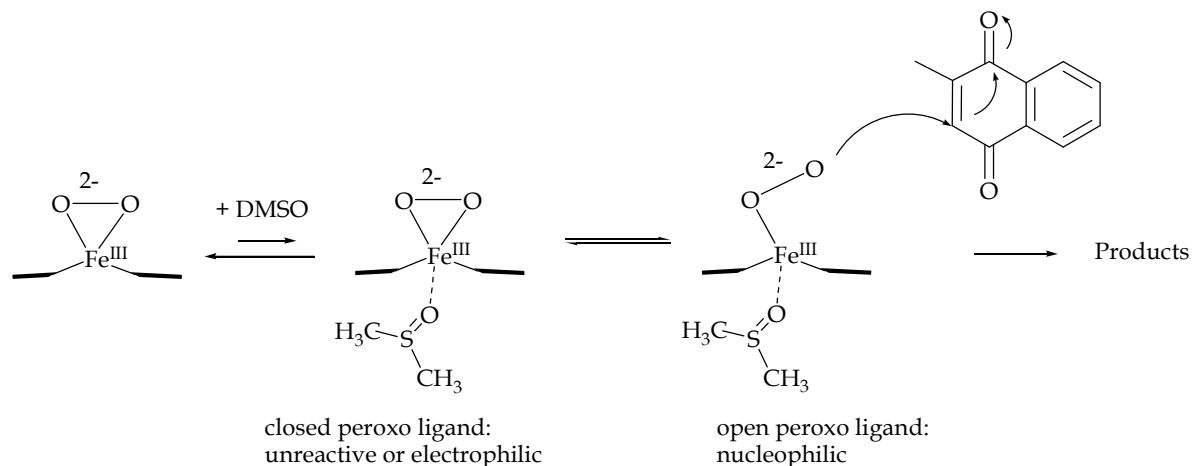
Scheme 15. Epoxidation of an electron-deficient olefin by the ferric perfluorinated peroxo complex in DMSO.

On the contrary, Nam and de Visser reported a remarkable axial ligand effect on the reactivity of the Mn^{III}-peroxo complex $[Mn^{III}(13\text{-}TMC)(O_2)]^+$ (**14**, 13-TMC=1,4,7,10-tetramethyl-1,4,7,10-tetraazacyclotridecane) in the deformylation of cyclohexanecarboxaldehyde (CCA) in the presence of H_2O_2.[71] The observed reactivity order of **14**-N_3>**14**-$OOCCF_3$>**14**-NCS>**14**-CN>**14** reflects an increase in the nucleophilicity of the $\{Mn^{III}O_2\}$ unit upon binding of anionic ligands that make the Mn^{III}-peroxo complex more electron-rich. Two factors are considered for the increased nucleophilicity of **14**-X: electronic and structural effects. First, the electronic effect is that binding of an electron-

[68] Kakei, H.; Tsuji, R.; Ohshima, T.; Morimoto, H.; Matsunaga, S.; Shibasaki, M. *Chem. Asian. J.* **2007**, 2, 257.
[69] Hara, K.; Park, S.-Y.; Yamagiwa, N.; Matsunanga, S.; Shibasaki, M. *Chem. Asian. J.* **2008**, *3*, 1500.
[70] Selke, M.; Valentine, J. S. *J. Am. Chem. Soc.* **1998**, 120, 2652.
[71] Annaraj, J.; Cho, J.; Lee, Y.-M.; Kim, S.Y.; Latifi, R.; de Visser, S.P.; Nam, W. *Angew. Chem. Int. Ed.* **2009**, *48*, 4150.

donating anionic axial ligand makes the Mn[III]-peroxo complex more electron rich,[72] resulting in an increase of the nucleophilicity character of the peroxo group. Nam showed that the binding of anionic ligands shifts the redox potential of **14**-X negatively, thus indicating that **14**-X becomes more electron-rich. Nam has also demonstrated that the Mn[III]-peroxo complexes with more electron donating axial ligands are more reactive in oxidative nucleophilic reactions. Thus, the reactivity order follows the electron-richness of the complexes in nucleophilic reactions. The structural effect is that binding of an axial ligand *trans* to the peroxo group may facilitate the conversion of the side-on peroxo group into an end-on peroxo, thus making it more nucleophilic (Scheme 16). This means that, upon binding, the axial ligand pulls the metal ion down into the coordination plane of the 13-TMC ligand, as in heme system (Scheme 16, **A**). As a consequence, the peroxo group experiences more repulsive interactions from atoms in the 13-TMC ring, resulting in the shift of the equilibrium toward the end-on coordination mode (Scheme 16, **B**).
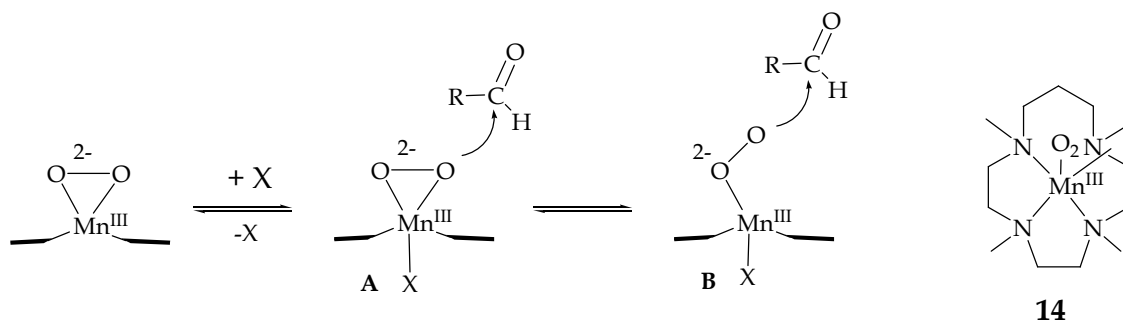
Scheme 16. Oxidative nucleophilic reaction by the Mn[III] -peroxo complex in the presence of an axial ligand (X).

1.3.3 Other reactivity

The co-ligand effects are not a prerequisite of oxidation reactions and similar effects have been observed also in other reactions, like asymmetric cyclopropanations. Nguyen and co-workers, noted that (salen)ruthenium(II) complexes are highly effective for cyclopropanation of olefins using the carbene precursor ethyl diazoacetate (EDA) (Scheme 17).[73] Furthermore, they have registered a significant ligand-accelerated catalysis effect for certain substrates through what is presumed to be axial ligand binding and further activation of the ruthenium carbene cyclopropanation intermediate. (Equation a, Scheme 18).[74]

[72] a) Raynolds, M. S.; Butler, A. *Inor. Chem.* **1996**, 35, 2378-2383. b) Butler, A.; Clague, M. J.; Meister, G. E. *Chem. Rev.* **1994**, 94, 625-638.
[73] Miller, J. A.; Gorss, B. A.; Zhuravel, M. A.; Jin, W.; Nguyen, S. T. *Angew. Chem. Int. Ed.* **2005**, 44, 3885-3889.
[74] Eveland, R. A.; Miller, J. A.; Nguyen, S. T. unpublished data.
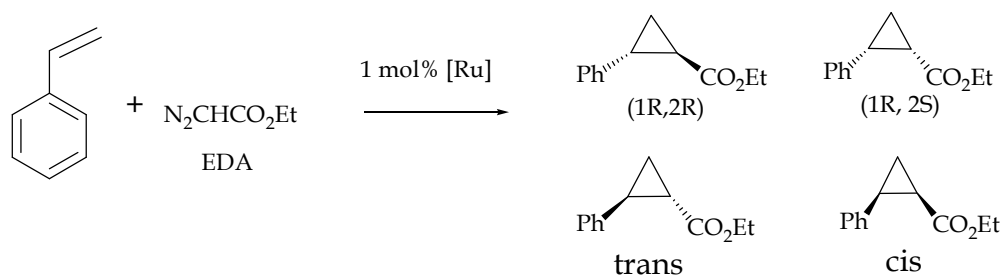
Scheme 17. Cyclopropanation of styrene catalyzed by Ru^{II} complexes using EDA as carbene precursor.
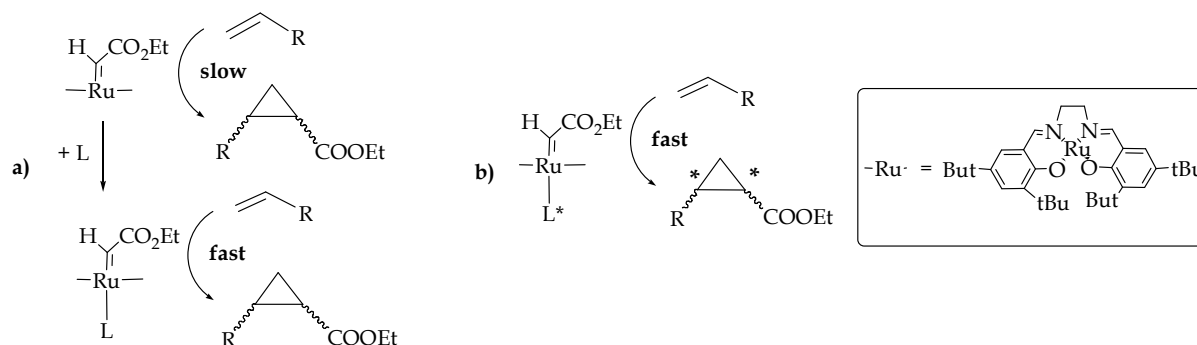
Scheme 18. a) CO-LAC in olefin cyclopropanation catalyzed by a (salen)ruthenium(II) complex. b) A chiral Lewis base L* ligated axially to an achiral (salen)ruthenium-carbene cyclopropanation intermediate could induce asymmetry.

On the bases of these studies, the authors attemped the use of chiral Lewis bases as axial ligand for achiral salen complexes (Equation b, Scheme 18) and found that the (*R*)-(+)-methyl *p*-tolyl **15** sulfoxide was the best chiral additive for the cyclopropanation of styrene affording the corresponding cyclopropanes with e.e.'s up to 57% (Table 8).

15
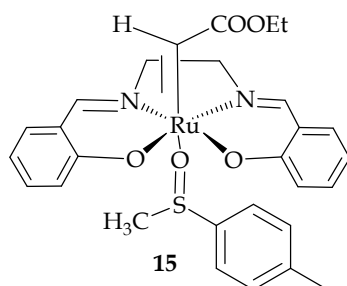
L*	Yield[%]	*cis/trans*	*cis* e.e. [%]	*trans* e.e. [%]
none	92	1 :7 :5	-	-
15	86	1 :7 :6	57 (*R,S*)	46 (*R,R*)

Table 8. The chiral additive ((*R*)-(+)-methyl *p*-tolyl sulfoxide) can bind the achiral (salen)ruthenium complex. The asymmetry of the additive is transmitted/amplified to the opposite axial position where a ruthenium carbene can interact stereoselectivity with an olefin.

Recently Yamada and co-workers,[75] described an interesting theoretical analysis of the cyclopropanation reaction pathway and the axial ligand effect for the 3-oxobutylideneaminatocobalt(II)-catalyzed system. The reaction pathway of the 3-oxobutylideneaminatocobalt(II)-catalyzed cyclopropanation (Scheme 19) consists in the reaction of cobalt(II) complex **16** with diazoacetate yielding thecobalt carbene complex **17**, which then reacts with styrene to regenerate the cobalt(II) complex **16**. The presence of an axial ligand L (such as *N*-methylimidazole) has a significant effect on both the enantioselectivity and reaction rates.
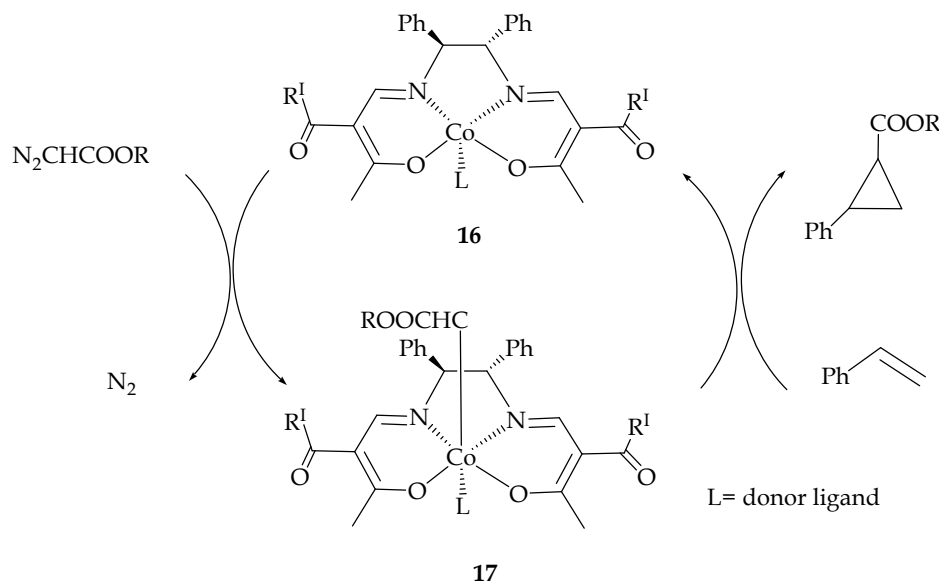
Scheme 19. Catalytic cycle of the cyclopropanation.

This reaction pathway was fully analyzed by density functional computational methods revealing that the axial donor ligand producs two prominent effects: one is the reduction of the activation energy for the formation of the cobalt carbene complex (thus a faster production of **17** was observed) and the increasing of the activation energy for the cyclopropanation step (thus a destabilization of the transition state of this step occurs in the presence of a donor ligand L) . The other is that the distance of the carbene carbon above the plane results shorter during the cyclopropanation step. Therefore, the stereoselection caused by the steric demanding groups in the chiral diamine is effectively enhanced by the addition of axial ligands.

Another example of LAC has been found in the one-pot synthesis of β-cyanohydrins from olefins in the presence of *bis*(trimethylsilyl)peroxide (BTSP) and TMSCN, promoted by catalytic amount of various zirconium catalysts (Table 9).[76] In this work Shibasaki reported that the reaction became much faster and cleaner in the presence of 20 mol % of Ph_3PO. From mechanistic studies it seems that the Zr catalyst plays a multiple roles acting as oxidant, Lewis acid, and nucleophile, in a tandem reaction process. The presence of a Lewis base coordinated to the zirconium centre should facilitate ligand exchange, a phenomenon that could be considered the key for promoting the two completely different steps involved in the

[75] Ikeno, T.; Iwakura, I.; Yabushita, S.; Yamada, T. *Organic Letters* **2001**, 4, 517-520.
[76] Yamasaki, S.; Kanai, M.; Shibasaki, M. *J. Am. Chem. Soc.* **2001**, 123, 1256.

reaction (epoxidation and epoxide-opening). Moreover the Lewis base should enhance the nucleophilicity of the zirconium cyanide.
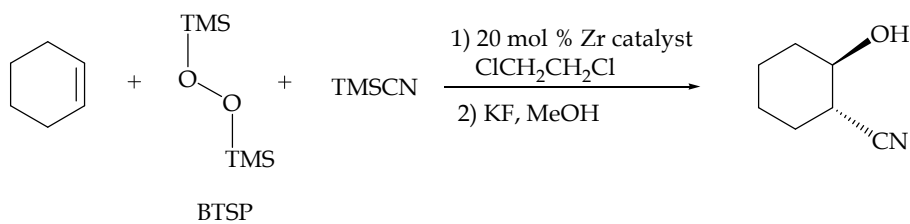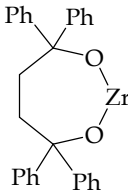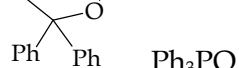
Zr catalyst	time	yield (%)
Zr(OnBu)₄	84 h	62
Zr(OiPr)₄	63 h	63
Zr(OtBu)₄	38 h	63
alone	15 h	68
Ph₃PO	1.5 h	94

Table 9. One-pot synthesis of β-cyanohydrins from olefins with various Zr catalysts and with Ph$_3$PO as additive.

1.4 Aim of the thesis

The work described in this thesis concern oxygen transfer processes mediated by d_0 metal complexes. In particular our attention has been focalized towards the reactivity of two classes of ligands: trisilanol polyhedral silsesquioxane and amine triphenolate.

In this respect, Chapter 2 describes the reactivity of a V(V) silsesquioxane complex (VO-POSS) in oxidation reactions towards various substrates such as sulfide, tertiary amine and secondary amine using cumyl hydroperoxide as the terminal oxidant. Moreover, the effects induced by added Lewis basic co-ligand in the VO(POSS) reactivity, selectivity and stereoselctivity of the oxygen transfer processes will be discussed. A proposal for the intermolecular activation, using MP2/TZVP calculations, will be presented.

Chapter 3 is dedicated to the synthesis and the sistematic study on the reactivity of eight aminotriphenolate d_0 metal complexes [Sc(III), Ti(IV), Zr(IV), Hf(IV), V(V), Nb(V), Ta(V), Mo(VI)]. The reactivity and selectivity properties ,both in presence and in absence of a strong Lewis Base (dimethylhexyl-*N*-oxide) as co-ligand, will be presented. The experimentals combined with theoretical calculations have furnished more insights on the characteristics of the reactive peroxo specie which will be presented.

In Chapter 4 the reactivity of a V(V) complex with *tri*-phenol amines bearing *tert*-butyl peripheral substituents in the oxidation of sulfides and hlides using hydrogen peroxide as

the terminal oxidant will be presented. The structural and reactivity analogies with the active site of the Vanadium haloperoxidases enzymes will be discussed.

Chapter 5 is dedicated to the synthesis of a new trisilanol polyhedral silsesquioxane ligand bearing long fluoroalkil chains. The very first results and the various synthetic strategies followed will be presented.

Chapter 2

Role of Intermolecular Interactions in Oxygen Transfer Catalyzed by Silsesquioxane Trisilanolate Vanadium(V)

Tol-S-Me $\xrightarrow{\text{CHP, 1}}$ Tol-S**O**-Me

Ph–CH₂–N(H)–CH₂–Ph $\xrightarrow{\text{CHP, 1}}$ Ph–CH=N⁺(**O**⁻)–CH₂–Ph

NEt₃ $\xrightarrow{\text{CHP, 1}}$ ⁻**O**–N⁺Et₃

1, R= *i*-butyl

CO-LIGAND EFFECT

REACTIVITY
CHEMOSELECTIVITY
STABILITY
STEREOSELECTIVITY
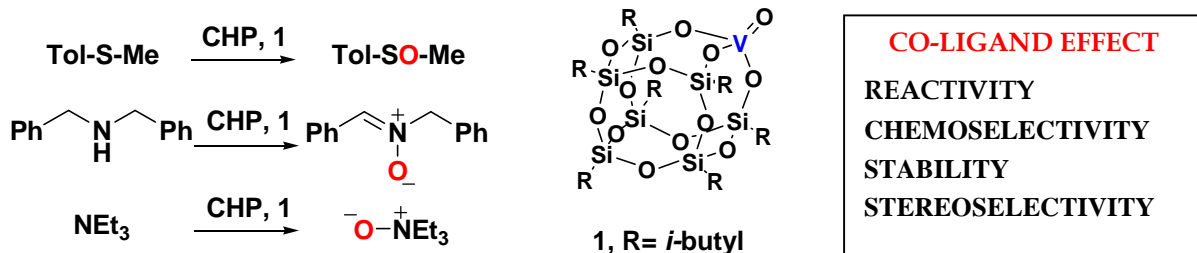
The polyhedral oligomeric silsesquioxane trisilanolate vanadium(V) complex **1** efficiently catalyzed oxidations at room temeperature using cumyl hydroperoxide as the terminal oxidant. Sulfoxidations and *N*-oxidations have been carried out yielding the corrisponding products in good yields. The addition of a Lewis base as a co-ligand can markedly affect reactivity, stability, chemo- and stereo-selectivity. A proposal for the intermolecular activation, using Gutmann analysis supported by MP2/TZVP calculations, is presented.

2.1 Introduction

The activation of peroxides by metal complexes has been the focus of intense research efforts because of its relevance to biochemical processes and its application in industrial oxidation processes.[1] Several complexes, inspired by natural metalloenzymes, have shown interesting catalytic properties.[2] Typically, a ligand is used to stabilize the metal, to increase its reactivity, and to direct the stereochemistry of the reaction.[3] A less explored alternative is the use of an extra ligand (coligand) able to bind the metal in addition to the ligand and thereby capable of tuning the catalytic properties of the complex.[4] This approach does not only offer the opportunity to module the catalytic systems with a defined reactivity and selectivity profile but also allows for a better understanding of the basic principles behind metal activation in synthetic and biological systems. In fact, intermolecular interactions can either stabilize transition states by charge redistribution or by the action on unstable intermediates. However, in a first approximation, the presence of a coligand (usually a Lewis base, LB) will decrease the catalyst (a Lewis acid) reactivity or even completely inhibit it.[5]

Several d^0 metal ions, such as Ti(IV), V(V), Mo(VI), and Re(VII), have shown the possibility to expand their coordination sphere in the presence of other ligands.[5,6] In some cases, this phenomenon results in a variation of the catalytic activity. As an example, earlier our group investigated the oxygen transfer to organic sulfur compounds catalyzed by Ti(IV) complexes, noticing that the coordination of a sulfoxide to the metal was responsible for a switch in the reactivity of the peroxometal functionality from electrophilic to nucleophilic.[6] Herein, it is provided an experimental evidence of a remarkable activation of a vanadium complex by intermolecular interactions. We also propose a mechanism for the activation, based on charge redistribution on the active peroxometal complex, which accounts for these results.

2.2 V(V)-*i*BuPOSS complex : synthesis, catalytic activity in oxygen transfer reactions and effects of the coligands.

Our intereset in the possible effect of extra ligands in catalysis came during the course of our studies on oxygen transfer reactions catalyzed by vanadium(V) silsesquioxane complex **1**. Oxidation mediated by vanadium compounds has been revitalized by the discovery of vanadium-dependent enzymes, haloperoxidases, producing an ever growing number of

---

[1] a) Bäckvall, J.-E.; *Modern Oxidation Methods*; Wiley-VCH: New York, **2004**. b) Limberg, C.; Meyer, F. *OrganometallicOxidation Catalysis (Topics in Organometallic Chemistry)*; Springer-Verlag: Berlin, **2007**.

[2] a) Berkessel, A.; Gröger, H. *Asymmetric Organocatalysis: From Biomimetic Concepts to Applications in Asymmetric Synthesis*; Wiley-VCH: New York **2005**. b) van Eldik, J. R. R. *Advanced Inorganic Chemistry*; Academic Press: New York, **2006**, Vol. 58: Homogeneous Biomimetic Oxidation Catalysis. c) Meunier, B.; *Biomimetic Oxidations Catalyzed by Transition MetalComplexes*; World Scientific Publishing Company: River Edge, NJ, **2000**. d) Que, L.; Tolman, W. B. *Nature*, **2008**, 455, 333-340.

[3] Berrisford, D. J.; Bolm, C.; Sharpless, K. B. *Angew. Chem. Int. Ed.* **1995**, 34, 1059-1070.

[4] a) Vogl, E. M.; Groger, H.; Shibasaki, M. *Angew. Chem. Int. Ed.* **1999**, 38, 1570-1577. b) Zhou, Y.; Shan, X.; Mas-Ballesté, R.; Bukowski, M. R.; Stubna, A.; Chakrabarti, M.; Slominski, V.; Halfen, J. A.; Münck, E.; Que, L. *Angew. Chem. Int. Ed.* **2008**, 47, 1896-1899.

[5] a) Kühn, F. E.; Santos, A. M.; Roesky, P. W.; Herdtweck, E.; Scherer, W.; Gisdakis, P.; Yudanov, I. V.; Di Valentin, C.; Rösch, N. *Chem. Eur. J.* **1999**, 5, 3603-3615. b) Bonchio, M.; Conte, V.; De Conciliis, M. A.; Di Furia, F.; Ballistreri, F. P.; Tomaselli, G. A.; Toscano, R. M. *J. Org. Chem.* **1995**, 60, 4475-4480.

[6] a) Bonchio, M.; Calloni, S.; Di Furia, F.; Licini, G.; Modena, G.; Moro, S.; Nugent, W. A. *J. Am. Chem. Soc.* **1999**, 121, 6258-6268. b) Redshaw, C.; Warford, L.; Dale, S. H.; Elsegood, M. R. J. *Chem. Commun.* **2004**, 1954-1955.

studies on biomimetic complexes.[7] The main interest has been directed toward oxidations of sulfides,[8] halides,[8,9] and allylic alcohols.[10] In the oxidation pathway followed by these complexes, it has been largely accepted that the mechanism begins with an electrophilic activation of the peroxide followed by a nucleophilic attack by the substrate on the η^2-coordinated peroxide.[11]

Vanadium POSS complexes,[12] originally synthesized by Feher in 1991,[12] had found application as photooxidation catalysts.[13,14] Their use in homogeneous solution has been held back because of the instability of the complex in the presence of hydroxylic reagents (e. g., hydroperoxides, alcohols, or water).[13] During the course of our studies on vanadium silsesquioxane **1** (VO-POSS), we cheeked the stability of **1** toward alkyl hydroperoxides, and we found that the complex was able to activate cumil hydroperoxide (CHP) and oxidize methyl *p*-tolyl sulfide **2** to the corresponding sulfoxide **3** (Scheme 1).
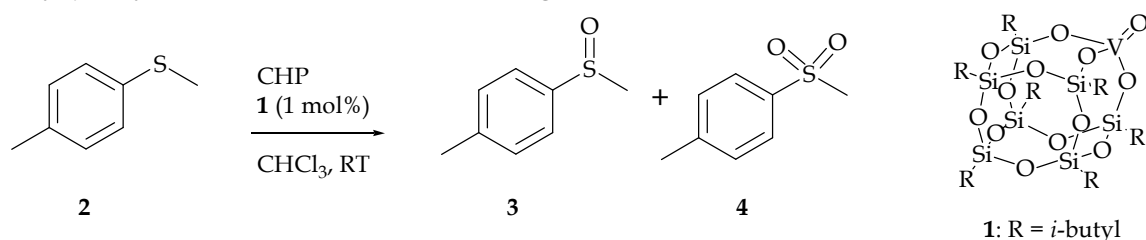
Scheme 1. V(V)-catalyzed oxidation of methyl *p*-tolyl sulfoxide **2**.

[7] a) Butler, A.; Clague, M. J.; Meister, G. E. *Chem. Rev.* **1994**, 94, 625-638. b) Conte, V.; Di Furia, F.; Licini, G. *Appl. Catal. A.* **1997**, 335-361. c) Butler, A. *Coord. Chem. Rev.* **1999**, 187, 17-35. d) van de Velde, F.; Arends, I. W. C. E. ; Sheldon, R. A. *Top. Catal.* **2000**, 13, 259-265. e) Rehder, D.; Santoni, G.; Licini, G.; Schulzke, C.; Meier, B. *Coord. Chem. Rev.* **2003**, 237, 53-63. f) Ligtenbarg, A. G. J.; Hage, R.; Feringa, B. L. *Coord. Chem. Rev.* **2003**, 237, 89-101. g) Crans, D. C.; Smee, J. J.; Gaidamauskas, E.; Yang, L. *Chem. Rev.* **2004**, 104, 849-902. h) Bolm, C. *Coord. Chem. Rev.* **2003**, 237, 245-256. i) Legros, J.; Dehli, J. R.; Bolm, C. *Adv. Synth. Catal.* **2005**, 347, 19-31. j) Rehder, D. *J. Inorg. Biochem.* **2008**, 102, 1152-1158.

[8] a) Santoni, G.; Licini, G.; Rehder, D. *Chem. Eur. J.* **2003**, 19, 4700-4708. b) Jeong, Y.-C.; Choi, S.; Hwang, Y. D.; Ahn, K.-H. *Tetrahedron Lett.* **2004**, 45, 9249-9253. c) Barbarici, A.; Maggi, R.; Muratori, M.; Sartori, G.; Sartorio, R. *Tetrahedron Asymm.* **2004**, 15, 2467-2473. d) Zeng, Q.; Wang, H.; Wang, T.; Cai, Y.; Weng, W.; Zhao, Y. *Adv. Synth. Catal.* **2005**, 347, 1933-1936. e) Drago, C.; Caggiano, L.; Jackson, R. F. W. *Angew. Chem. Int. Ed.* **2005**, 44, 7221-7223. f) Kelly, P.; Lawrence, S. E.; Maguire, A. R. *Eur. J. Org. Chem.* **2006**, 4500-4509. g) Mba, M.; Pontini, M.; Lovat, S.; Zonta, C; Bernardinelli, G.; Kündig, P. E.; Licini, G. *Inorg. Chem.* **2008**, 47, 8616-8618. h) Licini, G.; Mba, M.; Zonta, C. *Dal ton. Trans.* **2009**, 27, 5265-5277.

[9] a) Clague, M. J.; Keder, N. L.; Butler, A. *Inorg. Chem.* **1993**, 32, 4754-4761. b) Conte, V.; Di Furia, F. ; Moro, S. *Tetrahedron Lett.* **1994**, 35, 7429-7432. c) Colpas, G. J.; Hamstra, B. J.; Kampf, J. W.; Pecoraio, V. L. *J. Am. Chem. Soc.* **1994**, 116, 3627-3628. d) Colpas, G. J.; Hamstra, B. J.; Kampf, J. W.; Pecoraio, V. L. *J. Am. Chem. Soc.* **1996**, 118, 3469-3478. e) Hamstra, B. J.; Colpas, G. J.; Pecoraio, V. L. *Inorg. Chem.* **1998**, 37, 949-955.

[10] a) Bourhani, Z.; Malkov, A. V. *Chem. Commun.* **2005**, 4592-4594. b) Zhang, W.; Basak, A. ; Kosugi, Y. ; Hoshino, Y.; Yamamoto, H. *Angew. Chem. Int. Ed.* **2005**, 44, 4389-4391. c) Malkov, A. V.; Bourhani, Z.; Kočovský, P. *Org. Biomol. Chem.* **2005**, 3, 3194-3200. d) Barlan, A. U.; Zhang, W.; Yamamoto, H. *Tetrahedron* **2007**, 63, 6075-6087. e) Zhang, W.; Yamamoto, H.; *J. Am. Chem. Soc* **2007**, 129, 286-287. f) Li, Z.; Zhang, W.; Yamamoto, H. *Angew. Chem. Int. Ed.* **2008**, 47, 7520-7522.

[11] a) Balcells, D.; Maseras, F.; Lledós, J. *J. Org. Chem.* **2003**, 68, 4265-4274. b) Bortolini, O.; Conte, V. *J. Inorg. Biochem.* **2005**, 99, 1549-1577. c) Schneider, C. J.; Zampella, G.; Greco, C.; Pecoraro, C. L.; De Gioia, L. *Eur. J. Inorg. Chem.* **2007**, 515-523. d) Schneider, C. J.; Penner-Hahn, J. E.; Pecoraro, V. L. *J. Am. Chem. Soc.* **2008**, 130, 2712-2713.

[12] For a review on POSS ligands and complexes, see: a) Hanssen, R. W. J. M.; van Santen, R. A.; Abbenhuis, H. C. L. *Eur. J. Inorg. Chem.* **2004**, 4, 675-683. b) Wada, K.; Mitsudo, T. *Cat. Sur. Asia* **2005**, 9, 229-241.

[13] a) Feher, F. J.; Walzer, J. F. *Inorg. Chem.* **1991**, 30, 1689-1694. b) Wada, K.; Nakaashita, M.; Yamamoto, A.; Wada, H.; Mitsudo, T. *Chem. Lett.* **1997**, 1209-1210. c) Carniato, F.; Boccaleri, E.; Marchese, L.; Fina, A.; Tabuani, D.; Camino, G. *Eur. J. Inorg. Chem.* **2007**, 4, 585-591.

[14] Ohde, C.; Brandt, M.; Limberg, C.; Döbler, J.; Ziemer, B.; Sauer, J. *Dalton. Trans.* **2008**, 326-331.

The obtained results demonstrate a high catalytic activity of complex **1** itself, with quantitative conversion of the oxidant and minor formation of sulfone **4** (Table 1, entry 1).[15] We further noticed that the presence of a base able to act as a co-ligand in solution distinctively enhanced the catalytic activity of **1**. To shed more light onto this intriguing co-ligand effect, the sulfoxidation reaction in the presence of different co-ligands of increasing basic strenght (**3**, **5-9**, Figure 1) was carried out (Table 1).[16]
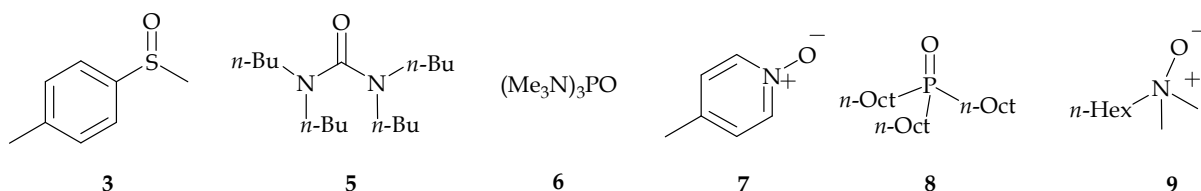

Figure 1. Lewis Bases **3**, **5-9** used as co-ligands.

Entry	Co-ligand	$t_{1/2}$ sec (equiv. co-ligand)[b,c]	[**3/4**] (equiv. co-ligand)[b]
1	None	6000	98:2
2	**3**	5580 (5), 5010 (150)	98:2 (5), 98:2 (150)
3	**5**	6060 (5), 4730 (150)	96:4 (5), 95:5 (150)
4	**6**	3100 (1), 3042 (5), 2200 (40), 1430 (80), 456 (150)	97:3 (1), 93:7 (5), 81:19 (40), 73:27 (80), 68:32 (150)
5	**7**	3525 (1), 2031 (5), 1280 (40), 570 (80), 476 (150)	95:5 (1), 96:4 (5), 94:6 (40), 91:9 (80), 82:18 (150)
6	**8**	628 (1), 290 (5), 217 (40), 235 (80), 230 (150)	93:7 (1), 95:5 (5), 93:7 (40), 92:8 (80), 82:18 (150)
7	**9**	361 (0.5), 250 (1), 233 (5), 195 (40), 200 (80), 200 (150)	85:15 (0.5), 88:12 (1), 87:13 (5), 85:15 (40), 84:16 (80), 84:16 (150)

[a] Reactions were carried out in CHCl$_3$ at 28 °C using [**2**]$_0$ = [CHP]$_0$ = 0.1 M and 1% mol of **1**. Quantitative yields based on the oxidant were obtained in all the reactions. Yields and **3/4** ratios were determined by ^{1}H NMR in the presence of DCE as internal standard in the crude reaction mixture after total oxidant consumption (iodometric test). [b] Co-ligand equivalents with respect to **1**. [c] Time required for a 50% decrease of the initial concentration of **2**.

Table 1. Oxidation of methyl *p*-tolyl sulfide **2** by CHP catalyzed by **1** (1%) in the presence of co-ligands **3**, **5-9** in chloroform.[a]

In all the reactions shown in Table 1, vanadium silsesquioxane **1**, which was prepared and characterized following a litterature procedure, was used at millimolar concentration, where it is present as a monomer.[13] The different co-ligands **3**, **5-9** have been choosen for their different electronic and steric properties, and have been tested in the range between 0.001

---

[15] For a comparison with other catalytic systems, see: Smith, T. S.; Pecoraro, V. L. *Inorg. Chem.* **2002**, 41, 6754-6760.

[16] No deoxygenated coligands have been observed at the end of the reaction. This to confirm that they are not acting as oxo-atom donors.

and 0.150 M (see Table 1 and Figure 2), which translates from equimolar to a 150-fold excess with respect to catalyst **1**.
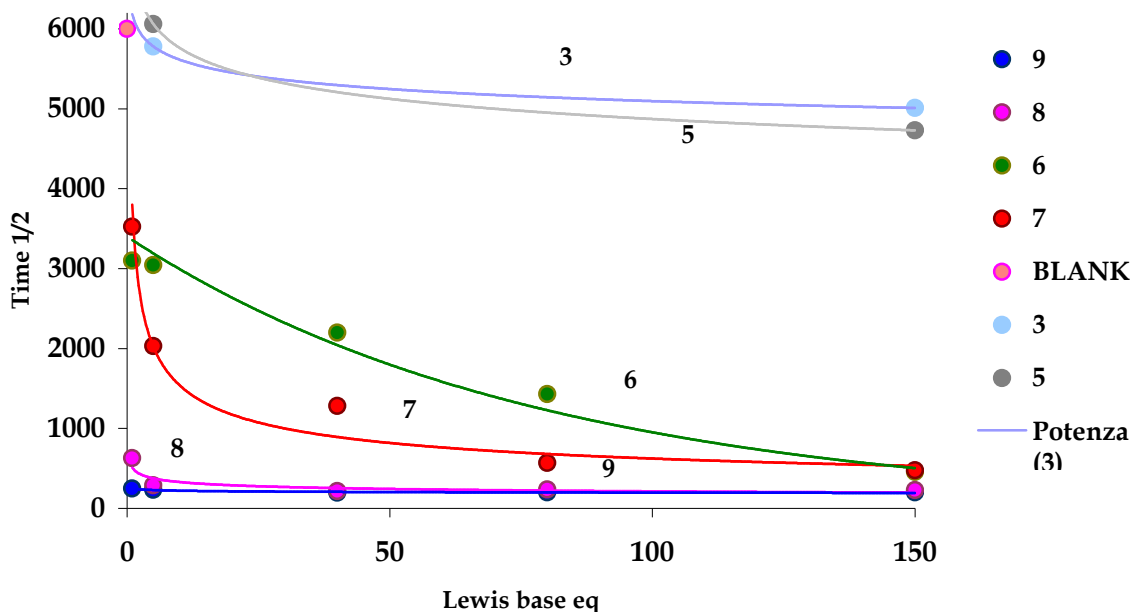

Figure 2. Half time of methyl *p*-tolyl sulfide **2** consuption at different concentrations of Lewis bases **3**, **5-9**.

In Figure 2 it is enphasized that reaction rates (expressed as half time of substrate consumption) increase in the presence of the LBs **3**, **5-9** with respect to the blank of the reaction and moreover, the accelerations are different in the presence of different LBs. It is interesting to note that also the concentrations of the same LB affect the reaction rates. In particular, the highest is the concentration of the LB the more enhanced is the reaction rate. This trend is pronounced for the LBs **7** and **6**. For the LBs **8** and **9** a maximum of acceleration can be found even at an equimolar LB/catalyst ratio.

As shown in Table 1, the addition of the co-ligands to the reaction mixtures results also in a variation in the sulfone/sulfoxide ratio [**3/4**] at the end of the reaction.

We noticed that these two effects (variation of the reactivity and variation of the selectivity) correlate with the electron richness of the co-ligand, as shown by the correlation with their electrostatic potential surfaces.[17] The more electron rich the co-ligand is (**8** or **9**), the more enhanced is the reactivity and the lower the excess required for maximizing the acceleration. As an example, the *N*-oxide **9** is able to increase the reaction rate 24 times already at a **1:9**= 1:1 ratio (Table 1, entry 7). The less electron-donating co-ligands (**3**, **5**) produce a small effect on the catalytic properties of complex **1** even when they are present in a large excess (Table 1, entries 2 and 3). On the other hand, the basic but more hindered **6** requires larger excesses to afford significant accelerations, in agreement with a less favorable coordination to the metal center (Table 1, entry 4), as showed in the [**6**]$_0$ versus reactivity profile shown in Figure 3. In this figure is also shown the variation of the sulfone concentrations at the end of the reaction

---

[17] A correlation among reactivity and electrostatic potential surfaces of the co-ligand has been found. See: Hunter, C. A. *Angew. Chem. Int. Ed.* **2004**, 43, 5310-5324.

versus the concentration of the LB **6** indicating that the amount of sulfone increase increasing the LB **6** concentration. This trend was also noted for the other LBs.
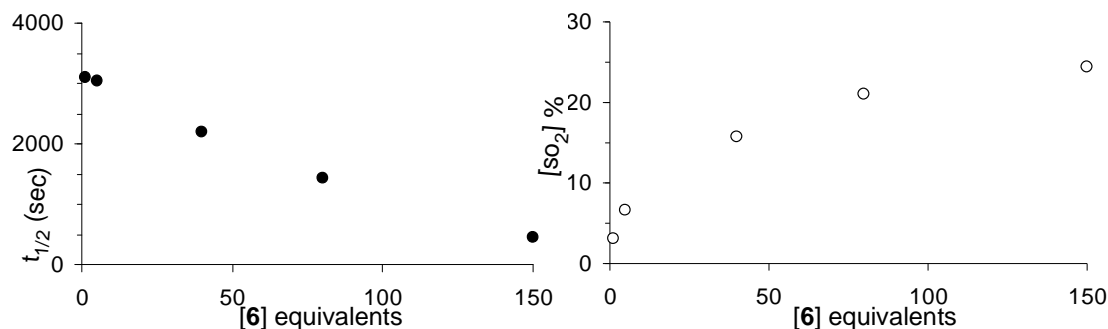
Figure 3. Variation of the half time of methyl-*p*-tolyl sulfide **2** consuption (left ●) and of the final concentration of methyl-*p*-tolyl sulfone **4** (right O) using $[2]_0 = [CHP]_0 = 0.1$ M, 1% mol of **1** and **6** (HMPA) (1-150 equiv. with respect to **1**) as co-ligand.

In order to further evaluate the catalytic activity of **1** in other oxygen transfer processes, and to further study the LBs effect toward other substrates we examined the oxidation of triethylamine **10** to the corresponding *N*-oxide **11** (Figure 4).[18]
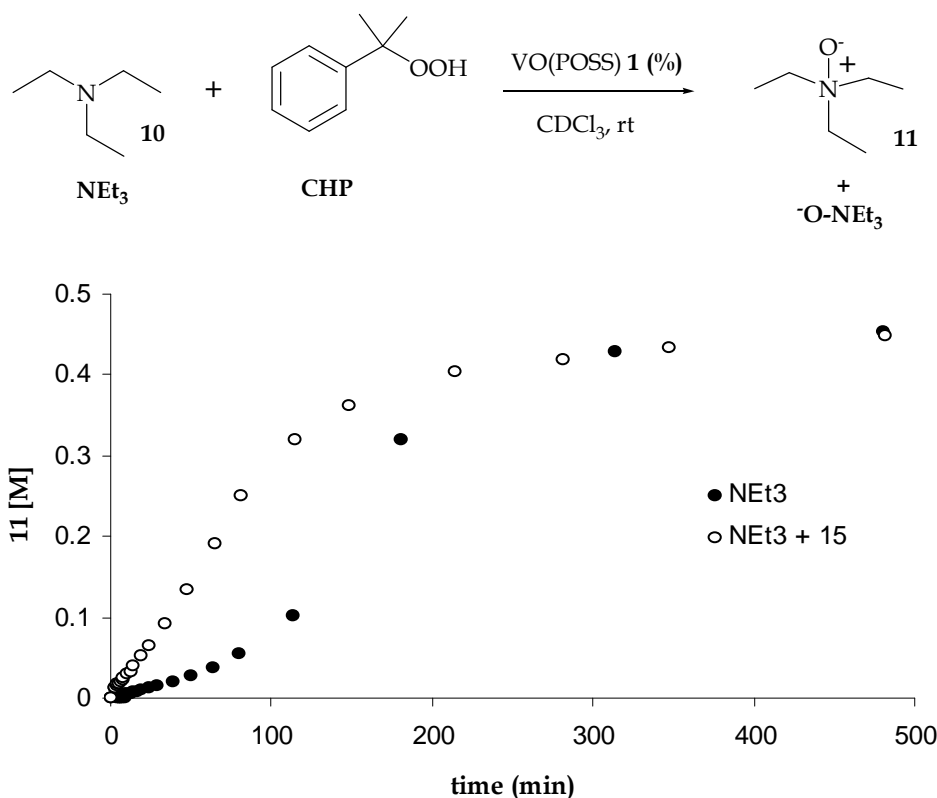
Figure 4. Plot of triethylamine-*N*- oxide **11** formation *vs* time (min) in the oxidation of triethylamine **10** (0.5 M) by CHP (0.5 M) in CDCl₃ at 28°C, catalyzed by **1** (1%) in presence (O) or in absence (●) of **9** (5%).

The raction displays a sigmoid profile (Figure 4, plain dots profile), suggesting that the initially formed *N*-oxide **11**, acting as a Leiws base coordinates to the metal center, increasing

---

[18] Colladon, M.; Scarso, A.; Strukul, G. *Green. Chem.* **2008**, 10, 793-798.

the catalytic activity of the system, in a typical autocatalytic process. As a confirmation, the addition of five equivalent of **9** to the starting mixture results in an increase of the reaction rate from the beginning and in comparable yields (Figure 4, empty dots profile).

We then tested the activity of the catalyst in the oxidation of dibenzylamine **12** to the corresponding nitrone **13**.[19] Nitrones are valuable synthetic intermediates for the synthesis of biologically active compounds,[20] as effective spin trap reagents[21] and as therapeutic agents.[22] In principle, the oxidative approach using hydrogen peroxide (or urea hydrogen peroxide) or alkyl hydroperoxide starting from corresponding secondary amines, provides the most direct and general method for preparing nitrones (Scheme 2).
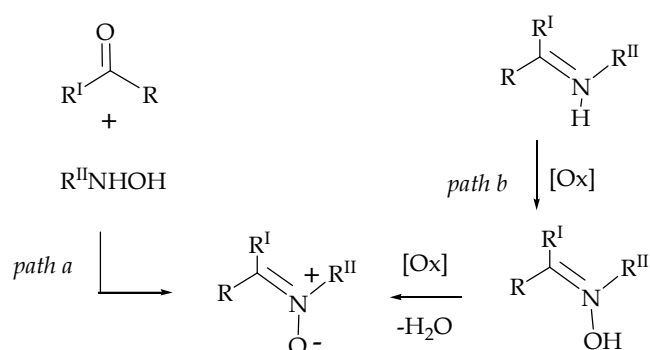
Scheme 2. Synthesis of nitrones via a) condensation of carbonyl compounds with N-monosubstituted hydroxylamine or b) the oxidation of secondary amines.

However, in most cases, in the direct synthesis a significant amount of hydroxylamine is recovered and hydrolysis of the catalyst by the stoichiometric amount of water that forms can occur and inhibit the process.

We observed that the oxidation of dibenzylamine **12** in the presence of **1** (10%) as a catalyst in chloroform, furnished nitrone **13** in a 66% yield (Figure 5). Instead, the addition of **9** (5 equivalent with respect to the catalyst) resulted in a final, much higher yield (90%). Indeed, the addition of only 1 equivalent of water, with respect to the catalyst, at the beginning of the reaction, resulted in a lower yield (51%) using only **1**. On the contrary, yields remained unvaried using **1** in the presence of **9** (90%). In this case the reaction is not accelerated, but the presence of the LB **9** seems to increase the stability of the catalyst toward the presence of the water molecules formed during the reaction.

[19] a) Forcato, M.; Nugent, W. A.; Licini, G. *Tetrahedron Lett.* **2003**, 44, 49-52. b) Zonta, C.; Cazzola, E.; Mba, M.; Licini, G. *Adv. Synth. Catal.* **2008**, 350, 2503-2506.

[20] a) Bloch, R. *Chem. Rev.* **1998**, 98, 1407-1438. b) Gothelf, K. V.; Jorgensen, K. A. *Chem. Rev.* **1998**, 98, 863-910. c) Cardona, F.; Goti, A. *Angew. Chem. Int. Ed.* **2005**, 44, 7832-7835.

[21] Villamena, F. A.; Xia, S. ; Merle, J. K.; Lauricella, R.; Tuccio, B.; Hadad, C. M.; Zweier, J. L. *J. Am. Chem. Soc.* **2007**, 129, 8177-8191, and reference cited therein.

[22] Slemmer, J. E.; Shacka, J. J.; Sweeney, M. I.; Weber, J. T. *Curr. Med. Chem.* **2008**, 15, 404-414.
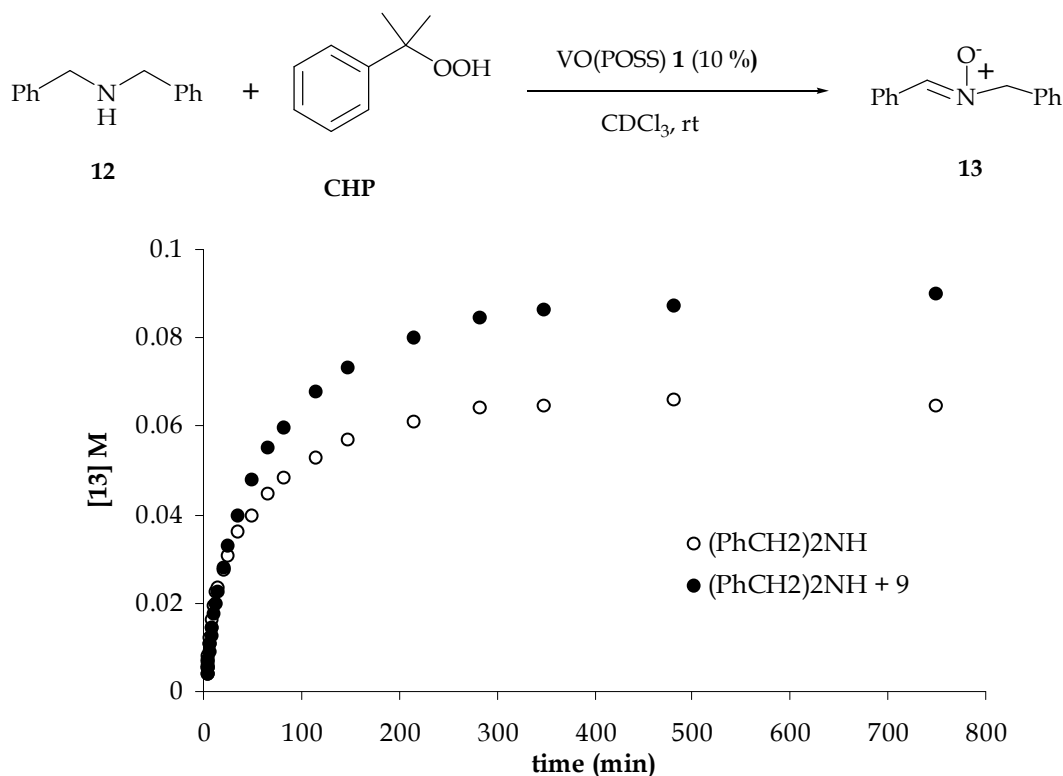
Figure 5. Plot of nitrone 13 formation *vs* time (min) in the oxidation of dibenzylamine 12 (0.1 M) by CHP (0.4 M) in CDCl$_3$ at 28°C, catalyzed by 1 (0.01 M) in presence (O) or in absence (●) of 9 (0.05 M).

An interesting evidence of the coordination of the co-ligands to the catalyst 1 were obtained via NMR spectroscopy (Figure 6). In Figure 6a) is presented the [51]V NMR spectra of the VO-POSS complex 1 in CDCl$_3$ in a 0.01 M concentration. Only a peak at -690.9 ppm is present. When 1 equivalent of *N*-oxide 9 with respect to the complex 1 is added to this solution a new signals appears at -605.9 ppm (Figure 6b). After the addition of a second equivalent of 9 only the peak at -605.9 ppm is detected.
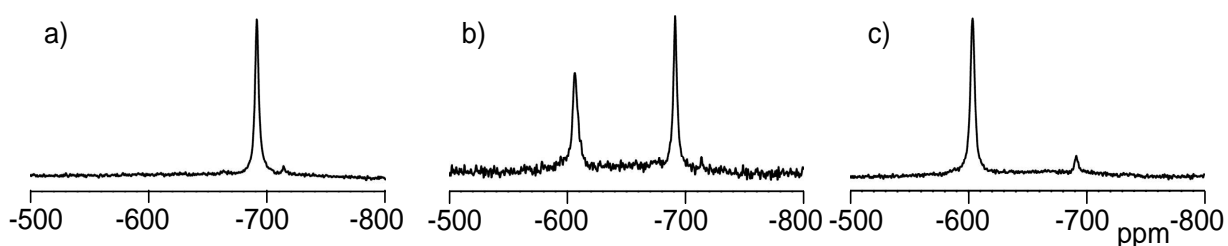
Figure 6. [51]V NMR spectra of 1 (0.01 M) in CDCl$_3$ at 28°C (a), in the presence of one equivalent of 9 (b) and in the presence of two equivalents of 9 (c).

R= *i*-butyl
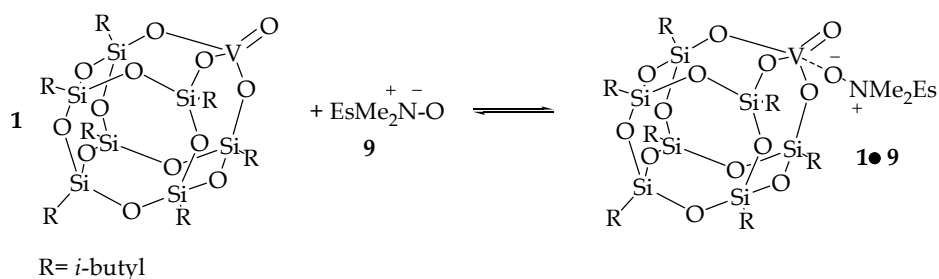
Scheme 3. Representation of the equilibrium present in solution between the complex 1 and the Lewis base 9.

We belive that the signal at -605.9 ppm corrisponds to the adduct **1•9** (Scheme 3). The presence of two peaks in the ^{51}V NMR spectra at a molar ratio of 1:1 between LB **9** and complex **1** indicates the presence of an equilibrium of coordination at the metal centre. Rising the concentration of the LB **9** the equilibrium shifts completely toward the new specie : the adduct **1•9**.

A definitive proof of the coordination of the coligand to the catalysts during the oxidation process, and in particular during the oxygen transfer step, came from the use of a chiral, enantiopure coligand, the phosphoric amide (*S, R, R*)-**14**. This co-ligand has been used to activate the catalyst and control the stereochemistry of the oxidation of methyl *p*-tolyl sulfide **2** (Scheme 4).[23] The final sulfoxide (*S*)-**3** was recovered in quantitative yield and with e.e. = 14%.

Scheme 4. Vanadium-catalyzed oxidation of methyl *p*-tolyl sulfide **2** using (*S,R,R*)-**14** as co-catalyst. $[2]_0 = 0.1$ M, $[1] = 0.001$ M, $[14] = 0.005$ M and $[CHP] = 0.010$ M.[15]
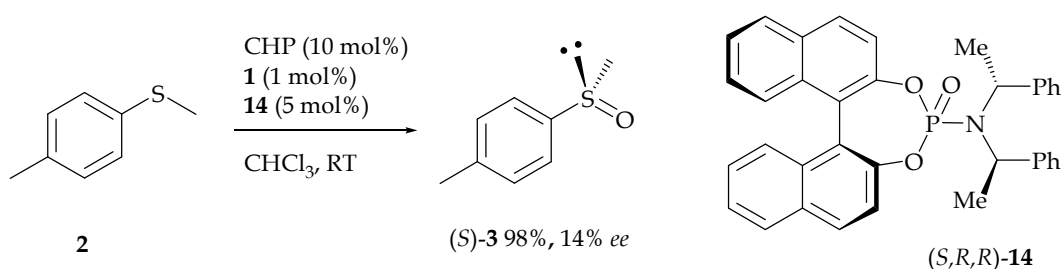
Even if this result is not exciting for the low value of e.e., it confirms our hypotesis of the coordination of the LB to the metal center during the catalytic process.

2.3 Coligand effects : stability and of the kinetic order in catalyst, substrate, oxidant and Lewis bases

The stability of catalyst **1** under turnover conditions (presence of hydroxylic species such as CHP and cumyl alcohol) has been investigated more in detail. The stability of **1** and **1•9** complexes at the end of rhe reaction of sulfoxidation of methyl *p*-tolyl sulfide **2** and in the presence of a large excess of CHP (up to 100 eqivalents) has been monitored via ^{51}V NMR. In both cases, the two species were present, unaltered (Figure 7 and 8). On the contrary, a new peak at –686.7 ppm appeared either upon standing for longer time after the completition of the reaction or when a solution of fresh catalyst **1** has been treated with a large excess of cumyl alcohol.[24] This peak has been assigned to the vanadium oxotricumyloxide **15**, which has been independently synthesized and characterized. Reactivity of **15** in sulfoxidation has been explored as well, and it was determined to be higher than 1 without the presence of a Lewis base (initial rate R_0(**15**)= 0.126 mmol/s vs R_0(**1**) = 0.019 mmol/s), confirming that **15** is not the active catalyst in the process. Furthermore, even if catalyst **15** forms during the course of the reaction, at a concentration lower than that detectable via ^{51}V NMR, its quantity

---

[23] Pizzuti, M. G.; Minnaard, A. J.; Feringa, B. L. *J. Org. Chem.* **2008**, 73, 940-947. Phosphoric amide **14** can also be generated in situ using the CHP/1 oxidation protocol starting from the corresponding phosphoroamidite.
[24] Reactions carried out in CHCl₃ at 28°C using $[2]_0=[CHP]_0=0.1$ M and 1 mol % of **15** furnished the sulfoxide **3** in 80 % yield, and the time required for a 50% decrease of the initial concentration of **2** is 990 s.

should increase along the reaction, determining a deviation from the first-order reactivity of 1, which is not observed.
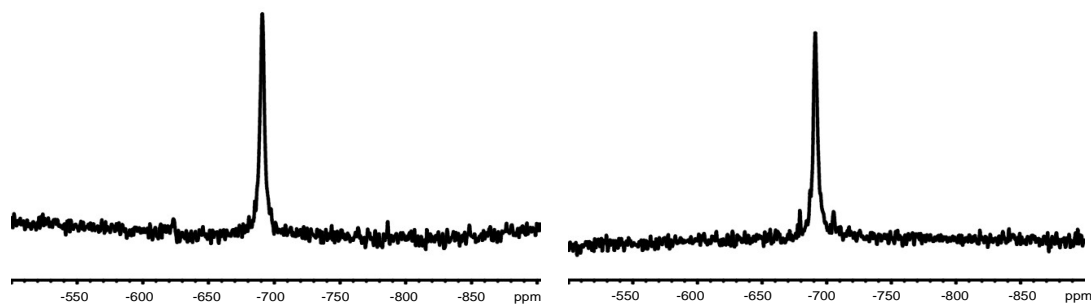
Figure 7. ^{51}V NMR Spectra of the catalyst **1** at the beginning and at the end of the oxidation of methyl p-tolyl sulfide **2** with CHP. A NMR tube was charged with a solution of the complex **1** in CDCl$_3$ (0.001 M), CHP (0.1 M) and methyl *p*-tolyl sulfide **2** (0.1 M).
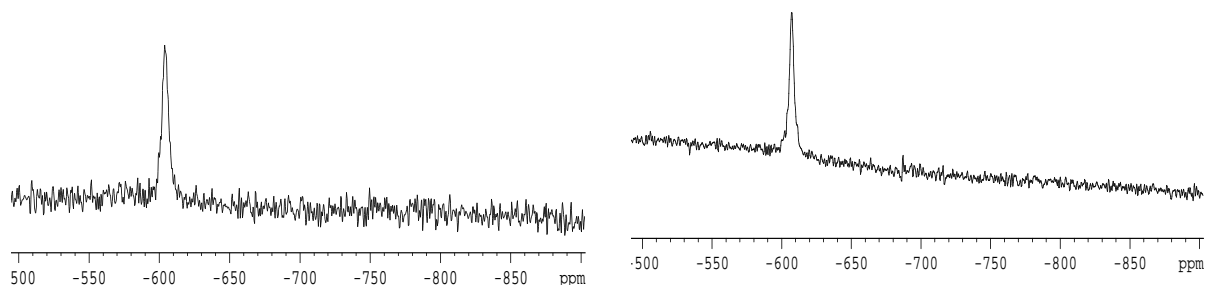
Figure 8. ^{51}V NMR Spectra of the catalyst **1** at the beginning and at the end of the oxidation of methyl *p*-tolyl sulfide **2** with CHP + DMNEO **9.** A NMR tube was charged with a solution of the complex **1** in CDCl$_3$ (0.001 M), CHP (0.1 M) and methyl *p*-tolyl sulfide **2** (0.1 M) and DMENO **9** (0.025 M).

A kinetic study in order to determine the order of the reaction in respect to the substrate and reactants has been carried out. The independent kinetic experiments demonstrated that the reaction proceeds with *first-order* reactivity in sulfide **2**, cumyl hydroperoxide (CHP), catalyst **1**, and Lewis base **6**. A saturation profile was observed using Lewis bases **8** and **9**. No sulfoxide inhibition was observed.
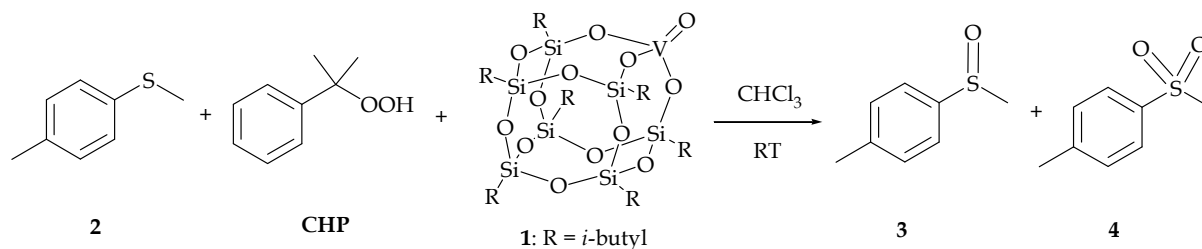
The oxidiation rates of methyl *p*-tolyl sulfide **2** were measured as a function of the initial concentration of catalyst **1** [0.0005 – 0.009 M], methyl *p*-tolyl sulfide **2** [0.04 M – 0.15 M], CHP [0.04 – 0.15 M].

$$\frac{d\,[\mathbf{2}]}{d\,\mathrm{t}} = -K_{\mathrm{obs}}\,[\mathbf{2}][\mathrm{CHP}][\mathbf{1}]$$

$$R_{\mathrm{t=0}} = K_{\mathrm{obs}}\,[\mathbf{2}]_0[\mathrm{CHP}]_0[\mathbf{1}]_0$$

and in the presence of a Lewis Base: **6**, **8** or **9** [0.001 – 0.150 M]
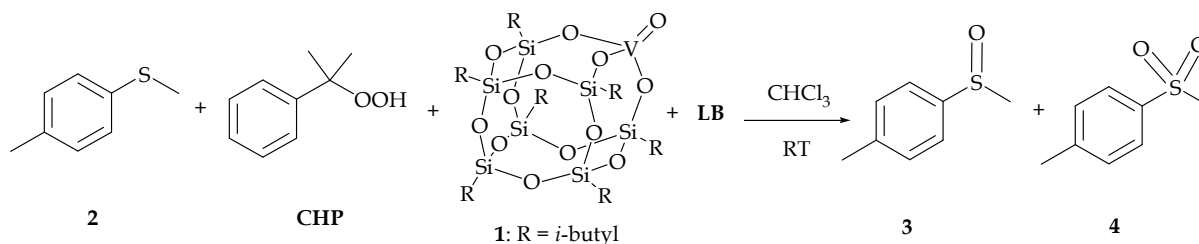
$$\frac{d\,[\mathbf{2}]}{d\,t} = -K_{obs}\,[\mathbf{2}][CHP][\mathbf{1}]\,[LB]$$

$$R_{t=0} = K_{obs}\,[\mathbf{2}]_0[CHP]_0[\mathbf{1}]_0[LB]_0$$

R_0 have been determined by least-square fitting of the experimental data according to the above described models.[25] The calculated initial rate, $R_{t=0}$, was plotted as a function of the varied specie giving a straight line for **1** (Figure 9), **2** (Figure 10) and **CHP** (Figure 11), supporting a pseudo-first order reaction for these species.
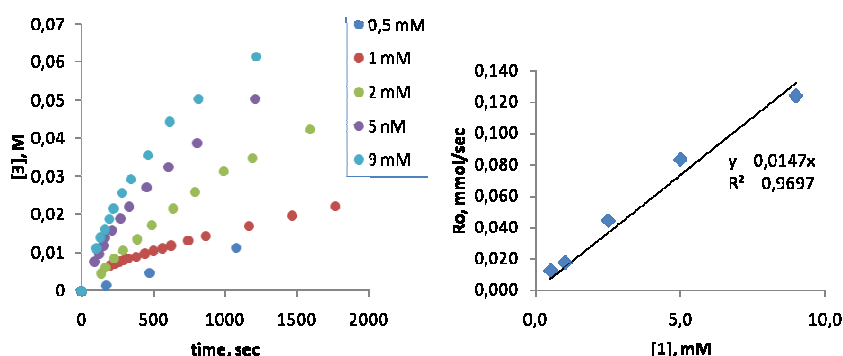
Figure 9. Determination of the kinetic order for VO-POSS **1** [0.0005 – 0.009 M], [**2**]₀=0.1 M, [**CHP**]₀=0.1 M in CDCl₃, 28°C.
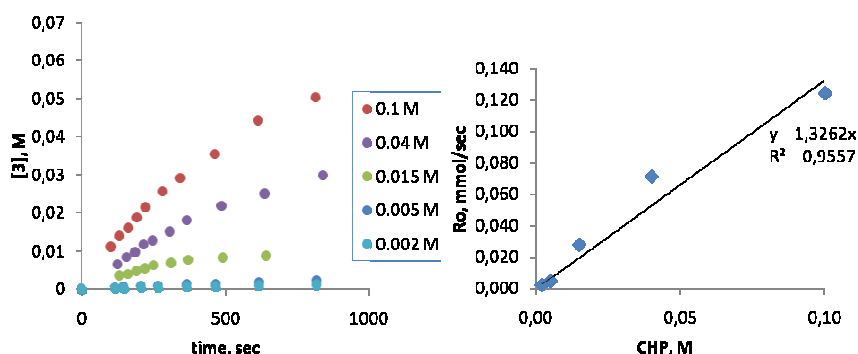
Figure 10. Determination of the kinetic order for **CHP** [0.002 – 0.1 M], VO-POSS [**1**]₀= = 0.009 M [**2**]₀=0.1 M in CDCl₃, 28°C.

[25] Scientist™- MicroMath® Scientific Software, P.O. Box 21550, Salt Lake City, Utah 84121, USA, **1995**
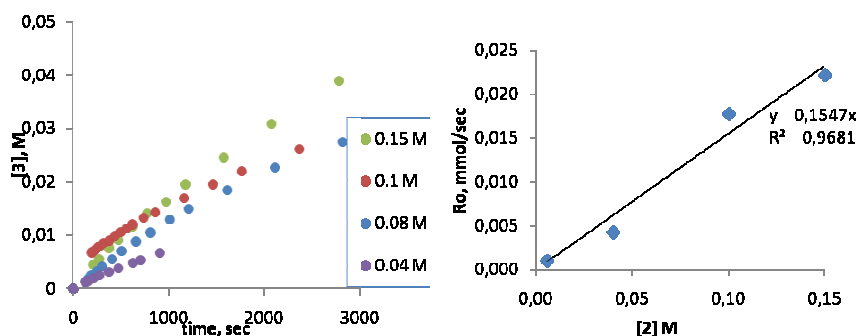
Figure 11. Determination of the kinetic order for methyl *p*-tolyl sulfide **2** [0.04 – 0.15 M] VO-POSS [**1**]$_0$= 0.001 M [**CHP**]$_0$= 0.1 M in CDCl$_3$, 28°C.

Saturation profiles have been obtained for **8** (Figure 12) and **9** (Figure 13) supporting the formation of the new catalytic specie **1•8**, **1•9**.
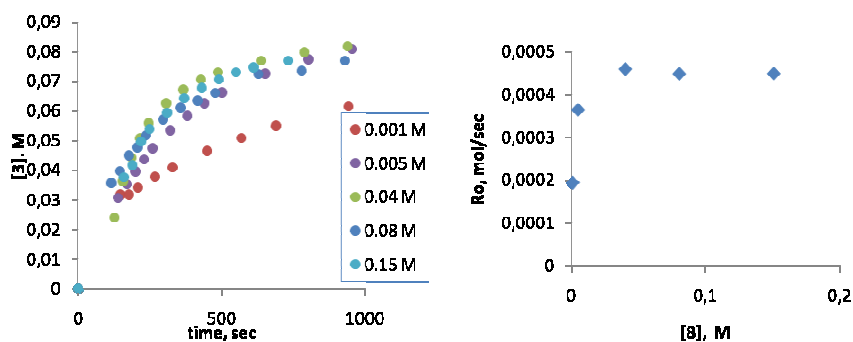
Figure 12. Determination of the kinetic order for *tris*-(*n*-octyl)phosphinoxide **8** [0.001 – 0.150 M] VO-POSS [**1**]$_0$= 0.001 M [CHP]$_0$=[**2**]$_0$= 0.1 M in CDCl$_3$, 28°C.
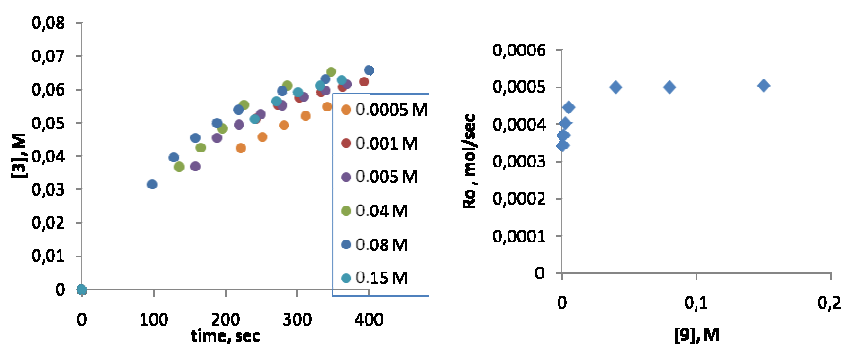
Figure 13. Determination of the kinetic order for dimethyl-*n*-hexyl N-oxide **9** [0.001 – 0.150 M] VO-POSS [**1**]$_0$= 0.001 M, [**CHP**]$_0$=[**2**]$_0$= 0.1 M in CDCl$_3$, 28°C.

With the same range of concentration, no saturation profiles have been obtained for **9** (Figure 14).
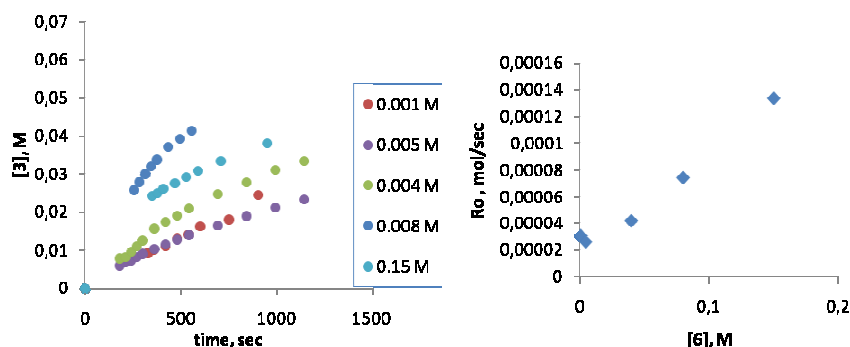
Figure 14. Determination of the kinetic order for HMPA **6** [0.001 – 0.150 M]; VO-POSS [**1**]$_0$= 0.001 M, [**CHP**]$_0$=[**2**]$_0$= 0.1 M in CDCl$_3$, 28°C.

2.4 A rational for the Lewis bases's activation : a computational study

In order to explain the reasons for the LB's activation, we recalled the extensively studied chemistry developed by Denmark in which a similar activation is observed even if the Lewis acid (silicon or selenium) is directly incorporated in the reactant.[26] In Denmark's studies, the presence of a LB is responsible for changing the electronic properties of the incorporated Lewis acid not only by enhancing its reactivity but also by selectively determining the stereochemistry of the reaction. The switch in reactivity is due to an electronic redistribution, which formally results in a more electropositive metal and in an increased electron density in the atoms attached to the silicon (or selenium), what is recalled as Gutmann analysis.[27] In other words, Gutman recognized that the distribution of the electron density in an acid-base adduct is not equal among the constituents atoms (Scheme 5). As reported by Jensen W. B. in "The Lewis Acid-Base Concepts":*"although a donor-acceptor interaction will result in a net transfer of electron density from the donor species to the acceptor species, it will, in the case of polyatomic species, actually lead to a net increase or "pileup" of electron density at the donor atom of the donor species and to a net decrease or "spillover" of electron density at the acceptor atom of the acceptor species. This results from the accompanynig changes in the intramolecular charge distribution induced by the primary donor-acceptor interaction. These disperse the net charge in electron density among all the atoms and in so doing, overcompensate for the initial changes induced at the donor and acceptor atoms. This result is important as it contradicts the usual assumption of the*

[26] a) Denmark, S. E.; Fu, J. *Chem Rev.* **2003**, 103, 2763-2793. b) Denmark, S. E.; Beutner, G. L.; Wynn, T.; Eastgate, M. D. *J. Am. Chem. Soc.* **2005**, 127, 3774-3789. c) Denmark, S. E.; Collins, W. R. *Org. Lett.* **2007**, 9, 3801-3804. d) Denmark, S. E.; Beutner, G. L. *Angew. Chem.* **2008**, 120, 1584-1663; *Angew. Chem. Int. Ed.* **2008**, 47, 1560-1638.

[27] Gaussian 03, Revision D.03, Frisch, M. J.; Trucks, G. W.; Schlegel, H. B.; Scuseria, G. E.; Robb, M. A.; Cheeseman, J. R.; Montgomery, Jr., J. A.; Vreven, T.; Kudin, K. N.; Burant, J. C.; Millam, J. M.; Iyengar, S. S.; Tomasi, J.; Barone, V.; Mennucci, B.; Cossi, M.; Scalmani, G.; Rega, N.; Petersson, G. A.; Nakatsuji, H.; Hada, M.; Ehara, M.; Toyota, K.; Fukuda, R.; Hasegawa, J.; Ishida, M.; Nakajima, T.; Honda, Y.; Kitao, O.; Nakai, H.; Klene, M.; Li, X.; Knox, J. E.; Hratchian, H. P.; Cross, J. B.; Bakken, V.; Adamo, C.; Jaramillo, J.; Gomperts, R.; Stratmann, R. E.; Yazyev, O.; Austin, A. J.; Cammi, R.; Pomelli, C.; Ochterski, J. W.; Ayala, P. Y.; Morokuma, K.; Voth, G. A.; Salvador, P.; Dannenberg, J. J.; Zakrzewski, V. G.; Dapprich, S.; Daniels, A. D.; Strain, M. C.; Farkas, O.; Malick, D. K.; Rabuck, A. D.; Raghavachari, K.; Foresman, J. B.; Ortiz, J. V.; Cui, Q.; Baboul, A. G.; Clifford, S.; Cioslowski, J.; Stefanov, B. B.; Liu, G.; Liashenko, A.; Piskorz, P.; Komaromi, I.; Martin, R. L.; Fox, D. J.; Keith, T.; Al-Laham, M. A.; Peng, C. Y.; Nanayakkara, A.; Challacombe, M.; Gill, P. M. W.; Johnson, B.; Chen, W.; Wong, M. W.; Gonzalez, C.; and Pople, J. A.; Gaussian, Inc., Wallingford CT, 2004.

organic chemist that the net changes in formal charges remain localized on the donor and acceptor atoms".[28]
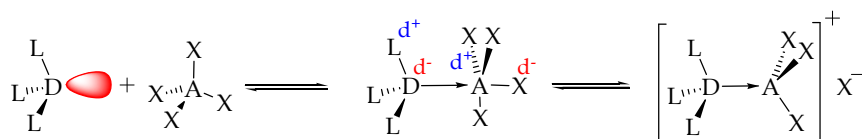
Scheme 5. Electronic redistribution resulting from Lewis acid-base complexation.

In order to explain the origin of the observed different reactivities, the faster reaction rates, and the increased sulfone formation in the presence of Lewis bases, we have to look as in Gutmann analysis at the changes in charge redistribution due to the coligand complexation. We believe that, in our case, the coordination of the coligand to the catalysts stabilizes the η^2 peroxometal intermediate, responsible for the oxygen transfer process, acceleration the reaction. In analogy to what has been shown for other Lewis acids, the coordination of a coligand should increase the electron density at the metal peroxide and decrease the density at the metal, thus stabilizing the η^2 intermediate, exactly the opposite effect.[26] In order to verify our hypothesis, calculations have been carried at the second-order Møller-Plesset perturbation (MP2) level using the TZVP basis set over model systems (Scheme 6).[26]
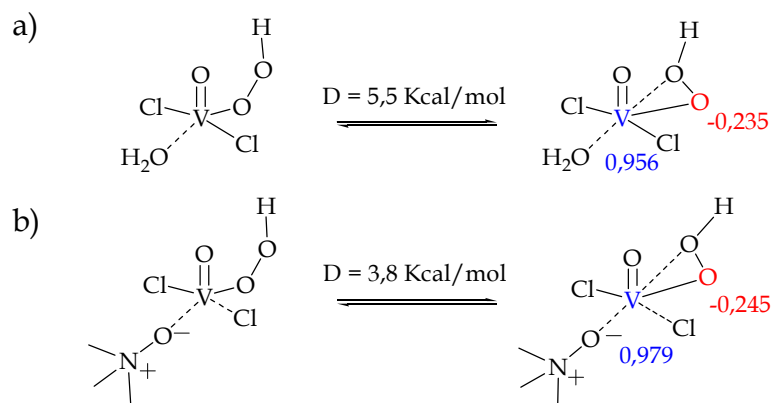
Scheme 6. Calculated energies (MP2/TZVP) for the formation of the η^2 complex in the presence of water (a) and trimethylamine-*N*-oxide (b) as co-ligands. The Mulliken electronic charge of the reactive oxygen (red) and metal (blue) are shown for the η^2 complex.

As shown, shifting from a poor Lewis base donor (water; Scheme 3a) to a stronger one (trimethylamine-*N*-oxide; Scheme 3b) results indeed in a relative stabilization of the η^2 reactive peroxo species. Moreover, the Mulliken charge analysis supports the increase of the electron density of the oxygen involved in the oxygen transfer process when an electron-rich atom is coordinated(-0.235 e *vs* -0.245 e). This also explains the higher nucleophilic character of oxygen, responsible for the increased sulfone/sulfoxide ratio observed with the more active co-ligands.

2.5 Conclusions

In summary, we found that vanadium-POSS **1** is an efficient catalyst in the oxygen transfer reactions to heteroatoms like sulfur and nitrogen using CHP as a primary oxidant.

---

[28] Jensen, W. B. *The Lewis Acid-Base Concepts,* Wiley-Interscience, New York, **1980**, pp. 135-142.

Furthermore, the presence of Lewis bases as coligands can markedly affect the reactivity in oxygen transfer reactions. The reactivity can be finely tuned using the different electronic, steric, and stereochemical characteristics of the coligand. This approach will allow for the use of a large variety of coligands via combinatorial methods for the development of tailor-made catalysts.

2.6 Experimental

General remarks

All chemicals were used as provided without further purifications. Vanadium oxytriisopropoxide , methyl *p*-tolyl sulfide, dibenzylamine, triethylamine (Et₃N), and (*S,R,R*)-(+)-(3,5-dioxa-4-phospha-cyclohepta[2,1-a;3,4-a]dinaphthalen-4-yl)bis(1-phenylethyl) amine were purchased from Aldrich. *N,N*-Dimethylhexylamine-*N*-oxide (DMENO) and cumene hydroperoxide (CHP) 80% solution in cumene were purchased from Fluka, and isobutyltrisilanol-POSSH₃ (isobutyl-POSSH₃; POSS = polyhedral oligomeric silsesquioxane trisilanolate) was purchased from Hybrid Catalysis (Eindhoven, NL).

¹H and ¹³C NMR spectra were recorded at 301 K on Bruker AC-300 and Bruker AC-250 instruments. ⁵¹V NMR spectra were obtained on a Bruker AC-300 instrument with a broadband probe and using VOCl₃ as an external standard. ESI-MS experiments were performed in a LC/MSD Trap-SL and XCT by flow injection analysis using *n*-hexane as a mobile phase. The V(V)-POSS complex was always handled and stored under an inert atmosphere. All of the product data are in agreement with what has been reported in the litterature.

Synthesis of Vanadium(V) Oxyisobutyl-POSS (1).

(*i*-PrO)₃VO (300 *μ*l, 1.29 mmol), dissolved in 1.70 mL of benzene, was added at room temperature to a solution of isobutyltrisilanol-POSSH₃ (1.025 g, 1.29 mmol) in 20 mL of benzene, under vigorous stirring. The mixture was stirred for 1.5 h until reaction completion. Filtration through a fine sintered glass funnel, and solvent removal in vacuo, led to the isolation of 900 mg of VO-isobutyl-POSS (1) as a white amorphous foam. The product characterization is in agreement with literature data.[13]

¹H NMR (300 MHz, CDCl₃): δ 1.93-1.81 (m, 7H, CHMe₂), 0.99 (d, 18H, J = 6.6 Hz, CH₃), 0.95 (d, 24H, J = 6.6 Hz, CH₃), 0.69 (d, 6H, J = 7.0 Hz, CH₂), 0.60 (d, 8H, J = 7.0 Hz, CH₂).

¹³C NMR (62.9 MHz, CDCl₃): δ 26.0 (CH₃), 26.0 (CH₃), 25.9 (CH₃), 24.2 (CH₂), 24.1 (CH₂), 24.1 (CH₂), 23.4 (CH), 23.0 (CH), 22.7 (CH).

⁵¹V NMR (300 MHz, CDCl₃): δ –694.95.

ESI-MS: 855.3 (M + H⁺). Calcd: 855.2. HRMS-ESI: 855.2520 (855.2166 calcd).

Synthesis of vanadium oxytricumyloxide (15)

(*i*-PrO)₃VO (100 μl, 0.423 mmol) was added to a solution of 2-phenyl-2-propanol (0.178 g. 1.269 mmol) in 10 ml of benzene, under vigorous stirring and inert atmosphere. The mixture was stirred for 30 minutes. Solvent removal *in vacuo* led to the isolation of 360 mg of product as a yellow oil.

^{1}H NMR (300 MHz, CDCl$_3$): δ 1.88 (s, 18H, CH$_3$), 7.28 (t, 1H, J = 7,3 Hz), 7.34 (t, 2H, J = 7,3 Hz), 7.53 (d, 2H, J = 7,7 Hz).

^{13}C NMR (62.9 MHz, CDCl$_3$): δ 32.3, 87.0, 124.8, 126.9, 128.3, 148.5. ^{51}V NMR (300 MHz, CDCl$_3$): δ –686.75.

Typical Procedure for Oxidation of Methyl *p*-Tolyl Sulfide (2).

An NMR tube was charged with a solution of complex 1 in CDCl3 (0.6 X 10^{-3} mmol, 0.51 mg), the internal standard (1,2-dichloroethane; DCE), cumyl hydroperoxide (0.06 mmol, 11.4 mg), and methyl p-tolyl sulfide 2 (0.06 mmol, 8.3 mg). The Lewis bases (**3**, **5**, **6**, **7**, **8**, **9**, and **14**) were added to a final volume of 0.6 mL. Concentrations of sulfide **2**, sulfoxide **3**, and sulfone **4** were determined by integration of the methyl group signals: *p*-Tol-S-Me (2.31 ppm),*p*-Tol-SO-Me (2.69), *p*-Tol-SO$_2$-Me (3.02 ppm) with respect to the internal standard, DCE (3.73 ppm). The final yield was determined after complete oxidant consumption (iodometric test) via ^{1}H NMR. Enantiomeric excess was determined by HPLC on a column [REGIS (*R*,*R*)-DACH DNB, isopropanol/hexane 40:60, and a flow rate of 1.0 mL/min].

Typical Procedure for Oxidation of Triethylamine (10).

An NMR tube was charged with a solution of complex **1** in CDCl$_3$ (3.0 x 10^{-3} mmol, 2.6 mg), the internal standard (DCE), CHP (0.3 mmol, 114 mg), and triethylamine **10** (0.3 mmol, 26 mg), and eventually **9** (0.015 mmol, 2.18 mg), with a final volume of 0.6 mL. Concentrations of triethylamine **10** and the corresponding *N*-oxide **11** were determined by integration of the methyl group signals: (*Me*CH$_2$)$_3$N (0.95 ppm) and (*Me*CH$_2$)$_3$NO (1.26 ppm) with respect to the internal standard, DCE (3.73 ppm). The final yield is determined via ^{1}H NMR after complete oxidant consumption (iodometric test). Yield: 99%; in the presence of **9**, 98%.

Typical Procedure for Oxidation of Dibenzylamine (12).

An NMR tube was charged with a solution of complex **1** in CDCl$_3$ (6.0 x 10^{-3} mmol, 5.1 mg), the internal standard (DCE), CHP (0.24 mmol, 45.7 mg), dibenzylamine **12** (0.06 mmol, 1.2 mg), and eventually DMENO **9** (0.03 mmol, 4.3 mg), with a final volume of 0.6 mL. Concentrations of dibenzylamine **12** and the corrisponding nitrone **13** were determined by integration of the methylene signals: (Ph*CH$_2$*)2NH (4.02 ppm) and (Ph*CH$_2$*)N$^+$O$^-$=(CHPh) (5.03 ppm) with respect to the internal standard, DCE (3.73 ppm). The final yield is determined via ^{1}H NMR after complete oxidant consumption (iodometric test). Yield: 66%, in the presence of **9**, 90%.

Typical Procedure for the determination of the kinetic order in catalyst 1.

An NMR tube was charged with a solution of cumyl hydroperoxide (0.06 mmol, 11.4 mg), the internal standard (1,2-dichloroethane; DCE), and methyl *p*-tolyl sulfide **2** (0.06 mmol, 8.3 mg). An appropriate volume of solutions (from 0.0024 M to 0.012M) of catalyst **1** in CDCl$_3$ was added to a final volume of 0.6 mL. Concentrations of sulfide **2**, sulfoxide **3**, and sulfone **4** were determined via ^{1}H NMR as described above.

Typical Procedure for the determination of the kinetic order in sulfide 2.

An NMR tube was charged with a solution of complex 1 in CDCl3 (0.6×10^{-3} mmol, 0.51 mg), the internal standard (1,2-dichloroethane; DCE) and cumyl hydroperoxide (0.06 mmol, 11.4 mg). An appropriate volume of solutions (from 0.8 M to 1.6 M) of methyl *p*-tolyl sulfide **2** in CDCl$_3$ was added to a final volume of 0.6 mL. Concentrations of sulfide **2**, sulfoxide **3**, and sulfone **4** were determined via ^{1}H NMR as described above.

Typical Procedure for the determination of the kinetic order in CHP.

An NMR tube was charged with a solution of complex 1 in CDCl3 (0.6×10^{-3} mmol, 0.51 mg), the internal standard (1,2-dichloroethane; DCE) and methyl p-tolyl sulfide 2 (0.06 mmol, 8.3 mg). An appropriate volume of solutions (from 0.04 M to 0.8 M) of cumyl hydroperoxide in CDCl$_3$ was added to a final volume of 0.6 mL. Concentrations of sulfide **2**, sulfoxide **3**, and sulfone **4** were determined via ^{1}H NMR as described above.

Typical Procedure for the determination of the kinetic order in 6, 8 and 9.

An NMR tube was charged with a solution of complex 1 in CDCl3 (0.6×10^{-3} mmol, 0.51 mg), the internal standard (1,2-dichloroethane; DCE), cumyl hydroperoxide (0.06 mmol, 11.4 mg), and methyl p-tolyl sulfide 2 (0.06 mmol, 8.3 mg). An appropriate volume of solutions (from 0.015 M to 0.08 M) of Lewis bases (**6**, **8**, and **9**) in CDCl$_3$ was added to a final volume of 0.6 mL. Concentrations of sulfide **2**, sulfoxide **3**, and sulfone **4** were determined via ^{1}H NMR as described above.

Computational details.

The molecular structures of the model complexes were optimized at second-order Møller-Plesset (MP2) perturbation levels as implemented in Gaussian 03. The Karlsruhe triple-zeta valence quality basis sets augmented with polarization functions (TZVP) were used as the standard basis set in this study.[27]

Chapter 3

Sulfoxidation as Tool for the Evaluation of the Oxygen Transfer Character of AlkylPeroxo d_0 Metals and the Effect of Co-Ligands on their Reactivity

Catalytic sulfoxidations using cumylhydroperoxide as primary oxidant has been tested in a series of eight aminotriphenolate d_0 metals complexes [Sc(III), Ti(IV), Zr(IV), Hf(IV), V(V), Nb(V), Ta(V), Mo(VI)]. The reactivity and selectivity properties ,both in presence and in absence of a strong Lewis Base (dimethylhexyl-N-oxide) as co-ligand, has been determined experimentally. The experimental values have been correlated with the Sanderson value of electronegativity. MP2/LANL2DZ theoretical calculations on model complexes have furnished more insights on the characteristics of the reactive peroxo specie. The experimentals combined with the theoretical calculations have offered the possibility to propose a general mechanism for the peroxide activation and reactivity.

3.1 Introduction

The possibility to activate peroxides with the help of metal complexes, in order to afford catalytic processes, has an important relevance in biochemical and artificial processes and it expands its potential in industrial applications .[1] The activation of the peroxide by the metal can occur via a radical pathway, in which the metal change his oxidation state along the course of the reaction, or an activation in which the metal activate the peroxide on in virtue of its Lewis Acidic properties. In the latter the metal does not change the oxidation state. While the first method of activation is more common to late transition metals, such as iron or copper, the second pathway is typical of early transition metal in d^0 oxidation state.[1]

Among the possible d^0 metal ions available, some have been used more effectively in oxygen transfer reactions. The more relevant example is the stereoselective allylic alcohol oxidation carried out by Sharpless using d^0 titanium(IV) tartrate complexes[2,3] but also other d^0 metal complexes have been used. As example Vanadium(V) complexes for sulfoxidations,[4] allylic alcohol oxidations,[5] haloperoxidation reactions;[6] and molibdenum(VI) epoxidation reactions since the pioneering work of Mimoun.[7] Other d^0 metals, such as Ta(V), Zr(IV) and Nb(V) have been used in oxidation transfer reactions but less extensively.[8]

Even if the mechanism of oxygen transfer has been, and continues to be, a controversial subject, it is becoming to be widely accepted that the mechanism involves a "Sharpless type"

[1] Backvall, J.-E. Modern Oxidation Methods; Wiley-VCH: New York, 2004. Limberg, C. and Meyer, F. Organometallic Oxidation Catalysis (Topics in Organometallic Chemistry); Springer-Verlag: Berlin, 2007.

[2] T. Katsuki, K. B. Sharpless, *J. Am. Chem. Soc.* **1980**, 102, 5974

[3] For more recent Ti(IV) catalyzed oxidations see: (a) Mba, M.; Prins, L.J.; Licini. G. *Org. Lett.* **2007**, *9*, 21-24. (b) Saito, B. Katsuki, T. *Tetrahedron Lett.* **2001**, *42*, 8333-8336. (c) Matsumoto, K.; Saito, B.; Katsuki, T. *Chem. Commun.* **2007**, 3619-3627. (d) Kondo, S.; Saruhashi, K.; Seki, K.; Matsubara, K.; Miyaji, K.; Kubo, T.; Matsumoto, K.; Katsuki, T. *Angew. Chem. Int. Ed.* **2008**, 10195-10198. (e) Sawada, Y.; Matsumoto, K, Katsuki, T. Angew. Chem. Int. Ed. 2009, 48, 7432-7435.

[4] (a) Santoni, G., Licini, G. and Rehder, D. *Chem. Eur. J.* **2003**, *19*, 4700– 4708. (b) Jeong, Y.-C., Choi, S., Hwang, Y. D. and Ahn, K.-H. *Tetrahedron Lett.* **2004**, *45*, 9249– 9253 (c) Barbarici, A., Maggi, R., Muratori, M., Sartori, G. and Sartorio, R. *Tetrahedron Asymm.* **2004**, *15*, 2467– 2473 (d) Zeng, Q., Wang, H., Wang, T., Cai, Y., Weng, W. and Zhao, Y. *Adv. Synth. Catal.* **2005**, *347*, 1933– 1936 (e) Drago, C., Caggiano, L. and Jackson, R. F. W. *Angew. Chem., Int. Ed.* **2005**, *44*, 7221– 7223 (f) Kelly, P., Lawrence, S. E. and Maguire, A. R. *Eur. J. Org. Chem.* **2006**, 4500– 4509 (g) Mba, M., Pontini, M., Lovat, S., Zonta, C., Bernardinelli, G., Kndig, P. E. and Licini, G. *Inorg. Chem.* **2008**, *47*, 8616– 8618.

[5] Bourhani, Z. and Malkov, A. V. *Chem. Commun.* **2005**, 4592– 4594 (b) Zhang, W., Basak, A., Kosugi, Y., Hoshino, Y. and Yamamoto, H. *Angew. Chem., Int. Ed.* **2005**, *44*, 4389– 4391 (c) Malkov, A. V., Bourhani, Z. and Koovsk, P. *Org. Biomol. Chem.* **2005**, *3*, 3194– 3200(d) Barlan, A. U., Zhang, W. and Yamamoto, H. *Tetrahedron* **2007**, *63*, 6075– 6087 (e) Zhang, W. and Yamamoto, H. *J. Am. Chem. Soc.* **2007**, *129*, 286– 287 (f) Li, Z., Zhang, W. and Yamamoto, H. *Angew. Chem., Int. Ed.* **2008**, *47*, 7520– 7522.

[6] (a) Clague, M. J., Keder, N. L. and Butler, A. *Inorg. Chem.* **1993**, *32*, 4754– 4761 (b) Conte, V., Di Furia, F. and Moro, S. *Tetrahedron Lett.* **1994**, *35*, 7429– 7432 (c) Colpas, G. J., Hamstra, B. J., Kampf, J. W. and Pecoraro, V. L. *J. Am. Chem. Soc.* **1994**, *116*, 3627– 3628 (d) Colpas, G. J., Hamstra, B. J., Kampf, J. W. and Pecoraro, V. L. *J. Am. Chem. Soc.* **1996**, 118, 3469– 3478 (e) Hamstra, B. J., Colpas, G. J. and Pecoraro, V. L. *Inorg. Chem.* **1998**, 37, 949– 955. (f) Podgorsek, A.; Zupan, M.; Iskra, J. *Angew. Chem. Int. Ed.* **2009**, *48*, 8424-8411.

[7] (a) Mimoun, H.; Seree de Roch, I.; Sajus, L. *Bull. Soc. Chem. Fr.***1969**, 1481–1492. (b) Mimoun, H.; Seree de Roch, I.; Sajus, L. *Tetrahedron* **1970**, *26*, 37–50. (c) Burke, A.J *Coord. Chem. Rev.* **2008**, *252*, 170-175. (d) Deubel, D.V.; Frenking, G.; Gisdakis, P.; Herrmann, W.A.; Rosch, N.; Sundermeyer, J. *Acc. Chem. Res.* **2004**, 37. (e) Dickman, M. H.; Pope, M. T. *Chem. Rev.* **1994**, *94*, 569–584

[8] (a) Kirihara, M.; Yamamoto, J.; Noguchi, T.; Itou, A.; Naito, S.; Hirai Y. *Tetrahedron* **2009**, *65*, 10477-10484. (b) Bonchio, M.; Licini, G.; Di Furia, F.; Mantovani, S.; Modena, G.; Nugent W.A. *J. Org. Chem.* **1999**, *64*, 1326–1330. (c) Watanabe, A.; Uchida, T.; Irie, R.; Katsuki, T. *Proc. Natl. Acad, Sci.* **2004**, *16*, 5737-5742. (d) Egami, H.; Katsuki, T. *Angew. Chem. Int. Ed.* **2008**, *47*, 5171-5174.

pathway (Scheme 1).[9] In this mechanism the active specie is an η^2 coordinated alkyl (or hydro) peroxo complex and the nucleophilic attack of the substrate to the electrophilic peroxo oxygen occurs along the antibonding σ^* (O_1-O_2) orbital.
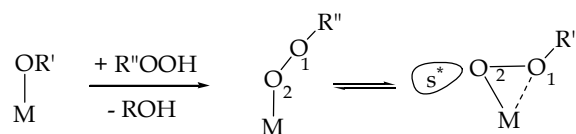
Scheme 1. Sharpless type pathway for the oxidation of nucleophiles.

However, despite the large interest in the subject, few studies are present comparing the electronic character in oxygen transfer reaction of different metal peroxo complexes.[10] Among these studies, it is worth of mention the contribution of the group of Rosch which studied the reactivity of d_0 peroxo complexes towards epoxidation.[11] What emerges from these studies is that the activity of the peroxo complexes is related to three factors: *i*) the strength of the M-O_1 and O_1-O_2 bonds (Scheme 1), *ii*) the charge in the O_2 oxygen atom and *iii*) the interaction between the unoccupied peroxo σ^* orbital and the HOMO of the substrate. Very interestingly, in the study they compared theoretically the behaviour of Cr(VI), Mo(VI) and W(VI) model complexes, it emerged clearly that the ionic radius of the metal ion was directly linked to the electronic charge on the reactive oxygen. The smallest the radius, the lower the charge on the reactive oxygen. However, because oxidation of olefins limits the study to few metals, we decided to start a systematic investigation using sulfoxidation as experimental tools to compare the reactivity among a much larger number of d_0 metal complexes. Sulfoxidation reactions can give us several potential advantages, one is the capability of most of d_0 metals to oxidize sulfides, giving rise to a wider analysis along the periodic table. Moreover, it is also possible to take advantage of the second oxidation step (sulfoxide to to sulfone) which can give more information on the nature of the reactive peroxo complex. The study has been planned preparing eight d_0 aminotri-ortho-*t*-butyl-phenolate metal complexes, namely Sc(III), Ti(IV), Zr(IV), Hf(IV), V(V), Nb(V), Ta(V) and Mo(VI), and testing their activity in sulfoxidation reactions. The aminotri-ortho-*t*-butyl-phenolate has been chosen because it has been shown for some of these complexes to afford a well defined coordination geometry and for the capability, given by the periferical ortho *t*-butyl substituents, to form highly stable monomeric complexes in solution.[3a,12]

In addition to this systematic study on the reactivity of different metal complexes in sulfoxidations, we have decided to combine an analysis on the effect of the reactivity of the presence of an external Lewis Base (dimethylhexyl-*N*-oxide). In fact, in some of our recent studies we have noticed that d_0 metal complexes can expand their coordination sphere

[9] For a discussion on the possible mechanism see: Comas-Vives, A.; Lledòs, Poli, R. *Chem. Eur. J.* **2010**, in press.

[10] (a) Ishiguro, K.; Sawaki, Y. *Bull. Chem. Soc. Jpn.* **2000**, *73*, 535-552. (b) Deubel, D.B.; Frenking, G.; Senn, H.M., Sundermeyer, J. *Chem. Commun.* **2000**, 2469-2470.

[11] Kuhn, F.E.; Santos, A.M.; Roesky, P.W.; Herdtweck, E.; Scherer, W.; Gisdakis, P.; Yudanov, I.V. Di Valentin, C.; Rosch *Chem. Eur. J.* **1999**, *5*, 3603-3615. (b) Di Valentin, C.; Gisdakis, P.; Yudanov, I.V.; Rosch, N. *J. Org. Chem.* **2000**, *65*, 2996-3004.

[12] Licini, G., Mba, M. and Zonta, C. *Dalton Trans.* **2009**, 5265.

coordinating a Lewis base, and the resulting complex displays a sensible difference on the reactivity, stability and selectivity in oxygen transfer reactions.[13] This as a consequence of an electronic rearrangement within the complex. Moreover, recently there has been a revitalised interested in the modification of the reactivities of peroxo complexes of Mn and Fe by external co-ligands.[14] The explanation of these effects can also offers the opportunity to explain the activity of biological complexes.

In this chapter we report a detailed study on the synthesis of eight aminetriphenolate complexes. These complexes have been studied towards the catalytic sulfoxidation of methyl-*p*-tolyl sulfide in presence and absence of a strong Lewis Base, dimethylhexyl-*N*-oxide. The experimental values will give an opportunity: *i)* to demonstrate a common catalytic pathway for all metal complexes, *ii)* to correlated the reactivity/selectivity of the different metals with Sanderson Electronegativity values and *iii)* to give an explanation for the change of catalytic activity generated by the Lewis Base, common for all the metals.

3.2 Synthesis of the complexes

Triphenolamine **1** has been prepared with a synthetic strategy recently developed in our group.[15] This is based on a threefold reductive amination of the corresponding substituted salicyl aldehyde (Scheme 2).
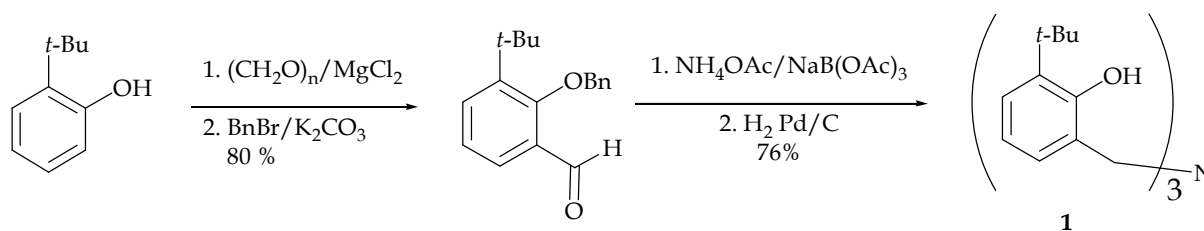
Scheme 2. Synthesis of *t*-butyltriphenolamine **1**.

The complexes were obtained by mixing the ligand **1** with an equimolar amount of an alkoxide precursor in $CDCl_3$ under nitrogen atmosphere, except for the case of molybdenum (VI) (Table 1). In the latter a methodology recently developed by Lehtonen for similar ligands, which uses MoO_2Cl_2 as metal source, was employed.[16] The formation of the complexes was followed by ^1H NMR spectroscopy. Different reaction times were necessary for the complete formation of the complexes. For all of reactions quantitative conversions were obtained as detected by the ^1H NMR of the crude of the reactions.

[13] (a) Bonchio, M., Conte, V., De Conciliis, M. A., Di Furia, F., Ballistreri, F. P., Tomaselli, G. A. and Toscano, R. M. *J. Org. Chem.* **1995**, *60*, 4475– 4480. (b) Bonchio, M., Calloni, S., Di Furia, F., Licini, G., Modena, G., Moro, S. and Nugent, W. A. *J. Am. Chem. Soc.* **1997**, *119*, 6935– 6936. (c) Bonchio, M., Licini, G., Modena, G., Bortolini, O., Moro, S. and Nugent, W. A. *J. Am, Chem. Soc.* **1999**, *121*, 6258– 6268. (d) Redshaw, C., Warford, L., Dale, S. H. and Elsegood, M. R. J. *Chem. Commun.* **2004**, 1954– 1955. (e) Lovat, S.; Mba, M.; Abbenhuis, H.C.L.; Vogt, D.; Zonta, C.; Licini, G. *Inorg. Chem.* **2009**, *48* 4724–4728.
[14] (a) Selke, M.; Valentine, J. S. *J. Am. Chem. Soc.* **1998**, 120, 2652. (b) Annaraj, J.; Cho, J.; Lee, Y.-M.; Kim, S.Y.; Latifi, R.; de Visser, S.P.; Nam, W. *Angew. Chem. Int. Ed.* **2009**, *48*, 4150.
[15] Prins, L.J.; Mba, M.; Kolarovic, A.; Licini, G. *Tetrahedron Lett.* **2006**, *47*, 2735-2738.
[16] Laurén, E.; Kivelä, H.; Hänninen, M.; Lehtonen, A. *Polyhedron* **2009**, *28*, 4051-4055.
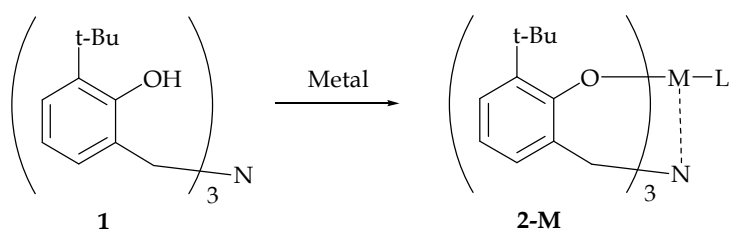
Metal[a]	Metal source	Yield[b]	Time[b]	Geometry[c]	L
Sc(III)	Sc(OiPr)$_3$	Quant.	4 days	Bpt	i-PrOH
Ti(IV)	Ti(OiPr)$_4$	Quant.	5 mins	Bpt	-OiPr
Zr(IV)	Zr(OtBu)$_4$	Quant.	5 mins	Bpt.	-OtBu
Hf(IV)	Hf(OtBu)$_4$	Quant.	5 mins	Bpt.	-OtBu
V(V)	VO(OiPr)$_3$	94%.	5 mins	Bpt.	=O
Nb(V)	Nb(OnEt)$_5$	Quant	5 min	Oct.	(-OnEt)$_2$
Ta(V)	Ta(OnBu)$_5$	Quant	5 mins	Oct	(-OnBu)$_2$
Mo(VI)	MoO$_2$Cl$_2$	73 %	12 hours	Oct	=O, –Cl

[a] Standard reaction conditions: equimolar solutions in CDCl$_3$ of ligand **1** and metal sources were mixed to a marked final volume of concentration 0.012 M operating under inert atmosphere (glove box). [b] Yields and time of formation of the complexes were determined by ^{1}H NMR. [c] Bpt: trigonal bipyramidal Oct: Octahedrical.

Table .1 Synthesis of *t*-butyl-aminotriphenolate complexes.

Coordination geometry of the final complexes were established evaluating the symmetry displayed by benzylic protons in the ^{1}H NMR spectra. In C$_3$ symmetric systems, such as **2-Ti**, the complex is formed as a racemic mixture, this as result of the helical wrapping of the ligand around the metal ion. The chirality of the complexes is reflected on the diastereotopicity of the benzylic methylene protons which translates in two doublets at 3.94 and 2.89 ppm. Couple of doublets are observed also for **2-V** (3,77 ppm bs and 2.90 ppm bs) indicating the formation of C$_3$ symmetric systems and thus a trigonal bipyrimidal coordination geometry (Figure 1). When the racemisation is faster than the NMR timescale the benzylic protons average and they result in a broad singlet. This is the case of **2-Sc** (3,48 ppm bs) **2-Zr** (3,48 ppm bs), **2-Hf** (3,51 ppm, bs). In the case of octahedrical arrangement, as in the case of **2-Mo**, a racemic mixture is also present. However, in this case the racemisation is always faster than the NMR scale and an average C$_S$ symmetry is observed. As result of the symmetry, 3 set of signals for the non equivalent methylene groups are observed, two doublets and a singlet. In the case of **2-Nb** and **2-Ta** broad singlets are observed. In this case the octahedral geometry is confirmed by the presence of two different alkoxide ligands coordinated to the metal (one apical and one equatorial). Moreover, in all the ^{1}H NMR

spectra is possible to notice the presence of the free alkoxide, with the correct stoichiometric ratio, and if present and ^{1}H NMR active, the coordinated ligands.
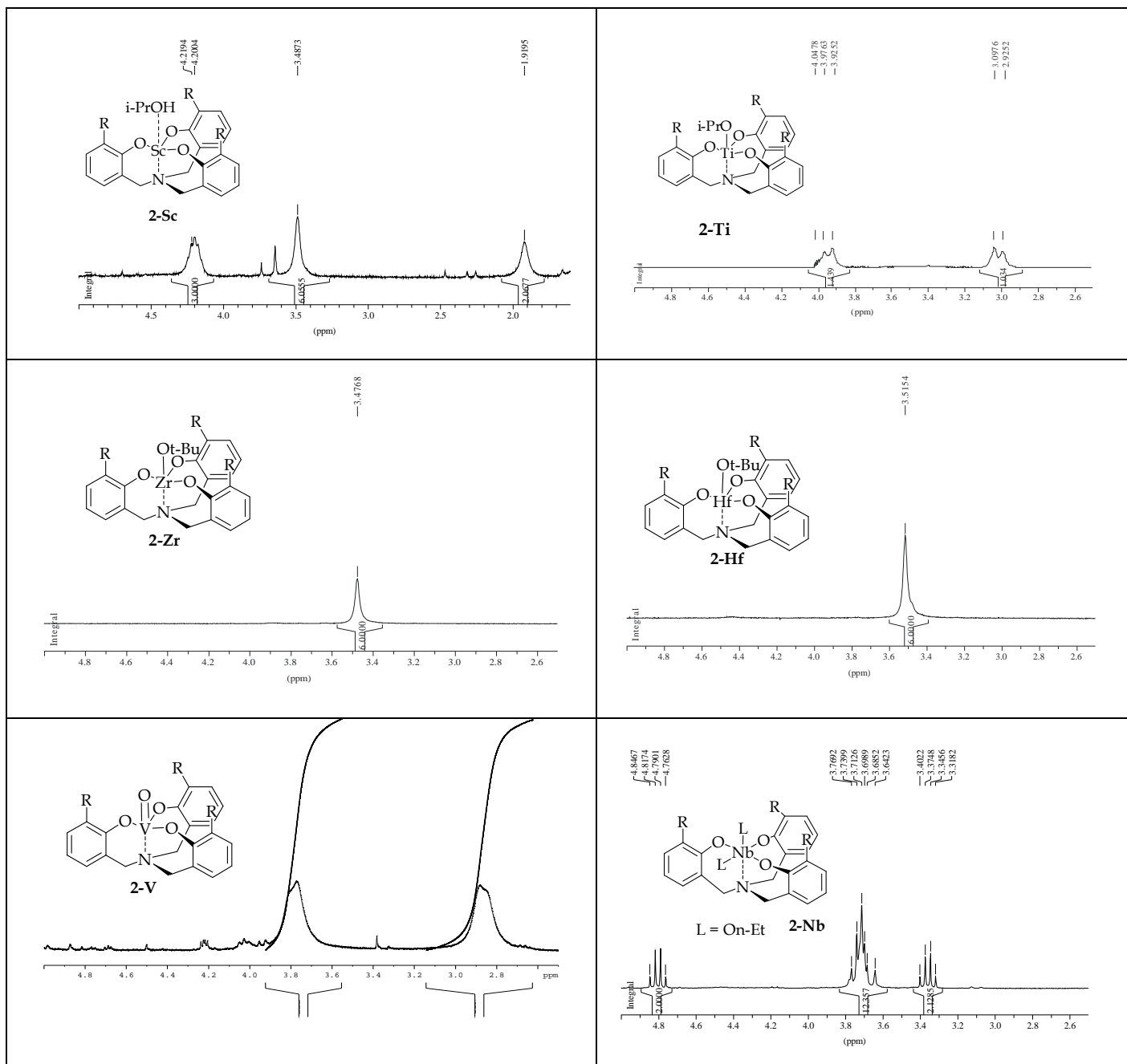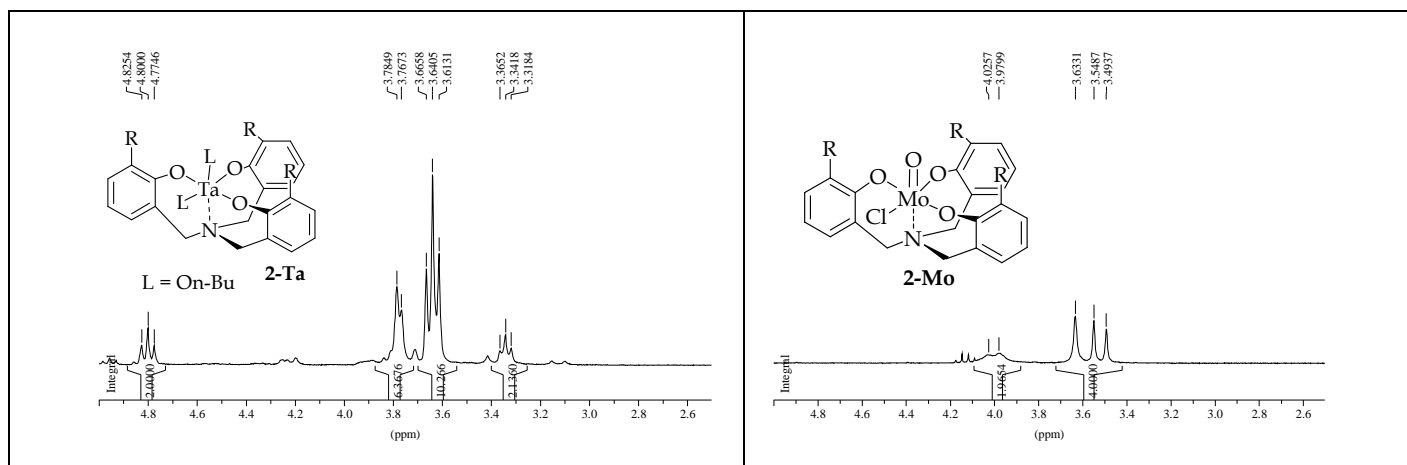
Figure 1. ^{1}H NMR spectra in CDCl$_3$ of the complexes 2 in the spectra region from 2.5 ppm to 5 ppm.

3.3 TPA Complexes Catalytic Activity

Previous studies on the catalytic activity toward sulfoxidation of **2-Ti** and **2-V** complexes have shown that these two catalysts are extremely active in activation of alkyl peroxides or hydrogen peroxide.[12] Moreover, they are also able to transfer quantitatively oxygen atoms also at very low catalyst loading. This particular feature is given by the high stability conferred by the polydentate ligand to the catalysts and by its capability to inhibit the formation of multinuclear specie. For these reasons we have decided to test the catalytic activity for sulfoxidation of methyl-*p*-tolyl sulfide **3** under the same conditions for all the complexes. Cumyl hydroperoxide (CHP) has been chosen as oxidant because this choice guarantees the formation of mono alkyl peroxo species. Reactions were carried out to a [substrate]$_0$ = [CHP]$_0$ = 0.1 M, and 1% of catalyst. Every catalytic tests was performed in presence and in absence of a strong Lewis Base, namely the dimethylhexyl-*N*-oxide **6**, at a concentration 0.005 M (5%), which correspond to five times the concentration of the catalyst. This concentration has found to saturatively coordinate vanadium complexes as shown in the prvious chapter. The results of all the catalytic tests are reported in Table 2. Initial rates for the first and second oxidation step were also calculated for all of the reaction (Table 2).

This particular feature is given by the high stability conferred by the polydentate ligand to the catalysts and by its capability to inhibit the formation of multinuclear specie. For these reasons we have decided to test the catalytic activity for sulfoxidation of methyl-*p*-tolyl sulfide **3** under the same conditions for all the complexes. Cumyl hydroperoxide (CHP) has been chosen as oxidant because this choice guarantees the formation of mono alkyl peroxo species. Reactions were carried out to a [substrate]$_0$ = [CHP]$_0$ = 0.1 M, and 1% of catalyst. Every catalytic tests was performed in presence and in absence of a strong Lewis Base, namely the dimethylhexyl-*N*-oxide **6**, at a concentration 0.005 M (5%), which correspond to five times the concentration of the catalyst. This concentration has found to saturatively coordinate vanadium complexes as shown in the prvious chapter. The results of all the catalytic tests are reported in Table 2. Initial rates for the first and second oxidation step were also calculated for all of the reaction (Table 2).

Table 2. Oxidation of methyl *p*-tolyl sulfide **3** with CHP

Complex[a]	Yield[b] (%)	Time (h)	4:5[b]	k_1[c] (mol^{-3} h^{-1})	k_2[c] (mol^{-3} h^{-1})	k_1/k_2
2-Sc	91	500	21:79	80	470	0,17
2-Sc + 6	80	5000	82:17	30	22	1,36
2-Ti	99	40	80:20	1583	380	4,17
2-Ti + 6	97	72	78:22	865	315	2,75
2-Zr	99	10	26:74	5188	25821	0,20
2-Zr +6	93	100	42:58	690	322	2,14
2-Hf	99	3	30:70	8030	31200	0,26
2-Hf +6	99	700	40:60	290	171	1,70
2-V	99	35	96:4	820	1	820
2-V + 6	99	1	90:10	46189	4450	10
2-Nb	99	550	92:8	442	49	9
2-Nb + 6	90	980	97:3	85	8	11
2-Ta	99	300	74:25	404	132	3
2-Ta + 6	88	2400	90:10	38	5	8
2-Mo	99	360	98:2	40	1	40
2-Mo + 6	99	300	90:10	147	7	21

[a] Standard reaction conditions: reactions were carried out in CHCl$_3$ at 28°C using [**3**]$_0$=[CHP]=0.1 M and 1% mol of complex **2** and 5% of **6** [b]Yields and **4/5** ratios were determined by ^{1}H NMR in the presence of DCE as internal standard in the crude reaction mixture after total oxidant consumption (iodometric test). [c] Kinetic constants have been calculated by non-linear fitting of the first 20% of the kinetic experiment.

The experimental data clearly highlight that all of the complexes own the capability to transfer oxygen from CHP to sulfide **3**. Moreover for most of the complexes the transfer is quantitative, and, in the worst case of **2-Sc+6** 80% yield was obtained. The lowest yields are associated to complexes that, in this experimental conditions, required long experimental time for completion of the reaction. This could be explained with a certain degree of possible

degradation of the catalyst under the reaction conditions. For the reaction in which the Lewis Base **6** is added it is confirmed that in the case of vanadium(V) the presence of Lewis Base results in an increased reactivity and also in a change of selectivity, as it was described in the previous chapter. Observation that can be translated, even in a in minor amount, only to the Mo(VI) complex. For all of the other metals, a reduction in the reactivity of the complexes was observed.

From the experimental data has been possible to extrapolate kinetic constants for the first oxidation process from the sulfide to the sulfoxide (k_1), and for the second oxidation process from sulfoxide to sulphone (k_2, Table2). This has been calculated by non-linear fitting of a second-order equation to the first 20% of the reaction. This choice has been made in order to: have a minimal effect of the degradation of the complex on the measured kinetic parameter, and to avoid the effect which can have the coordination of formed sulfoxide to the reactivity of the metal complex. Beside the observation on the high selectivity toward sulfoxide displayed by **2-V** and **2- Mo**, kinetic values are not straightforward to interpret. Moreover it is not clear why **2-V** and **2- Mo** complexes display acceleration, while the other shows only a reduction on the reactivity. The only straightforward interpretation is that more acidic metals complexes, such as **2-V** and **2-Mo** (Figure 2 and 3), have the tendency to form exclusively the sulfoxide **4**, while the less acid metals, such **2-Zr** (Figure 4), tend to favour the second oxidation process. In order to find out a correlation of the intrinsic properties of the different metal complexes with their reactivity we choose to compare the different kinetic values for the complexes using the Sanderson Electronegativity values.
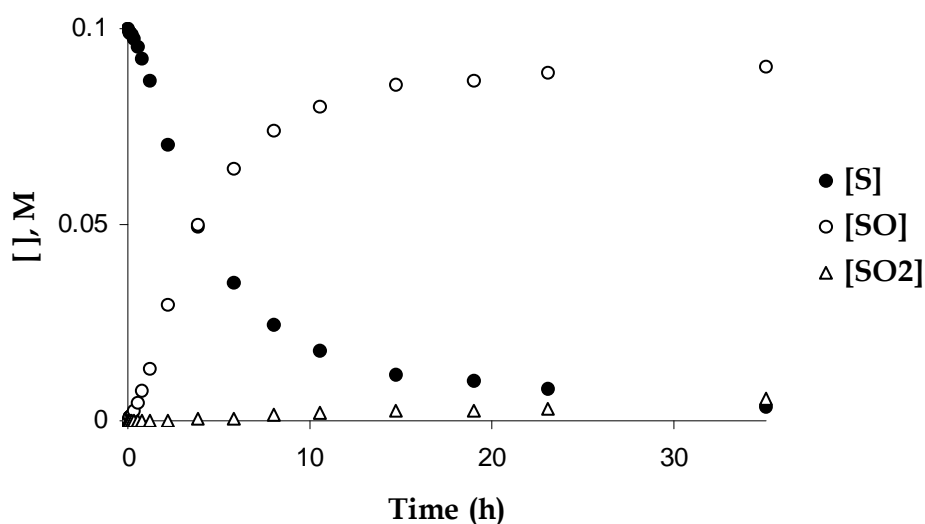
Figure 2. Oxidation of methyl *p*-tolyl sulfide **3** to methyl *p*-tolyl sulfoxide **4** and methyl *p*-tolyl sulfone **5** with CHP catalyzed by complex **2-V**. Reaction conditions: [**3**]$_0$=[CHP]$_0$= 0.1 M, [**2-V**]=1%, 28°C, CDCl$_3$. Concentrations were determined by ^{1}H NMR (DCE as internal standard) on the crude reaction mixture after total oxidant consumption (iodometric test).
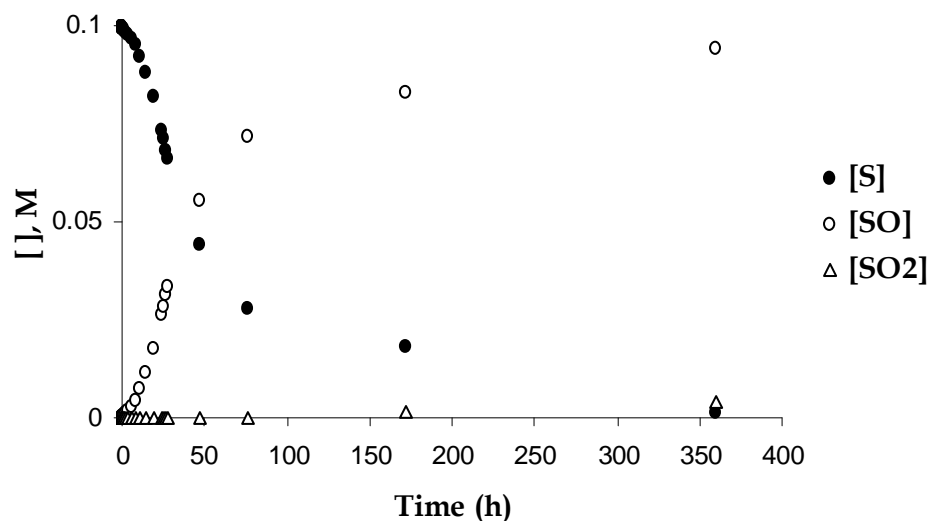
Figure 3. Oxidation of methyl *p*-tolyl sulfide **3** to methyl *p*-tolyl sulfoxide **4** and methyl *p*-tolyl sulfone **5** with CHP catalyzed by complex **2-Mo**. Reaction conditions: $[3]_0 = [CHP]_0 = 0.1$ M, **[2-Mo]**=1%, 28°C, CDCl$_3$. Concentrations were determined by ^{1}H NMR (DCE as internal standard) on the crude reaction mixture after total oxidant consumption (iodometric test).
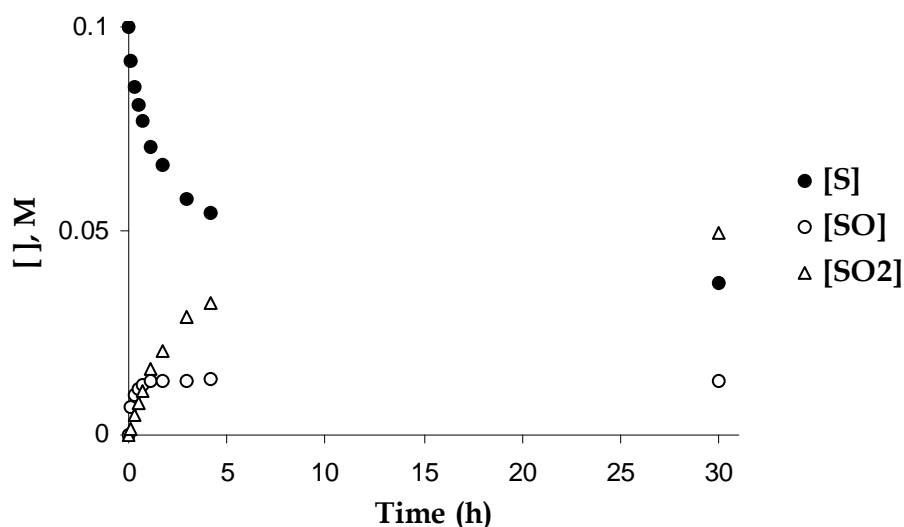
Figure 4. Oxidation of methyl *p*-tolyl sulfide **3** to methyl *p*-tolyl sulfoxide **4** and methyl *p*-tolyl sulfone **5** with CHP catalyzed by complex **2-Zr**. Reaction conditions: $[3]_0 = [CHP]_0 = 0.1$ M, **[2-Zr]**=1%, 28°C, CDCl$_3$. Concentrations were determined by ^{1}H NMR (DCE as internal standard) on the crude reaction mixture after total oxidant consumption (iodometric test).

3.4 Reactivity comparison: Sanderson Electronegativity Values

Sanderson electronegativity (SE) values allows to have a parameter indicating the characteristic of the metals.[17] These values are based on the principle that the ability of an

---

[17] (a) Sanderson, R. T. *Science* **1951**, *114*, 670-672. (b) T. Sanderson, Chemical Bonds and Bond Energy, Academic Press, New York, 1976. (c) Sanderson, R. T. *J. Am. Chem. Soc.* **1983**, *105*, 2259-2261. (d) Sanderson, R.T. *Inorg. Chem.* **1986**, *25*, 3518-3522. (e) Jeong, N.C.; Lee, J.S.; Tae, E.L.; Lee, Y.J.; Yoon, K.B. *Angew. Chem. Int. Ed.* **2008**, *47*, 10128-10132.

atom or ion to attract electrons to itself is dependent upon the effective nuclear charge felt by the outermost electrons. In first approximation they are in straight correlation among the ratio between the formal oxidation state over the ionic radius.

However, it is not possible to correlate directly the reactivity and selectivity of the different metal complexes with this electronegativity parameter. Too many factors are contributing to the observed catalytic properties of a complex. In each complex the observed reactivity depends by several parameters which can be summarised, in first approximation, to: the characteristic of the metal peroxo complex, the geometry adopted by the complex, the energy requested for coordination of the alkyl peroxide and the steric factors governing the approach of the reacting molecules to the formed alkyl-peroxo complex. In order to highlight only the metal peroxo complex features, thus removing the other factors, we compare the relative rates of the metal complex within the same ligand. In other words, we are comparing the relative reactivities and in particular:

- the ratio between the rate constants of the first and second oxidation obtained using the catalyst **2-M** ($k_{1(2\text{-M})}/ k_{2(2\text{-M})}$),
- the ratio between the rate constants of the first and second oxidation of the complex **2-M** in the presence of Lewis Base **6** (5 equiv) ($k_{1(2\text{-M+6})}/ k_{2(2\text{-M+6})}$),
- the ratio between the first oxidation rate constants of the complex **2-M** without and with the Lewis Base **6** ($k_{1(2\text{-M})}/ k_{1(2\text{-M+6})}$),
- the ratio between the second oxidation rate constants of the complex **2-M** without and with the Lewis Base **6** ($k_{2(2\text{-M})}/ k_{2(2\text{-M+6})}$).

These values are reported in Table 3 and the correlations with Sanderson's Electronegativity value is in Figure 5.

2-M	Sanderson's EN	$k_{1(2\text{-M})}/k_{2(2\text{-M})}$	$k_{1(2\text{-M+6})}/k_{2(2\text{-M+6})}$	$k_{1(2\text{-M})}/k_{1(2\text{-M+6})}$	$k_{2(2\text{-M})}/k_{2(2\text{-M+6})}$
2-Sc	1,02	0,2	1,4	2,7	21
2-Ti	1,50	4,2	2,7	1,8	1,2
2-Zr	0,90	0,2	2,1	7,5	80
2-Hf	0,96	0,3	1.7	28	182
2-V	2,5	820	10	0,02	10^{-4}
2-Nb	1,4	9,0	11	5,2	6,1
2-Ta	1,2	3,1	8	11	26
2-Mo	2,2	40	21	0,3	0,1

Table 3. Electronegativity values for the elements and relative ratios for the rate constants (see values reported in Table 2).

What it clearly emerges examining the data reported in Figure 5 is that there is indeed a good correlation in all the four graphs between SE values and the relative reaction rates. In Figure 5a is possible to note a straight correlation among the ratio of the first and second

oxidation with the SE value. This support the fact that the most acidic metals have the tendency to favour the first oxidation in favour of the second, while with the less acid ones the second oxidation is favoured. This is a consequence of the tendency of metals such as vanadium(V) and molybdenum(VI) to forms bond with the reactive oxygen with small charge separation among the two atoms. The bonds, due to the smaller difference in electronegativity, have larger covalent character and the resulting oxygen atom is less electron-rich. On the other hand, less electronegative atoms, such as zirconium, bonds to reactive oxygen with a more defined ionic character. This makes the reactive oxygen more electron-rich and thus more available to the oxidation of the sulfoxide **4**. The introduction of the Lewis Base **6** in the reaction mixture results in a marked variation in the reactivity (Figure 5, graph b).
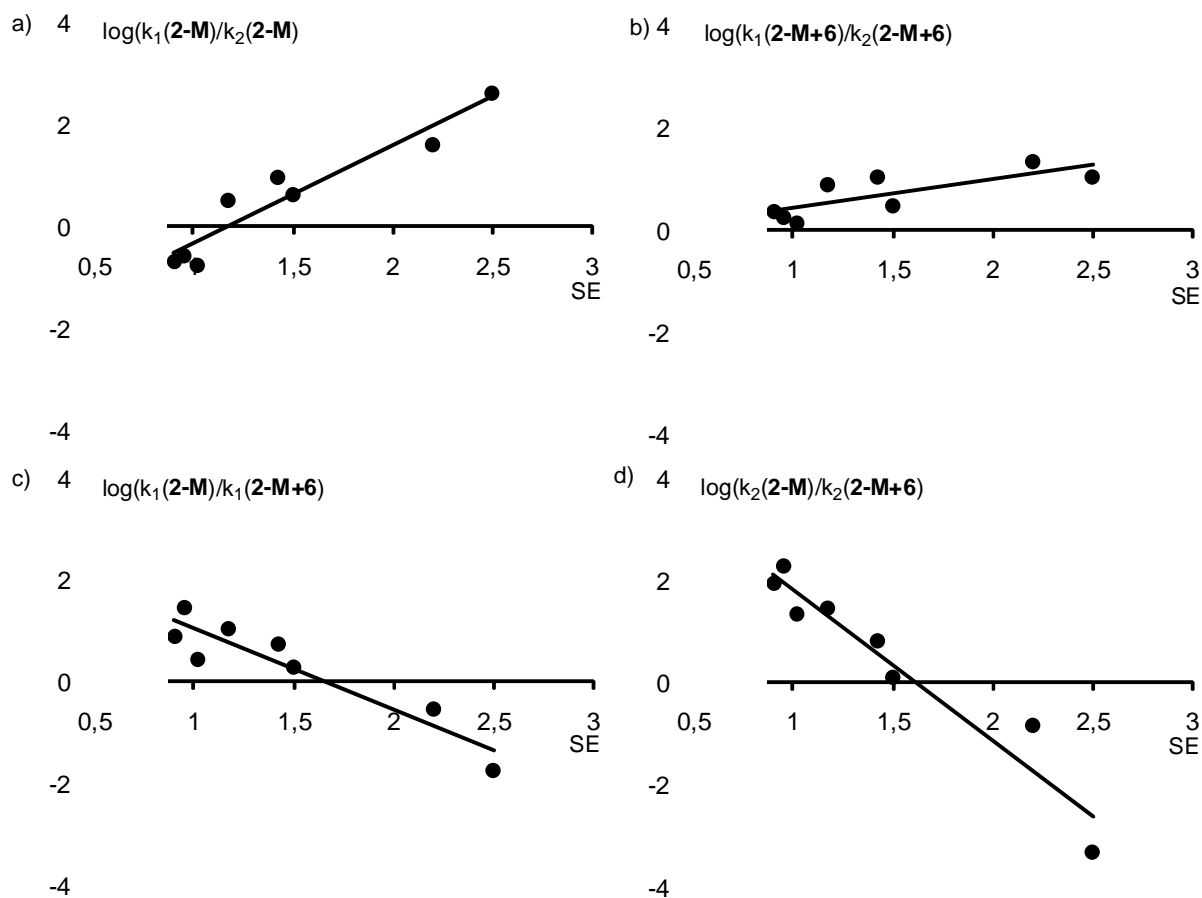
- **Figure 5.** Plot of the relative reactivities *vs* the Metal Sanderson Electronegativity values. a) ratio between the rate constants of the first and second oxidation obtained using the catalyst **2-M** ($k_{1(2\text{-}M)}$/ $k_{2(2\text{-}M)}$). b) ratio between the rate constants of the first and second oxidation of the complex **2-M** in the presence of Lewis Base **6** (5 equiv) ($k_{1(2\text{-}M+6)}$/ $k_{2(2\text{-}M+6)}$). c) ratio between the first oxidation rate constants of the complex **2-M** without and with the Lewis Base **6** ($k_{1(2\text{-}M)}$/ $k_{1(2\text{-}M+6)}$). d) ratio between the second oxidation rate constants of the complex **2-M** without and with the Lewis Base **6** ($k_{2(2\text{-}M)}$/ $k_{2(2\text{-}M+6)}$).

Even if a correlation is still present, the differences of the complexes for the first or the second oxygen transfer is less pronounced. The reactivity trend is similar to the one shown in Graph a but the metals display a less marked difference among them. In fact, while in absence of Lewis Base the k_1 over k_2 range was varying from 0,2 to 820, the addition of the Lewis Base reduce this range from 1,4 to 21. Acidic metals decrease their preference toward

the first oxidation step, and in a reverse mode, less acid metal ions have the tendency to decrease their preference toward the second oxidation step.

Interesting correlation are also observed when we compare the rate of the first and second oxidation constant (k_1 and k_2) in presence or absence of the Lewis Base (Figure 5, graphs c and d). In this case, while for more electronegative metals the introduction of a Lewis base results in a marked increased in reactivity for the first oxidation step, for the less electronegative metals there is a reduction in the reactivity. Similar considerations, with a more marked correlation, can be drawn for the analysis of the second oxidation with and without the Lewis Base (Figure 5d).

3.5 MP2 Calculations

The observed reactivity obtained with the different metal complexes, and the variations obtained in presence of the Lewis Base **6,** need further explanations. While the general reactivity of the complex can be explained in terms of the polarization of the metal-peroxo bond, more difficult is to understand the variations on the reactivity observed in presence of Lewis Base. In order to explain the reasons for the Lewis Base activation/deactivation process we recall our study on the VO-POSS chemistry described in the previous chapter.[13e] In this study an important acceleration in the reaction rates was observed in the oxidations catalysed by the VO-POSS complex when a Lewis Base was present in the system. The explanation, which recalled the Denmark studies in Lewis Base Catalysis, was attributed to a switch in reactivity due to an electronic redistribution which formally results in a more electropositive metal and in an increased electron density in the oxygen atoms. In the previous case, the Lewis Base acceleration of the reaction was explained by the stabilization of the η_2 peroxometal intermediate responsible for the oxygen transfer process. Also in this case calculations have been carried at the second-order Møller-Plesset perturbation (MP2) method using the DGDZVP basis set over V(V) and Zr(IV) model systems. These two metals represent the extreme possible scenarios both as far as the electronegativity scale, the activation/deactivation scale and also the chemoselectivity are concerned (Scheme 3).
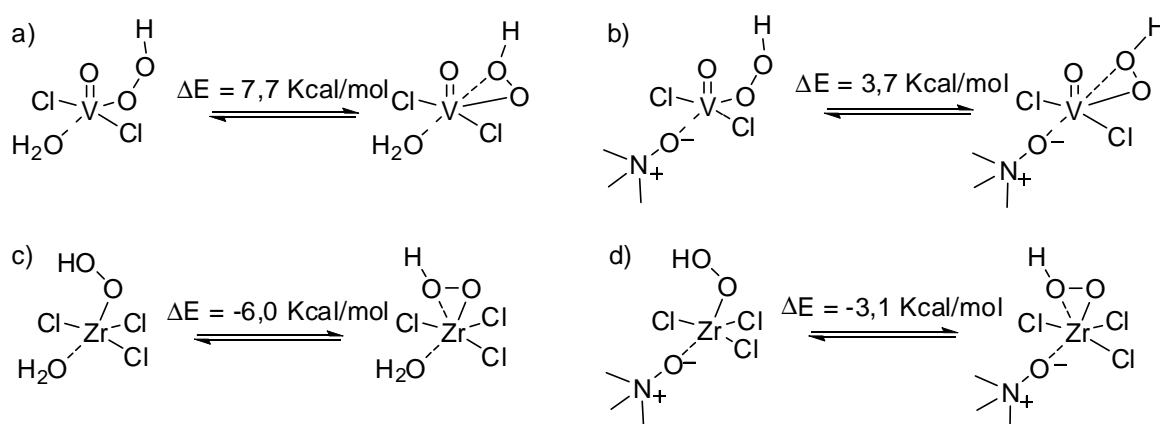
Scheme 3. Calculated energies (MP2/DGDZVP) for the formation the equilibra among the end-on and the η_2 peroxo complex in the presence of water (a,c) and trimethylamine-*N*-oxide (b,d) as coligands for model V(V) (a,b) and Zr(IV) (c,d) complexes.

In analogy with what we found in the previous studies on VO-POSS system, for the V(V) model complex, shifting from a poor donor (water) (Scheme 3, a), to a stronger donor (trimethylamine-*N*-oxide) (Scheme 3, b) results in a relative stabilization of the η_2 reactive peroxo specie. Thus in the experimental system, the higher concentration of η_2 peroxo when the Lewis Base is coordinated translates into an increased reactivity. In an opposite way, for the Zr(IV) catalyst, the shift from a poor to a strong Lewis Base donor, results in a destabilisation of the η_2 coordinated peroxo. This fact decreases the amount of active complex in solution and consequently its reactivity. The analysis of the relative stability of the peroxo complexes gives an explanation the experimentally observed variation of the reactivity. A different analysis has to be performed for the explanation of the different chemoselectivity observed for the two complexes, with the two different Lewis bases.

In order to get more information on the chemoselectivity towards the relative amount of sulfoxide **4** or sulfone **5** obtained, Mulliken charge analysis was performed on the peroxo complexes reported on Figure 6. The charge analysis on the metal center and peroxo oxygen atoms is consistent with the relative values of elctronegativity of the metals and the ionic *vs* covalent bond character of the peroxo complexes. Indeed, in the case of V(V), the more electronegative metal, the charge separation in the V-O bond is small ($qV-qO_1 = 1.7$ e). Instead, in the case of Zr(IV) a more marked polarization, as we recalled as ionic character, of the bond is observed ($qV-qO_1 = 2.3$ e). As a consequence of this phenomenon, the resulting reactive oxygen is more electron-rich in the Zr(IV) than in the V(V) complex. This fact, in first approximation, explains the preference of V(V) complexes in the oxidation of electron-rich sulfides, while **2-Zr** has a strong preference towards the oxidation of the less electron-rich sulfoxide. At the same time, the more ionic Zr-O bond allows for an easier formation to the η_2 coordinated peroxo group.
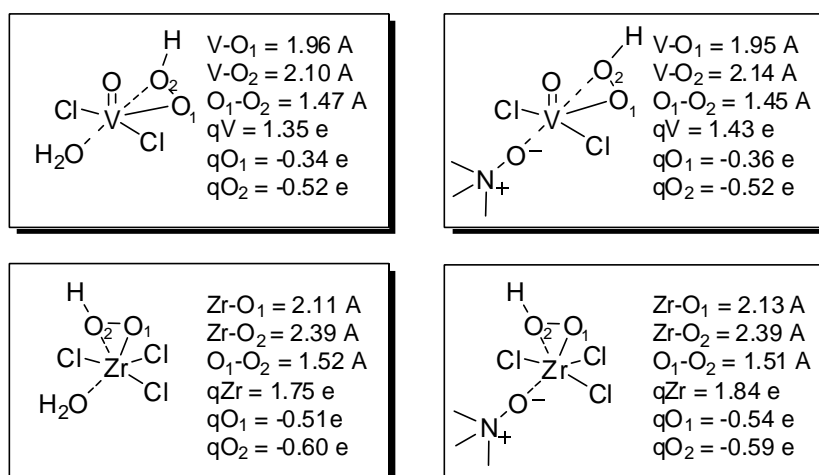
Figure 6 . Calculated geometrical parameters and Mulliken electronic charges (MP2/DGDZVP) for the model complexes in the presence of water and trimethylamine-*N*-oxide as co-ligands.

The introduction of a stronger Lewis Base induces a similar electron reorganisation in both the model complexes. The Lewis Base induces a stronger polarisation for the metal-peroxo bond and therefore the metal centre becomes more positive and the oxygen atom more negative. However, the extra-ionic character for the V(V) gives an extra stabilisation of the η_2

peroxo group, while in the Zr(IV) system the same phenomenon results in a destabilisation of the η_2 peroxo group.
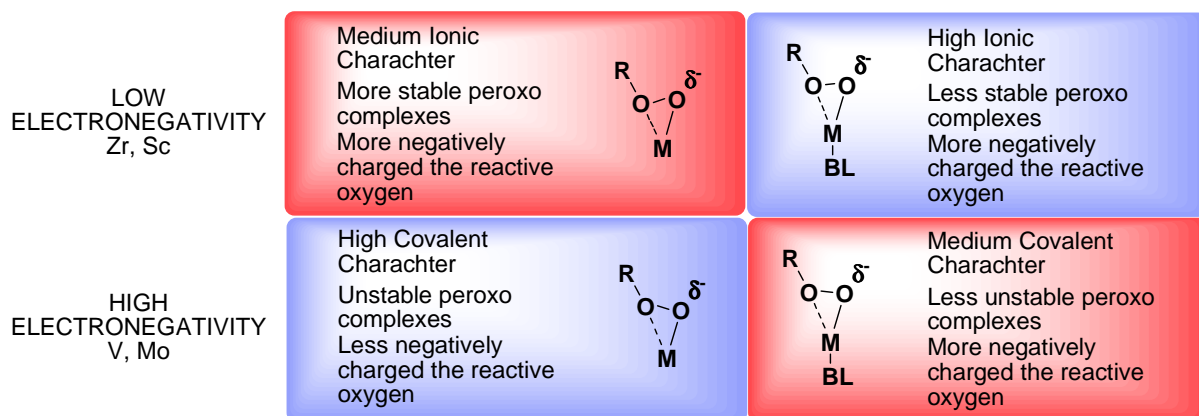
Figure 7. Common charchteristics of the peroxo complexes studied by theoretical calculations

The increased preference for the sulfoxide oxidation of the V(V)-Lewis Base complex is explainable in term of charge rearrangement. The reactive oxygen atom in the V(V)-LB complex is more electron-rich and this makes it more prone to react with the sulfoxide. Less straightforward seems the explanation of the Zr(IV) catalyst reactivity at the present time. More detailed calculations on the geometry and energies of the transition states of these model systems will be necessary in order to get more information of the observed switch in chemoselectivity.

3.6 Conclusions

Eight aminotriphenolate d_0 metals complexes [Sc(III), Ti(IV), Zr(IV), Hf(IV), V(V), Nb(V), Ta(V), Mo(VI)] has been synthesised and tested in methyl *p*-tolyl sulfide oxidation with cumyl hydroperoxide both in presence and in absence of a strong Lewis base (dimethylhexyl-*N*-oxide). Their kinetic parameters in term of reactivity and chemoselectivity have been determined. These values have been found to correlate with the Sanderson values of electronegativity, allowing to get important highlights into the observed reactivity of these complexes and the characteristic the reactive peroxo species. More information have been obtained with the aid of MP2/DGGZVP theoretical calculations on model complexes, allowing the correlation between the reactivity and chemoselectivity observed with the properties of the metal peroxo bonds. This study offer to present an unifying study on the reactivity of the metal peroxo complexes. Moreover, it offers the opportunity to have a general descriptor for the reactivity of the peroxo metal complexes of d^0 metals.

3.7 Experimental

General remarks

All chemicals and dry solvent have been purchased from Aldrich, Fluka and Strem and used as provided, without further purifications. Triphenolamines were synthesized as previously reported.[15]

Flash chromatographies have been performed with Macherey-Nagel silica gel 60 (0.04-0.063 mm, 230-400 mesh). The NMR spectra have been recorded on a Bruker AC 250 (^{1}H: 250.13 MHz; ^{13}C: 62.9 MHz) or a Bruker AV 300 (^{1}H: 300.13 MHz; ^{13}C: 75.5 MHz) spectrometer. Chemical shift (δ) have been reported in parts per million (ppm) relative to the residual undeuterated solvent as an internal reference (CDCl$_3$: 7.26 ppm for ^{1}H NMR and 77.0 ppm for ^{13}C NMR; CD$_3$OD: 4.84 ppm for ^{1}H NMR and 49.05 ppm for ^{13}C NMR). The following abbreviations have been used to explain the multiplicities: s = singlet, d = doublet, t =triplet, dd = double doublet, m = multiplet, br = broad. APCI-MS spectra have been obtained on a LC/MS Agilent series 1100 spectrometer in positive mode, by direct flow injection using methanol as mobile phase, with ESI-ion trap mass detector. High-resolution mass spectra have been obtained with ESI-TOF Mariner™ Biospectrometry™ Workstation of Applied Biosystem by flow injection analysis; exact mass measurements have been obtained by external calibration with two appropriate lock mass compounds. All moisture sensitive compounds have been handled under controlled atmosphere (nitrogen) in a glovebox Mbraun MB 200MOD, equipped with a MB 150 G-I recycling system.

Synthesis of Vanadium(V) complex 2-V.

Complex **2-V** was prepared in glovebox by slowly addition of a solution of VO(Oi-Pr)$_3$ (0.615 mmol) in dry THF (1mL) to a solution of the ligand **1** (0.610 mmol) in dry THF (5 mL). An immediate change in colour of the solution was observed (from colourless to dark-red). The solution was stirred for 1 hr at rt and then the solvent was evaporated under vacuum leading to a dark-red solid, which was repeatedly washed with small volumes of hexane and dried in vacuum. Yield: 94%.

^{1}H-NMR (300 MHz, CDCl$_3$): δ 1.53 (27H, *s*), 2.87 (3H, *bs*), 3.77 (3H, *bs*), 6.89 (3H, *t*, J= *7.5* Hz), 7.03 (3H, *d*, J = 7.3 Hz), 7.24 (3H, *d*, J = 7.3 Hz). ^{13}C-NMR (50 MHz, CDCl$_3$): δ 29.9 (*CH$_3$*), 35.3 (*C*), 57.6 (*CH$_2$*), 123.3 (*CH*), 125.7 (*CH*), 126.8 (*C*), 128.1 (*CH*), 136.5 (*C*), 143.9 (*C*). ^{51}V-NMR (78.28 MHz, CDCl$_3$): δ -389.07 , (78.28 MHz, CD$_3$OD): δ -396.2.   IR (KBr, cm^{-1}): 752, 891, 945, 1080, 1188, 1236, 1426, 2952, 3081. APCI-MS: 568.25 [M + H]$^+$, calc. 568.26. Anal. Calcd. for C$_{33}$H$_{42}$NO$_4$V: C 69.83, H 7.46, N 2.47. Found: C 69.38, H 7.51, N 2.35.

Synthesis of Scandium(III) complex 2-Sc:

Complex **2-Sc** was prepared in glovebox by mixing homogeneous solutions of the ligand **1** (0.24 M) and Sc(Oi-Pr)$_3$ (0.24 M) in CDCl$_3$ in a 1:1 ratio. Analyzing the reaction mixture via ^{1}H-NMR the quantitative formation of the complex was observed after 3 days. The complex solution (0.012 M) was used for kinetics experiments without further purifications and without removing the three equivalents of i-PrOH released from the metal precursor.

^{1}H-NMR (250 MHz, CDCl$_3$): δ 7.16 (d, 3H, J = 7.5 Hz, ArH), 6.96 (d, 3H, J = 7.3 Hz, ArH), 6.61 (t, 3H, J = 7.5 Hz, ArH), 3.48 (s, 6H, NC*H$_2$*), 1.41 (s, 27H, *t*-Bu).
^{13}C-NMR (62.9 MHz, CDCl$_3$): δ 161.76 (C), 135.98 (C), 128.71 (CH), 126.62 (CH), 125.03 (C), 116.70 (CH), 59.46 (CH$_2$), 34.89 (C), 29.74 (CH$_3$).

In the NMR spectra resonances relative to free iso-propanol released in the reaction are present: ^{1}H-NMR (250 MHz, CDCl$_3$): δ 4.02 (m, 1H, CHMe$_2$), 1.28 (6H, d, J = 5 Hz, CH(CH$_3$)$_2$). ^{13}C-NMR (50 MHz, CDCl$_3$): δ 66.05 (CH), 25.45 (CH$_3$).

Synthesis of Titanium(IV) complex 2-Ti:

Complex **2-Ti** was prepared in glovebox by mixing homogeneous solutions of the corresponding ligand **1** (0.1M) and Ti(O*i*-Pr)$_4$ (0.18 M) in CDCl$_3$ in a 1:1 ratio to a final concentration 0.01 M of the complex obteining a bright yellow solution which was use for kinetic experiments without further purifications and without removing the three equivalents of *i*-PrOH released from the metal precursor.

^{1}H-NMR (300 MHz, CDCl$_3$): δ 7.19 (d, 3H, J = 7.8 Hz, ArH), 6.96 (d, 3H, J = 6.5 Hz, ArH), 6.77 (t, 3H, J = 7.5 Hz, ArH), 5.24 (hept, 1H, J = 6.1 Hz, CHMe$_2$), 3.94 (d, 3H, J = 13.0 Hz, NCH$_2$), 2.89 (d, 3H, J = 13.0 Hz, NCH$_2$), 1.51 (6H, d, J = 6.1 Hz, CH(CH$_3$)$_2$), 1.45 (s, 27H, *t*-Bu). ^{13}C-NMR (62.9 MHz, CDCl$_3$): δ 162.7 (C), 136.4 (C), 127.8 (CH), 126.4 (CH), 125.2 (C), 120.3 (CH), 80.2 (CH, *i*-Pr), 58.6 (CH$_2$), 35.1 (C), 29.7 (CH$_3$), 26.7 (CH3, *i*-Pr). ESI-MS: 580.3605 (M+H$^+$), calc. 580.2906.

In the NMR spectra resonances relative to free iso-propanol released in the reaction are present: ^{1}H-NMR (250 MHz, CDCl$_3$): δ 4.04 (hept, 1H, J = 6.1 Hz, CHMe$_2$), 1.22 (6H, d, J = 6.1 Hz, CH(CH$_3$)$_2$). ^{13}C-NMR (62.9 MHz, CDCl$_3$): δ 64.5 (CH), 25.1 (CH$_3$).

Synthesis of Zirconium(IV) complex 2-Zr:

Complex **2-Zr** was prepared in glovebox by mixing homogeneous solutions of the corrisponding ligand **1** (0.051 M) and Zr(O*t*-Bu)$_4$ (0.051 M) in CDCl$_3$ in a 1:1 ratio to a final concentration 0.0128 M of the complex. The solution was use for kinetic experiments without further purifications and without removing the three equivalents of *t*-BuOH released from the metal precursor.

^{1}H-NMR (250 MHz, CDCl$_3$): δ = 7.22 (dd, 3 H, J = 7.8 and 1.6 Hz,ArH), 6.98 (dd, 3 H, J = 7.4 and 1.4 Hz, ArH), 6.75 (t, 3 H, J = 7.6 Hz, ArH), 3.44 (s, 6 H, NCH$_2$), 1.50 (s, 9 H, C (CH$_3$)$_3$), 1.46 (s, 27 H, C(CH$_3$)$_3$). ^{13}C-NMR (62.9 MHz, CDCl$_3$): δ = 159.71 (C), 137.05 (C), 128.30 (CH), 126.72 (CH), 124.62 (C), 119.22 (CH), 60.89 (C, *t*-Bu), 59.02 (CH$_2$), 32.90 (ZrOC(CH$_3$)), 29.54 (CH$_3$, *t*-Bu).

In the NMR spectra resonances relative to free *tert*-butanol released in the reaction are present: ^{1}H-NMR (250 MHz, CDCl$_3$): δ 1.24 (9H, s, C(CH$_3$)$_3$). ^{13}C-NMR (62.9 MHz, CDCl$_3$): δ 69.05 (C), 31.23 (CH$_3$).

ESI-MS: m/z = 580.4 (M – 41, –OMe legante apicale in sostituzione di–O^{t}Bu, protonato). ESI-MS (CH$_3$OH + HCOOH 0.1 %, modalità negativa): m/z = 680.3 (M + 17, –OOCH legante apicale in sostituzione di–O^{t}Bu, addotto con anione formiato).

Synthesis of Hafnium(IV) complex 2-Hf:

Complex **2-Hf** was prepared in glovebox by mixing homogeneous solutions of the corrisponding ligand **1** (0.0495 M) and Hf(O*t*-Bu)$_4$ (0.0495 M) in CDCl$_3$ in a 1:1 ratio to a final

concentration 0.0124 M of the complex. The solution was used for kinetic experiments without further purifications and without removing the three equivalents of *t*-BuOH released from the metal precursor.

^{1}H-NMR (250 MHz, CDCl$_3$): δ 7.24 (d, 3H, J = 7.8 Hz, ArH), 6.95 (d, 3H, J = 7.7 Hz, ArH), 6.69 (t, 3H, J = 7.8 Hz, ArH), 3.51 (s, 6H, NC*H*$_2$), 1.48 (9H, s, C (C*H*$_3$)$_3$), 1.46 (s, 27H, *t*-Bu).

ESI-MS: 721.2 (M(-*t*-bu)+Na$^+$).

In the NMR spectra resonances relative to free *tert*-butanol released in the reaction are present: ^{1}H-NMR (250 MHz, CDCl$_3$): δ 1.24 (9H, s, C(C*H*$_3$)$_3$).

Synthesis of Niobium(IV) complex 2-Nb:

Complex **2-Nb** was prepared in glovebox by mixing homogeneous solutions of the corrisponding ligand **1** (0.039 M) and Nb(O*n*-Et)$_5$ (0.0796 M) in CDCl$_3$ in a 1:1 ratio to a final concentration 0.01 M of the complex obteining a bright green solution which was used for kinetic experiments without further purifications and without removing the three equivalents of *n*-EtOH released from the metal precursor.

^{1}H-NMR (250 MHz, CDCl$_3$): δ 7.26 (dd, 1H, J = 10 and 2.5 Hz, ArH), 7.22 (dd, 2H, J = 10 and 2 Hz, ArH), 6.95 (tt, 3H, J = 15 and 2.5 Hz, ArH), 6.74 (t, 2H, ArH), 6.72 (t, 1H, ArH), 4.81 (q, 2H, *CH*$_2$CH$_3$), 3.71 (m, 6H, NC*H*$_2$), 3.36 (q, 2H, *CH*$_2$CH$_3$), 1.56 (s, 9H, CH*(CH)*$_3$), 1.46 (t, 3H, CH$_2$*CH*$_3$), 1.40 (s, 18H, CH*(CH)*$_3$), 0.55 (t, 3H, CH$_2$*CH*$_3$).

^{13}C-NMR (62.9 MHz, CDCl$_3$): δ 158.7 (C), 137.63 (C), 126.6 (CH), 125.9 (CH), 121.5 (C), 120.7 (CH), 58.7 (CH$_2$), 35.01 (C), 31.81 (CH$_2$, *n*-Bu), 30.76 (CH$_3$), 18.65 (CH$_3$, *n*-Bu).

In the NMR spectra resonances relative to free *n*-butanol released in the reaction are present: ^{1}H-NMR (250 MHz, CDCl$_3$): δ 3.71 (q, 6H, *CH*$_2$CH$_3$), 1.24 (t, 9H, CH$_2$*CH*$_3$). ^{13}C-NMR (62.9 MHz, CDCl$_3$): δ 58.71 (CH$_2$, *n*-BuOH), 18.52 (CH$_3$, *n*-BuOH).

Synthesis of Tantalum(IV) complex 2-Ta:

Complex **2-Ta** was prepared in glovebox by mixing homogeneous solutions of the corrisponding ligand **1** (0.0479 M) and Ta(O*n*-Bu)$_5$ (0.0479 M) in CDCl$_3$ in a 1:1 ratio to a final concentration 0.012 M of the complex. The solution was used for kinetic experiments without further purifications and without removing the three equivalents of *n*-BuOH released from the metal precursor.

^{1}H-NMR (250 MHz, CDCl$_3$): δ 7.26 (d, 1H, J = 10 Hz, ArH), 7.22 (d, 2H, J = 7.5 Hz, ArH), 6.93 (m, 3H, ArH), 6.70 (m, 3H, ArH), 4.80 (t, 2H, *CH*$_2$(CH$_2$)$_2$CH$_3$), 3.76 (m, 6H, NC*H*$_2$), 3.34 (t, 2H, *CH*$_2$(CH$_2$)$_2$CH$_3$), 1.54 (s, 9H, CH*(CH)*$_3$), 1.39 (s, 18H, CH*(CH)*$_3$), from 1.6 to 1.1 (multiplets, 20H, CH$_2$*(CH*$_2$)$_2$CH$_3$ and OHCH$_2$*(CH*$_2$)$_2$CH$_3$)

^{13}C-NMR (62.9 MHz, CDCl$_3$): δ 158.14, 138.99, 129.38, 127.31, 122.65, 119.17, 63.01, 61.54, 56.43, 35.081, 34.98, 30.01, 29.73, 19.14, 14.14, 14.08.

ESI-MS: 828.2 (M + H$^+$), calc. 827.4.

In the NMR spectra resonances relative to free *n*-butanol released in the reaction are present: ^{1}H-NMR (250 MHz, CDCl$_3$): δ 3.64 (6H, t, J= 5 Hz OH*CH*$_2$(CH$_2$)$_2$CH$_3$), from 1.6 to 1.1

(multiplets, 12H OHCH$_2$(CH$_2$)$_2$CH$_3$), 0.92 (9H, t, J= 7.5 Hz OHCH$_2$(CH$_2$)$_2$CH$_3$). ^{13}C NMR (62.9 MHz, CDCl$_3$): δ 61.12(CH$_2$), 34.98(CH$_2$), 19.10 (CH$_2$), 13.69(CH$_3$).

Synthesis of Molibdenum(VI) complex 2-Mo:

1 mmol (200 mg) of milled MoO$_2$Cl$_2$ and 1 mmol (503 mg) of the ligand precursor **1** were mixed with 50 ml of toluene and the stirred suspension was heated to the reflux temperature for 18 h. Resulting intense blue solution was filtered through a short pad of silica and evaporated to yield complex **2-Mo** as a violet solid in 500 mg (80 %) yield.

^{1}H-NMR (250 MHz, CDCl$_3$): δ 7.40 (dd, 1H, J = 7.8 and 1.37 Hz, ArH), 7.34 (dd, 2H, J = 7.8 and 1.82 Hz, ArH), 7.15 (dd, 3H, J = 9.17 and 1.37 Hz, ArH), 6.98 (m, 3H, ArH), 3.99 (d, 1H, J = 11.45, NCH$_2$), 3.6 (d, 1H, J = 21.1, NCH$_2$), 3.49 (s, 1H, NCH$_2$), 1.59 (s, 9H, CH*(CH)$_3$*), 1.47 (s, 18H, CH*(CH)$_3$*).

^{13}C-NMR (62.9 MHz, CDCl$_3$): δ 159.84 (C), 141.40 (C), 140.4 (CH), 128.71(CH), 128.11(C), 125.61(CH), 60.23(CH) 35.45(CH), 35.43(CH), 30.54 (C), 30.40 (C).

ESI-MS: 672.3 (M + Na$^+$), 688.1 (M + K$^+$).

Typical Procedure for Oxidation of Methyl *p*-Tolyl Sulfide (2).

An NMR tube was charged with a solution of the complexes **2-M** in CDCl$_3$ (0.6 X 10^{-3} mmol), the internal standard (1,2-dichloroethane; DCE), cumyl hydroperoxide (0.06 mmol, 11.4 mg), and methyl *p*-tolyl sulfide **3** (0.06 mmol, 8.3 mg). The Lewis Base **6** (0.003 mmol, 0.43 mg) was added to a final volume of 0.6 mL. Concentrations of sulfide **3**, sulfoxide **4**, and sulfone **5** were determined by integration of the methyl group signals: *p*-Tol-S-Me (2.31 ppm),*p*-Tol-SO-Me (2.69), *p*-Tol-SO$_2$-Me (3.02 ppm) with respect to the internal standard, DCE (3.73 ppm). The final yield was determined after complete oxidant consumption (iodometric test) via ^{1}H NMR.

Fitting of the kinetic experimental data.
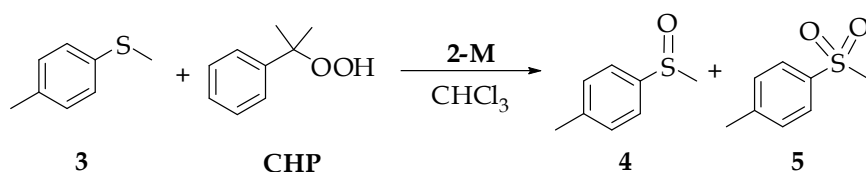
The kinetic law for the reaction in Scheme X is:

$$\frac{d[\mathbf{4}]}{dt} = k_1[\mathbf{3}][\mathbf{CHP}][\mathbf{2\text{-}M}][\mathbf{6}] - k_2[\mathbf{4}][\mathbf{CHP}][\mathbf{2\text{-}M}][\mathbf{6}]$$

and:

$$\frac{d[\mathbf{5}]}{dt} = k_2[\mathbf{4}][\mathbf{CHP}][\mathbf{2\text{-}M}][\mathbf{6}]$$

Incorporating the catalyst **2-M** and the Lewis Base **6** the equations become:

$$\frac{d[\mathbf{4}]}{d\mathrm{t}} = k_1^{'}[\mathbf{3}][\mathbf{CHP}] - k_2^{'}[\mathbf{4}][\mathbf{CHP}]$$
and:
$$\frac{d[\mathbf{5}]}{d\mathrm{t}} = k_2^{'}[\mathbf{4}][\mathbf{CHP}]$$

R_0 have been determined by least-square fitting of the experimental data according to the above described models. [18]

---

[18] Scientist™- MicroMath® Scientific Software, P.O. Box 21550, Salt Lake City, Utah 84121, USA, **1995**

Chapter 4

Oxovanadatrane complexes

as functional and structural models of

haloperoxidases

1f= 0.05-5%   **TMB + H$_2$O$_2$ + H$^+$ + Br-(Cl$^-$)**

TON(Br$^-$) = 1260

TOF(Br$^-$)= 220 h^{-1}

up to 92% (Br$^-$)
40% (Cl$^-$)   **TMBBr(Cl) + 2 H$_2$O**

TMB =1,3,5-trimethoxybenzene

R^1$\cdot$S$\cdot$R^2 + H$_2$O$_2$ **1f** = 0.01-1%

TON = 9900

TOF= 8000 h^{-1}

R^1$\cdot$S$\cdot$R^2 + H$_2$O   up to 99%

t-Bu

1f
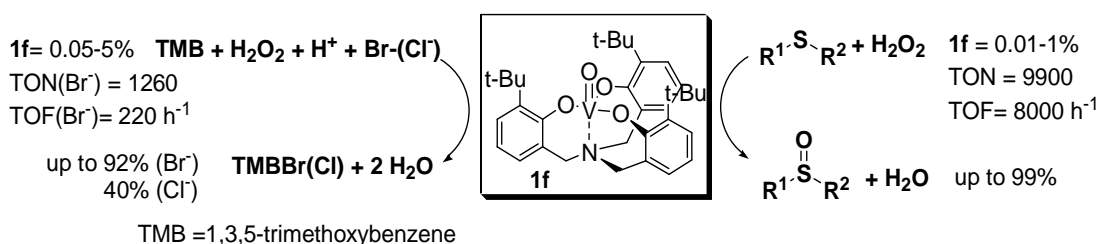
The coordination chemistry and catalytic activity of *C$_3$*-symmetric triphenolate amino complexes have been investigated. In this context, V(V)-oxo triphenolate amino complex **1** has been synthesized: it possesses a TBP geometry which emulates the one found in Vanadium haloperoxidases (VHPOs). This chapter describes that that V(V)-complex **1f** bearing *tert*-butyl peripheral substituents is a structural and functional model of VHPOs. The complex catalyzes efficiently sulfoxidations at room temperature using hydrogen peroxide as terminal oxidant yielding the corresponding sulfoxides in quantitative yields and high selectivities (catalyst loading down to 0.01%, TONs up to 9900, TOF up to 8000 h^{-1}) as well as chlorination and bromination of trimethoxybenzene (catalyst loading down to 0.05%, TONs up to 1260, TOF up to 220 h^{-1}).

4.1 Introduction

The first isolation of a vanadium haloperoxidase enzyme (VHPOs) from the marine algae *Ascophyllum nodosum* date back to 1984.[1] It is now known that this vanadium-dependent enzymes, found in most marine algae, seaweed, and in some lichens[2] and fungi,[3] are able to oxidize halides 'X⁻' to the corresponding 'X⁺' species in the presence of hydrogen peroxide. Once formed, oxidized halides can react with suitable organic sunbstrates to form halogenated organic compounds (Scheme 1).[4] These products probably are part of the defense mechanisms of the organisms in which the VHPOs are found. For example, HOX (hypoalous acids) and some of the organohalogens produced by VHPOs may prevent fouling by microorganisms or may act as antifeeding system.[5]

$$X^- + H_2O_2 \xrightarrow{\text{VHPO}} X^+ \quad \text{oxidized halide}$$

$$\text{(e.g. HOX, } X_2, X_3^-, \text{ Enzyme-X)}$$

Organic substrate / H_2O_2

$$X^-\text{Org} + H_2O \qquad\qquad O_2 + X^- + H_2O + H^+$$
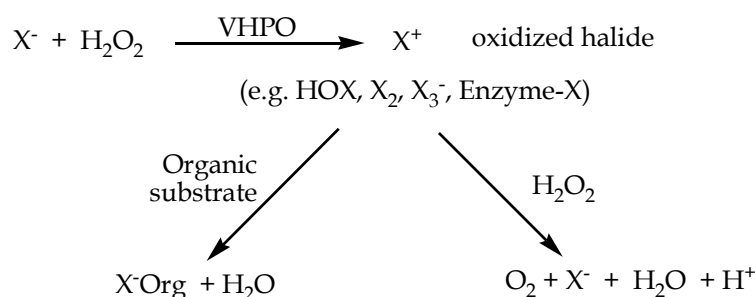
Scheme 1. Summary of the general reactivity of VHPOs with halide (X^-).

The nomenclature for the haloperoxidases has traditionally been based on the most electronegative halide which can be oxidized by hydrogen peroxide catalyzed by the enzyme. Thus chloroperoxidases (VCPOs) catalyze the oxidation of chloride, bromide and iodide; bromoperoxidases (VBPOs) catalyze the oxidation of bromide and iodide, while iodoperoxidases (VIPOs) catalyze the oxidation of only iodide. There are no fluoroperoxidases because hydrogen peroxide does not have the potential to oxidize fluoride.[6]

A variety of halogenated products have been isolated from natural organisms, some of these compounds are simple, volatile halohydrocarbons (such as bromoform, dibromomethane, etc.) others are more interesting halogenated indole or terpene compounds possessing a variety of biological and pharmacological effects, such as antifungal, antibacterial, antiviral, antiinflammatory or even antineoplastic activity.[7]

---

[1] Vilter, H. *Phytochemistry* **1984**, *23*, 1387.

[2] Plat, H.; Krenn, E.; Wever, R., *Biochemical Journal* **1987**, *248*, 277.

[3] van Schijndel, J. W. P. M.; Vollenbroek, E. G. M.; Wever, R. *Biochimica et Biophysica Acta* **1993**, *1161*, 249.

[4] (a) Butler, A. *Coord. Chem. Rev.* **1999**, *187*, 17. (b) Butler, A.; Carter, J.; Simpson, M. In Handbook on Metalloproteins; Bertini, I., Sigel, A., Sigel, H., Eds.; Marcel Dekker Inc.: New York, Basel, 2001; pp 153-179.

[5] Soedjak, H. S.; Walker, J. V.; Butler, A. *Biochemistry* **1995**, 34, 12689-12696.

[6] Butler, A.; Walker, J. V. *Chem. Rev.* **1993**, 93, 1937-1944.

[7] (a) Neidleman, S. L.; Geigert, J. L.; Biohalogenation; Ellis Horwood Ltd. Press: New York, 1986. (b) Butler, A.; Walker, J. V. *Chem. Rev.* **1993**, *93*, 1937.

In the past lots of studies have been carried out in order to reveal the nature of the active site and the mechanism of action. The first crystal structure of a vanadium chloroperoxidase enzyme was isolated from the fungus *Curvularia inaequalis* in 1996,[8] and a year later was published the X-ray analysis of the peroxo adduct that is the enzyme's active form.[9] In the native state the vanadium ion is characterized by a trigonal bipyramidal geometry, where three oxygen atoms belong to the equatorial plane and one oxygen occupies an axial position. The other apical ligand is His496, which links the metal ion to the protein, whereas Lys353, Arg360, His404, and Arg490 are involved in hydrogen bonds with the oxygen atoms of the cofactor. In the peroxo derivative of the enzyme, the peroxide is bound side-on to the vanadium centre in a η^2-fashion and the cofactor is characterized by a strongly distorted tetragonal pyramidal geometry, with two oxygen atom type and one peroxo atom in the equatorial plane, while His496 and the other peroxo atom occupy axial positions (Figure 1).[10]
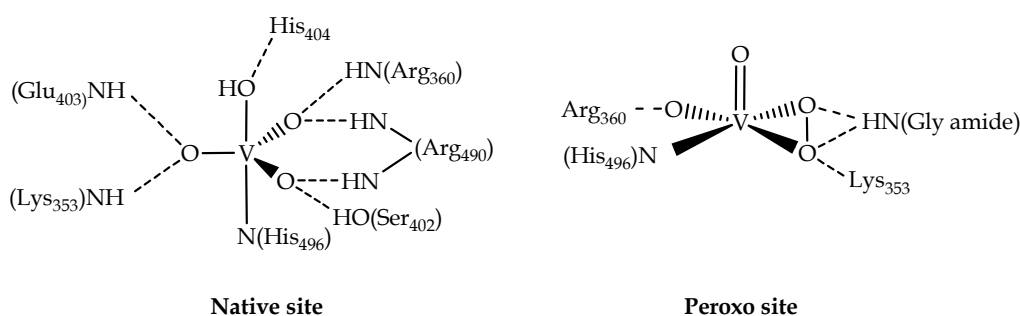

Native site **Peroxo site**

Figure 1. The native and peroxo vanadium site in VCPO.[10]

The active site of the enzyme is located on top of the second four-helix bundle of the enzyme structure and a channel allows the entrance of hydrogen peroxide, X⁻ and a possible organic substrate.[1,11,12] In one side the channel is composed of hydrophobic residues, while the other side is mainly hydrophilic.[1] However, the crystal structures of these type of enzymes revealed that VHPOs are composed of one or more subunits of around 60-70 KDa and have only one bounded vanadium atom for each subunit (Figure 2).[13]

[8] Messerschmidt, A.; Wever, R. *Proc. Natl. Acad. Sci. USA* **1996**, 93, 392.

[9] Messerschmidt, A.; Prade, R.; Wever, R. *Biol. Chem.* **1997**, 378, 309.

[10] Ligtenbarg, A. G. J.; Hage, R.; Feringa, B. L. *Coord. Chem. Rev.* **2003**, 89.

[11] Almeida, M.; Filipe, S.; Humanes, M.; Maia, M. F.;Melo, R.; Severino, N.; Da Silva, J. A. L.; Frausto da Silva, J. J. R.; Wever, R. *Phytochemistry* **2001**, *57*, 633.

[12] Tschirret-Guth, R.A.; Butler, A. *J. Am. Chem. Soc.* **1994**, *116*, 411.

[13] Weyand, M.; Hecht, H.-J.; Kieû, M.; Liaud, M.-F.; H. Vilter, H.; Schomburg, D. *J. Mol. Biol.* **1999**, *293*, 595-611.
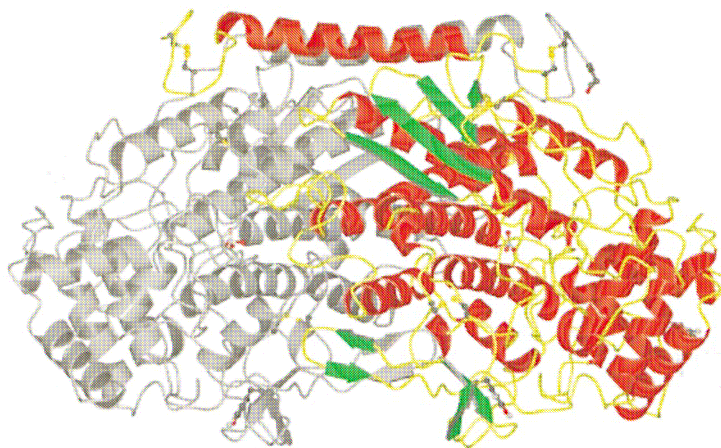
Figure 2. Ribbon-type representation of the VBPO dimer isolated from brown alga *Ascophyllum nodosum*. In the coloured monomer α–helices are reported in red, β-strands in green and coil in yiellow. A vanadate group is present in each monomer.[13]

The VHPOs require one equivalent of vanadium for activity.[14] The vanadium centre does not appear to undergo redox cycling during turnover and is proposed to function as a Lewis acid: the role of the metal is to serve as a strong Lewis acid in the activation of the primary oxidant hydrogen peroxide.

A general consensus currently exists for the mechanism of halide oxidations for VHPOs, which is a "ping-pong" mechanism: hydrogen peroxide coordinates to the vanadium centre, forming the peroxovanadate active specie. The rate-determining step in the catalytic cycle is the nucleophilic attack of the halide on the protonated protein-peroxide complex, generating a X^+ specie, which immediately reacts with the organic substrates and halogenates them. This step will generate singlet oxygen in the absence of a suitable organic substrate, and has been investigated in detail with Cl^-, Br^-, I^-.

As mentionated above, the apical hydroxyl group of the enzyme is hydrogen bonded to a hystidine residue (His404) in a protein environment. This hydrogen bond makes the OH^- group more nuclephilic. When a peroxide molecule approaches the active site, the OH^- unit is protonated and HOO^- is generated. The weakly ligated water molecule dissociates from vanadium ion and a side-on bound peroxide intermediate is formed after the departure of another water molecule. Subsequently attack of a chloride ion at a peroxo oxygen and the uptake of a proton from a surrounding water molecule leads to the generation of hypoahalous acid (HOX) and restoration of the native state (Scheme 2).

---

[14] de Boer, E.; van Kooyk, Y.; Tromp, M.; Wever, R. *Biochim. Biophys. Acta* **1986**, *869*, 48.
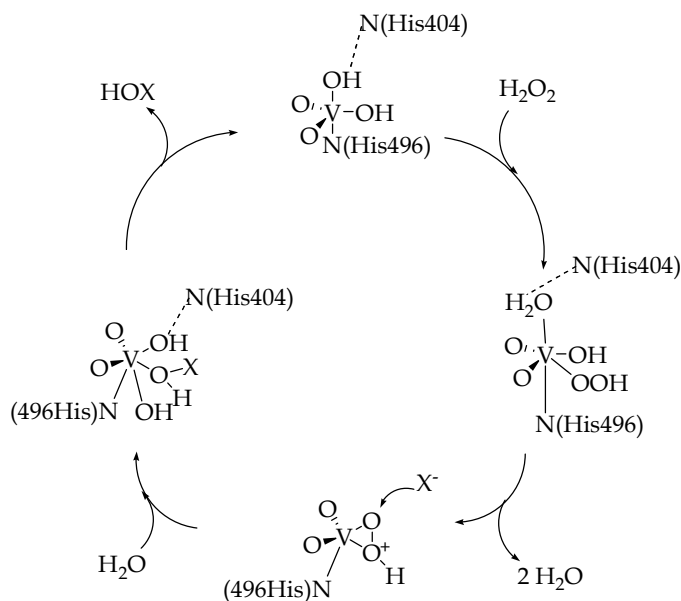
Scheme 2. Proposed catalytic mechanism of VHPOs.[10]

According to the literature, the oxygen transfer involves the attack of the substrate on the deprotonate peroxo oxygen: before the nucleophilic attack of the substrate the peroxo moiety is protonated to hydroperoxo and Lys353 seems to polarize the peroxidic bound.[1] Besides, the oxidation reaction towards halides increases in velocity adding acids and the spectroscopic data are consistent with the protonation of one or more sites of the peroxidic species.

In theory, every nucleophilic organic compound, which can gain access to the VHPOs active site and which have an oxidation potential lower than the reduction potential of hydrogen peroxide, could be oxidized by these enzymes. This is the case of sulfides. It was demonstrated that VHPOs are able to catalyze stereoselective sulfoxidations.[15,20] Depending on the substrate, up to 91% e.e. could be achieved. Moreover, different enzymes may produce opposite enantiomers, starting from the same substrate. As an example, the enzymes obtained respectively from *Ascophillum nodosum* and from *Corallina pilulifera* activate the hydrogen peroxide in the oxidation of thioanisole, affording the corresponding sulfoxide with high yields and selectivities, exceeding 95% enantiomeric excess of (*R*)-enantiomer for the first enzyme, and 55% e.e. of (*S*)-enantiomer, for the second one (Scheme 3).[16]

[15] (a) Andersson, M. A.; Willetts, A.; Allenmark, S. G. *J. Org. Chem.* **1997,** *62*, 8455. (b) Dembitsky, V. M. *Tetrahedron* **2003**, *59*, 4701.

[16] ten Brink, H.B.; Schoemaker, H.E.; Wever, R. *Eur. J. Biochem.* **2001**, *268*, 132.
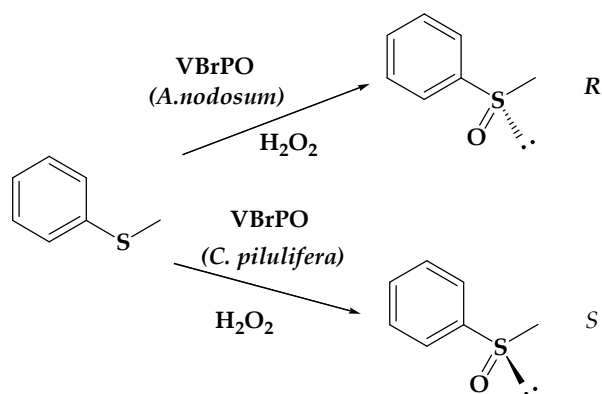
Scheme 3

Complementary stereoselective sulfoxidation by means of different haloperoxidases can be reached using a heme-containing chloroperoxidase from marine fungus *Caldariomyces fumago*, and VBrPO from *Corallina officinalis*: using hydrogen peroxide as the oxygen source the enzymes catalyze the oxidation of 2,3-dihydrobenzothiophene with excellent and opposite enantioselectivity, as shown in Scheme 4.[20]
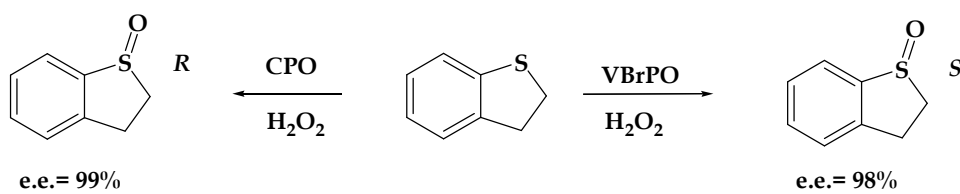
Scheme 4

The enzymatic mechanism of sulfide oxidation seems to be the same of the one operating in the halide oxidation: a two-electrons transfer mechanism.[10]

4.2 Functional and structural models of VHPOs

To get a better understanding of the working mechanism of the vanadium haloperoxidase enzymes, the role of vanadium and then to utilize them as efficient catalyst in oxidation reactions, a variety of vanadium compounds have been studied as functional models for V-haloperoxidases.[17] These complexes are reactive, towards the oxidation of sulfides and halides, in analogy with the VHPOs.[18] The role of the ligands in the VHPOs models is crucial: in fact in the absence of ligands, which stabilize the monomeric complex, vanadium establishes a series of oligomeric and protonating equilibria, depending on his concentration and on the acidic conditions. In recent years several vanadium complexes of multidentate ligands containing O and N donor sites were tested for catalysis in oxidation reactions.

In particular, different tripodal amine-based ligands have been largely employed to obtain monomeric V(V) complexes and they have been tested in the activation of hydrogen peroxide (Figure 3).[2,3] These ligands are ideal to model same of the donor types considered

[17] Butler, A. in: Reedijk, J; Bouwman, E. (Eds.) Bioinorganic Catalysis, 2nd ed (Charter 5), Marcel Dekker, New York, 1999,

[18] Bolm, C. *Coord. Chem. Rev.* **2003**, 245.

likely to be found at the active site of the enzyme such as carboxylate, alcohol, amide, and pyridine donors.
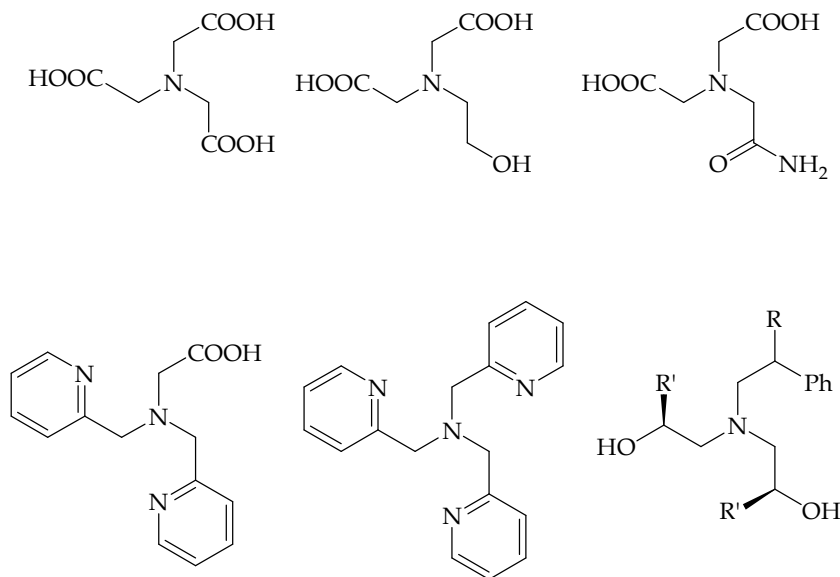
Figure 3. Ligands whose V(V) complexes heve been tested for catalysis of bromide or sulfide oxidation.

For each ligand the monomeric complex is obtained using a 1:1 ratio vanadium precursor/ligand. Addition of hydrogen peroxide affords a new monomeric metal peroxidic species, effective in halide oxidations and sulfoxidations.

The sulfide oxidation has proven to be highly similar to halide oxidation by these complexes (Scheme 5).[19] Once the initial oxoperoxovanadium complex is protonated, the substrate engages in a nucleophilic attack on the protonated peroxide ligand. The product distribution displays almost exclusively sulfoxide products, with little presence of further oxidation products, points to an electrophilic rather than radical mechanism. Scheme 6 reports a representation of the halide oxidation mechanism. The only difference, between the halide and sulfide oxidation mechanism, is the acid equivalent required for reactivity. In halide oxidation the acid is consumed in each cycle. In sulfide oxidation the acid is not consumed.

---

[19] Smith, T. S.; Pecoraro, V. L. *Inorg. Chem.* **2002**, 41, 6754-6760.
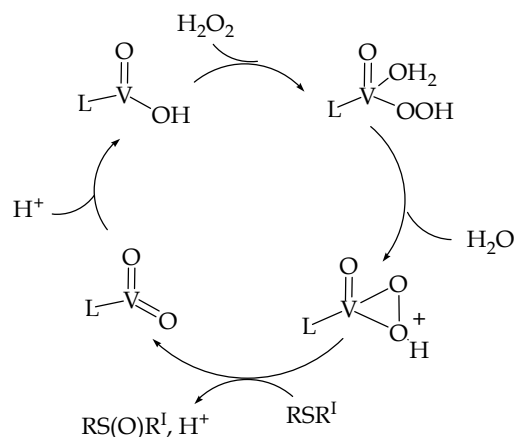
Scheme 5. Complete scheme for the catalytic cycle of sulfide oxidation by monoperoxovanadium(V) tripodal amine complexes.[19]
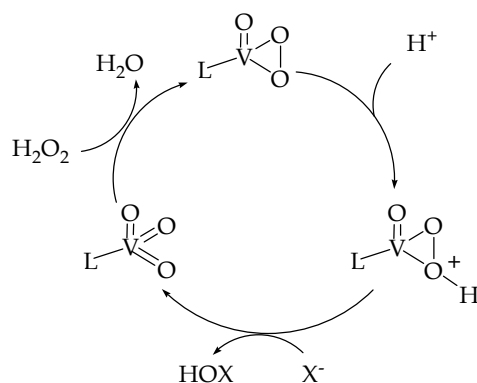
Scheme 6. Simplcistic halide oxidation mechanism.[19]

4.3 V(V)amine tri-phenolate complexes: synthesis and structural study

Concerning vanadium chemistry with amine tri-phenolate ligands, only one study has been reported, showing V(V)oxo complexes formation via reaction between the ligand precursor and VO(Oi-Pr)$_3$.[20] The family of tetradendate amine tri-phenolate ligands strongly binds to the metal and enables "fine tuning" of the complex structure, seeming to provide a "natural environment" for vanadium. We could obtain similar complexes (**1d-f**) and we tested their ability to catalyze the oxidation of sulfides and halides with hydrogen peroxide.[21]

1a R^1 = R^2 = Cl
1b R^1 = R^2 = Me
1c R^1 = R^2 = t-Bu
1d R^1 = R^2 = H
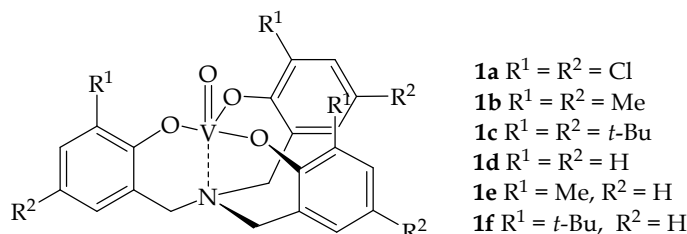**1e** R^1 = Me, R^2 = H
1f R^1 = t-Bu, R^2 = H

Figure 8. C_3-symmetric V(V) amine triphenolate complexes.

[20] Groysman, S.; Goldberg, I.; Goldschmidt, Z.; Kol, M. *Inorg. Chem.* **2005**, *44*, 5073.

[21] Mba, M.; Pontini, M.; Lovat, S.; Zonta, C.; Bernardinelli, G.; Kündig, E. P.; Licini, G. *Inorg. Chem.* **2008**, *47*, 8616.

Reaction of tris-phenolamines[22] with VO(O*i*-Pr)$_3$ in dry THF under nitrogen yielded complexes **1d-f** as deep red crystalline solids in high yields (92-94%). The observed complexation behaviour is in complete accordance with the structurally similar complexes **1a-c** described in literature, which contain additional *para* substituents on the phenolic moiety.[20]

Complexes **1e** and **1f** (R^1= Me and *t*-Bu, respectively) show highly symmetric ^{1}H NMR spectra, in agreement with the formation of single C_3-symmetric, mononuclear species, with a single ^{51}V NMR signal (-381.9 ppm and -389.1 ppm, CDCl$_3$, respectively), whereas complex **1d** shows a complicate, non-symmetric ^{1}H NMR spectrum and two different signals in ^{51}V NMR (-396.8 and -428.8 ppm, CDCl$_3$) indicative of the presence of aggregates or a mixture of species in solution (Table 1).

Complex	δ (ppm) in CDCl$_3$
VO(O*i*-Pr)$_3$	-625.8
1d	-396.83 , -428.78
1e	-381.90
1f	-389.07

Table 1. ^{51}V NMR Chemical shift values (ppm) for **1d-f** complexes, in CDCl$_3$ as solvent.

For example, the ^{1}H NMR spectra of the oxovanadatrane complex **1f** and the corrisponding ligand show the maintenance of the high symmetry of the ligand into the complex. The enantiomeric benzylic protons of the ligand become diastereotopic in the complex, resulting as two broad singlets (Figure 5).
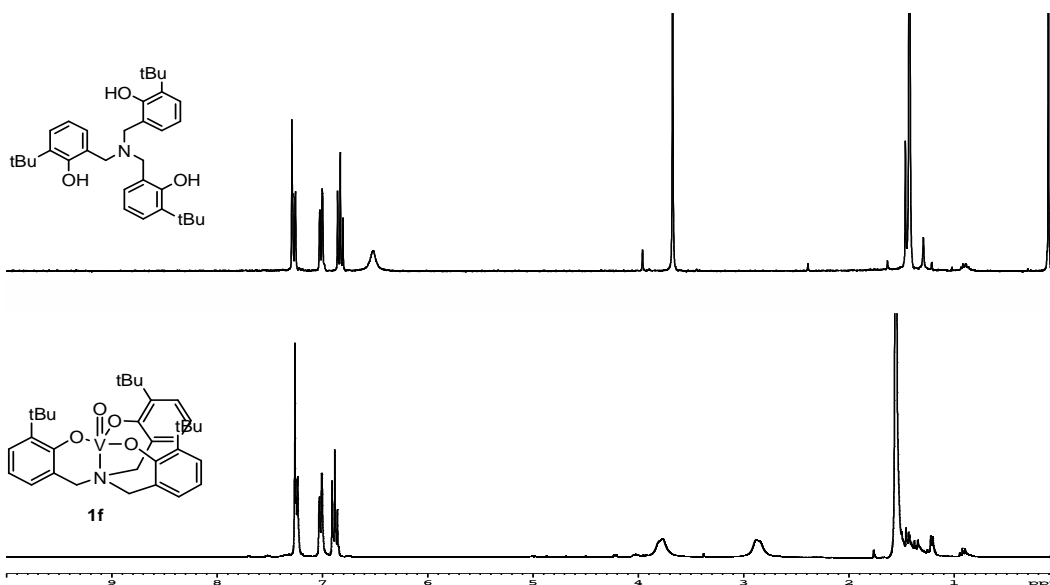

Figure 5. ^{1}H NMR spectra (300 MHz, CDCl$_3$) respectively of **1f** (R^1= *t*-Bu) and its corresponding free ligand.

[22] Prins, L. J.; Mba, M.; Kolarović, A.; Licini, G. *Tetrahedron Lett.* **2006**, *47*, 2735.

At lower temperatures these methylene signals consistently resolve in a clear AB system, due to the slowing down of the racemization process between the to propeller-like chiral enantiomers (Δ-Λ) (Figure 6).
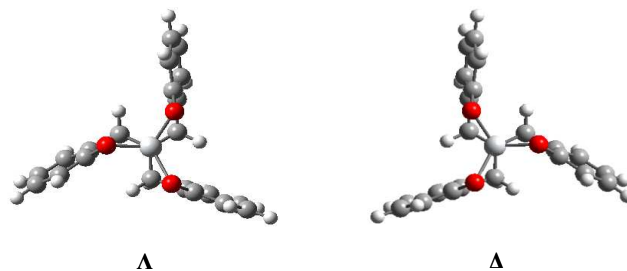
Figure 6. Clockwise (Δ) and counter-clockwise (Λ) enantiomeric conformations of amine tri-phenolate complexes.

The X-ray structure of complex **1f**, crystallized from dichloromethane/hexane, is consistent with what we observe in solution, by NMR spectroscopy, and it is structurally analogous to the reported X-ray structures of complexes **1a-c**.

The solid-state structure reveals a monomeric pentacoordinate complex, which adopts a trigonal bypiramidal geometry (Bpt), with the oxo function occupying the axial position, *trans* to the central nitrogen. The V centre is positioned slightly above the phenolate oxygens plane, pointing towards the oxo function. The V-N bond is weak, being effected by the *trans* effect of a strong π-donor oxo ligand (Figure 7).[1]
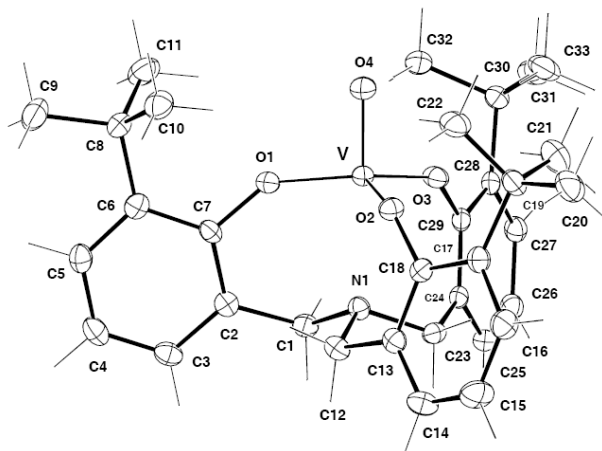
Figure 7. X-ray structure of **1f**, recorded at 150 K.

The coordination environment of vanadium in these structures mimicks, to a large extent, the coordination environment of the metal centre in vanadate-dependent HPOs. In fact both structures have a trigonal bypiramidal geometry and in both cases the ligand set around the metal is [O₄N], with the amine ligand occupying an axial position. In the amine triphenolate complexes the oxo function occupies the second axial position, whereas in the active site of the enzyme this position is occupied by a hydroxo or an aqua ligand.

Bond Lengths, Å	
V-O1	1.809(1)
V-O2	1.807(1)
V-O3	1.807(1)
V-O4	1.604(1)
V-N1	2.416(2)

Angles, degrees			
O1-V-O2	122.50(6)	O1-V-O3	117.42(6)
O1-V-O4	97.75(6)	O1-V-N1	81.36(6)
O2-V-O3	114.18(6)	O2-V-O4	97.68(7)
O2-V-N1	81.16(6)	O3-V-O4	98.98(7)
O3-V-N1	83.22(6)	O4-V-N1	177.79(6)

Table 2. Selected bond lengths (Å) and angles (degrees) for crystal structure of **1f**, with reference to atom labelling reported in Figure 7. See experimental part for details on crystal data and structure refinement.

4.4 V(V)amine tri-phenolate complexes: catalytic activity

The use of multidentate amine triphenolate ligands for complexation of the metal affords a great advantage due to the high stability of the metal complexes, which allows low catalyst concentrations without the loss of catalyst integrity. Second, a nearly occupation of all coordination sites of the metal by a single ligand reduces the chances of formation of multimeric and often undefined metal-species under catalytic conditions.

In this contest the reactivity of complexes **1d-f** as functional models of VHPOs was examined in the sulfides and halides oxidation.

4.4.1 Oxidation of sulfides to the corresponding sulfoxides

Although the oxidation of sulfides by vanadium complexes is not new,[23,24,25,26] the exact mechanism by which it is accomplished is still a subject of study.

The active species in the process is a V(V) complex associated with and/or generated by hydrogen peroxide or an organic hydroperoxide. There are two possible mechanisms of sulfide oxidation, an electrophilic route[26a] and a radical one.[25d] The first one is more prevalent and proceeds via nucleophilic attack by sulfide on a coordinated peroxide.[27,28]

To study the catalytic activity of 1d-f in sulfoxidation reactions, we used hydrogen peroxide as terminal oxidant. The use of hydrogen peroxide is highly advantageous, since it is non-

[23] (a) Nakajima, K.; Kojima, M.; Fujita, J. *Chem. Lett.* **1986**, 1483. (b) Nakajima, K.; Kojima, M.; Toriumi, K.; Saito, K.; Fujita, J. *Bull. Chem. Soc. Jpn.* **1989**, *62*, 760. (c) Nakajima, K.; Kojima, K.; Kojima, M.; Fujita, J. *Bull. Chem. Soc. Jpn.* **1990**, *63*, 2620. (d) Ballistreri, F.P.; Tomaselli, G.A.; Toscano, R.M.; Conte, V.; Di Furia, F. *J. Am. Chem. Soc.* **1991**, *113*, 6209. (e) Vetter, A.H.; Berkessel, A. *Tetrahedron Lett.* **1998**, *39*, 1741.

[24] (a) Bortolini, O.; Di Furia, F.; Modena, G. *J. Mol. Catal.* **1982**, *16*, 61. (b) Di Furia, F.; Modena, G.; Seraglia, R. *Synthesis* **1984**, 325.

[25] Bolm, C.; Bienewald, F. *Angew. Chem. Int. Ed. Engl.* **1995**, *34*, 2640.

[26] Drago, C.; Caggiano, L.; Jackson, R.F.W. *Angew. Chem. Int. Ed.* **2005**, *44*, 7221.

[27] Butler, A.; Clague, M.J.; Meister, G.E. *Chem. Rev.* **1994**, *94*, 625.

[28] (a) Di Furia, F.; Modena, G. *Rev Chem. Intermed.* **1985**, *6*, 51. (b) Di Furia, F.; Modena, G. *Pure Appl. Chem.* **1982**, *54*, 1853.

toxic, inexpensive and yields water as the only side product. To work under homogeneous conditions and follow the reaction course via ^{1}H-NMR, sulfide oxidations were performed in methanol-d_4 using a 10% catalyst loading and a 1:1 ratio of thioanisole 2a and H_2O_2 (35% in water) (Table 3).
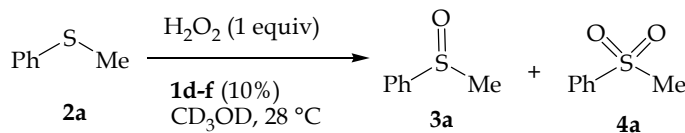
Entry	Catalyst	Time(min)[b]	Yields (%)[c]	3a:4a [c]
1	**1d**	720	7	>99:1
2	**1e**	10	89	99:1
3	**1f**	10	99	99:1
4	--	720	3	>99:1

[a]Reaction conditions: $[2a]_o = [H_2O_2]_o = 0.09$ M, 10% catalyst CD$_3$OD, 28 °C. [b]Time required for complete oxidant consumption. [c]Determined on the oxidant by ^{1}H NMR (CD$_3$OD, 300 MHz), DCE as internal standard, and quantitative GC analysis on the crude reaction mixture after complete oxidant consumption (iodometric test).

Table 3. Oxidation of **2a** by aqueous H_2O_2 (35%) catalyzed by **1d-f**.[a]

We were pleased to find that, in the presence of the mononuclear complexes **1e-f**, sulfide **2a** was oxidized to the corresponding sulfoxide **3a** in high yields, with almost complete sulfoxide selectivity and in very short reaction times (10 min) (Table 3, entries 1 and 2). In contrast, complex **1d** (R^1=H) gave very low conversions and only after extended reaction times (7%, 12 h). While the reaction performed without V(V) catalyst afforded even lower conversions.

Because complex **1f** revealed to be the most active and efficient catalyst and, in addition, does not require to be handled under inert atmosphere, our studies were continued testing only the catalytic performances of complex **1f**.

Substrate/Catalyst Ratio. Catalyst loading is an aspect of major importance for catalytic systems, since it determines the cost of the process. Results reported in Table 4 show the effect of increasing the substrate/catalyst ratio on the oxidation of thioanisole **2a** with hydrogen peroxide.

Using V(V)-amino triphenolate complex **1f** as catalyst, 10:1 and 100:1 and 1000:1 ratios were used. Substrate concentrations were varied from 0.1 to 1 M (Table 4, entries 1-2, catalyst loading 1% and 0.1%, respectively). Fast reactions with high yields were obtained in all cases. Catalyst concentration was further decreased (0.001 M- 0.0001 M), using a constant substrate concentration ($[2a]_0 = 1.0$ M) (Table 4, entries 2-4).

#	$[2a]_o$ (M)	1f (%)	$t_{1/2}$ (min)[b]	yields (%)[c]	$3a:4a$[c]	time (min)[d]	TON	TOF (h^{-1})[e]
1	0.1	1	6	97	96:4	25	97	240
2	1.0	0.1	24	98	98:2	80	980	1330
3	1.0[f]	0.1	6	98	97:3	20	980	8000
4	1.0	0.01	265	97	97:3	850	9700	1790
5	1.0[f]	0.01	110	99	98:2	255	9900	2667

[a]Reactions conditions: **2a**:H_2O_2 =1:1, 28 °C, CD_3OD,. [b]Time for 50% decrease of $[H_2O_2]_o$. [c]Determined on the oxidant by ^1H NMR (CD_3OD, 300 MHz) in the presence of DCE as internal standard and quantitative GC analysis on the crude reaction mixture after total oxidant consumption (iodometric test). [d]Time required for total oxidant consumption. [e]Determined at 20% conv. [f]Reactions performed with H_2O_2 (70%).

Table 4. Oxidation of thioanisole 2a by acqueous H_2O_2 (35%) catalyzed by 1f. Effect of concentration and catalyst loading.[a]

In particular, using 0.1% catalyst and 70% aqueous H_2O_2 comparable yields and reaction times of the reaction performed with 1% catalyst could be achieved with remarkable TOF (8000 h^{-1}) (Table 2, entry 3).
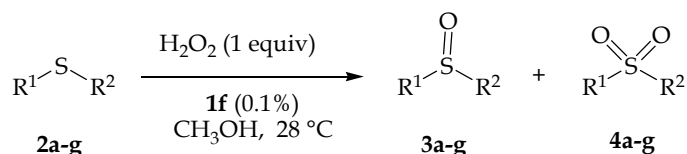
The catalyst loading was then further decreased to 0.01% without affecting the efficiency of system but simply slowing down the reactions (Table 2, entries 4-5). Also in this case the use of more concentrated H_2O_2 increases the system performances: the reaction is complete in less than 5 hours, with 9900 TON and still significative TOF (2667 h^{-1}).

The system reported here is more efficient than the vanadium-dependent bromoperoxidases, which present TONs of 450-520 in 20 hours.[6] Moreover, to the best of our knowledge, the **1f**/H_2O_2 system seems to be the most active VHPOs model so far reported, as far as TONs (9900 in 4 h) and TOFs (up to 8000) are concerned.[3a]

Scope of the reaction. The general scope of the V(V)-based catalytic system has been examined. A series of alkyl aryl, and dialkyl sulfides was oxidized and optimized conditions were used: $[2a\text{-}g]_0=[H_2O_2]_0=0.5$ M, 0.1% of catalyst, working on a preparative scale (8 mmol).

In analogy with what observed previously for **2a**, in all cases the oxidation with H_2O_2 afforded the corresponding sulfoxides in short reaction times (1-4 h), quantitative yields, also in isolated products, and very high selectivity for the sulfoxide formation. Dialkyl sulfides were oxidized faster than the corresponding aryl alkyl ones (Table 5, entries 4 and 5), being methyl-*p*-nitrophenyl sulfide **2g** the less reactive substrate (Table 5, entry 7).

All these results are consistent with the occurrence of an electrophilic oxygen transfer process and prove the generality and applicability of the method also on preparative scale.

$$R^1 \diagdown S \diagdown R^2 \xrightarrow[\substack{\textbf{1f} (0.1\%) \\ CH_3OH,\ 28\ ^\circ C}]{H_2O_2\ (1\ equiv)} R^1 \diagdown \overset{\displaystyle O}{S} \diagdown R^2 \quad + \quad R^1 \diagdown \overset{\displaystyle O\ \ \ O}{S} \diagdown R^2$$

Entry	Sub.	R^1	R^2	Yields (%)[b]	3:4	Time (min)[c]
1	**2a**	Ph	Me	98 (98)	99:1	120
2	**2b**	*p*-Tol	Me	>99 (99)	99:1	120
3	**2c**	*p*-Tol	*n*-Bu	96 (94)	> 99:1	120
4	**2d**	Ph	Bn	>99 (99)	> 99:1	90
5	**2e**	*n*-Bu	*n*-Bu	99 (91)	> 99:1	60
6	**2f**	*p*-MeO-C_6H_4	Me	98 (94)	> 99:1	100
7	**2g**	*p*-NO$_2$-C_6H_4	Me	98 (70)	97:3	240

[a]Reaction conditions: [**2a-g**]$_0$:[H_2O_2]$_o$=0.5M, **1f** 0,1%, 28 °C, MeOH [b]Determined by quantitative GC analysis on the crude reaction mixture after total oxidant consumption (iodometric test). Isolated yields are given in brackets. [c]Time required for total oxidant consumption.

Table 5. Oxidation of sulfides 2a-g by aqueous hydrogen peroxide (35%) catalyzed by 1f (0.1%).[a]

4.4.2 Oxidation of halides

The activity of complex **1f** was tested also in halides oxidation. As mentioned earlier, a number of VHPO model studies concerning the mechanistic details of halides oxidation have been performed. Altought the first detailed mechanistic study of a vanadium-assisted halide oxidation by H_2O_2 was with dixovanadium(V) in aqueous solution,[29] some of the most successful reactivity studies have been performed in non-aqueous enviroment. The use of a less polar solvent enables researchers to study the behaviour of complexes in more hydrophobic environments. The energetics of protein folding dictate that the more hydrophobic residues reside on the interior of the protein where the active site is often located. As hydrophobic pokets cannot be created with ease using model compounds, the use of a less polar solvent, such as *N,N*-dimethylformamide (DMF), is a useful (although somewhat extreme) method for mimicking this non-polar environment.[30] The first study performed in DMF solution was reported by Butler et al. The catalytic species used to investigate the halide oxidizing properties of artificial models of VHPOs were the vanadium(V) oxo complexes of *N*-(2-hydroxyphenyl)salicildenamine and *N*-(2-carboxyphenyl)salicylidenamine ligands reported in Scheme 7. [31]
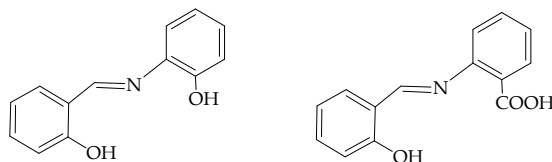
Scheme 7.

[29] de la Rosa, R. I. ; Clague, M. J. ; Butler, A. *J. Am. Chem. Soc.* **1992**, 114, 760-761.
[30] Slebodnick, C.; Law, N. A.; Pecoraro, V. L. *Biomimetic Oxidations Catalyzed by Transition Metal Complexes*, 2000, Imperial College Press, Chapter 5, pp. 227.
[31] Clague, M. J.; Keder, N. L.; Butler, A. *Inorg. Chem.* **1993**, 32, 4754-4761.

The reactions were performed in the presence of H_2O_2 as oxidant, tetrabutylammonium bromide (TBAB) as halogen source and 1,3,5-trimethoxybenzene (TMB) as organic substrate. One very important factor arised from this study is that the reaction become catalytic only with the addition of stoichiometric amounts of acid (HCl or $HClO_4$)(Scheme 8).
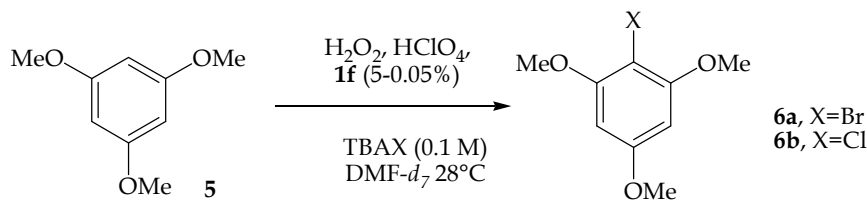
Scheme 8

In the absence of acid no reaction occurs. As mentioned above, further studies on model compounds of VHPOs has been carried out after this first work, and all of these results have suggested that the vanadium complexes must be protonated (presumibely at the peroxide) to become active. Furthermore, the acid requirement is esplicabile also in light of the overall reaction stoichiometry in which the presence of protons are needed to drive the net reaction.

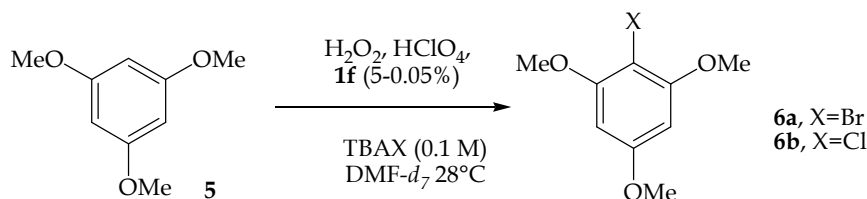$$H_2O_2 + Br^- + TMB \longrightarrow BrTMB + H_2O + OH^-$$
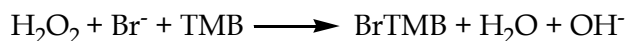
Although much progress has been made in recent yers toward achieving bromide oxidation with model complexes, Cl⁻ oxidation has remained relatively elusive. This is probabily due to the difficulties encountered by the model complexes to achieve efficient chloride oxidation. By studying the rate dependance on acid, estimated pK_a's for the protonated peroxovanadate complexes in acetonitrile have been obtained and range from 5.5-6.0, depending on the ligand. The pK_a's of HBr or HI in acetonitrile are also in this range, while the pK_a of HCl is ca. 9. Thus, one likely explanation for the lack of chloride oxidaton in acetonitrile is that the chloride buffers the reaction, preventing the formation of the active protonated peroxovanadate complex.[30]

In our work we have studied and compared the reactivity of the complex **1f** in halides oxidation with other models present in the litterature. To do this we performed the reactions under the same conditions described by Butler *et al.*[31] ($[\mathbf{1f}]_0 = 1$ mM, $[H_2O_2]_0 = 8$ mM, $[TBAB]_0 = 100$ mM, $[\mathbf{5}]_0 = 20$ mM, $[HClO_4]_0 = 3$mM in DMF) in presence of 1,3,5-trimethoxybenzene **5** as substrate for halogenation.[2a,b] Under the reaction conditions described in entry 1 Table 6, the bromination proceeds almost instantaneously to the mono brominated product **6a**. Yields slightly exceed 100%, based on the limiting reagent that, in this case, is the acid, (Table 6, entry 1). Working in absence of acid afforded only 2.5% of **6a**, consistently with the expected stoichiometry of the reaction that requires also one equivalent of acid (Table 6, entry 2).[2a,b]

Increasing both H_2O_2 and acid up to a **5**:H_2O_2:$HClO_4$=1:1:1 ratio gave **6a** in 87% yield, which could be further increased up to 92% working in the presence of a 2-fold excess of H_2O_2 (Table 6, entries 3 and 4).

In order to test the catalyticity of the system, the catalyst amount was decreased to 0.5% and 0.05%: **6a** was obtained in high yields (87%) with TON=173 in the first case (Table 6, entry 7) and 63% yield with a TON up to 1260 in the second one (Table 6, entry 8).

#	X	1f (%)	$[H_2O_2]_o$ (mM)	$[H^+]_o$ (mM)	[6a,b] (mM)	$t_{1/2}$[b] (min)	Yield[c] (%)	TON
1	Br	5	8	3	3.3	< 5	110	3.3
2	Br	5	40	-	0.5	--		0.5
3	Br	5	20	20	17.3	17	87	17
4	Br	5	40	20	18.4	6	92	18
5	Br[d]	5	40	20	10.7	250	54	11
6	Br	--	20	20	2.2	--	11[e]	--
7	Br	0.5	20	20	17.3	33	87	173
8	Br	0.05	20	20	12.6	1440	63	1260
9	Br[d]	0.05	20	20	6.0	>5000	30	600
10	Cl	5	8	3	1.2	--	40[e]	1.2
11	Cl	5	40	20	1.1	--	5[e]	1.1

[a] Reaction conditions: DMF-d_7, 28 °C using $[5]_o$=20 mM, $[TBAX]_o$=0.1 M, X=Br or Cl. [b] Time for a 50% decrease of $[H_2O_2]$o. [c] Based on the limiting agent $HClO_4$ and determined by ^1H NMR (DCE as internal standard) on the crude reaction mixture after total oxidant consumption (iodometric test). [d] $VO(acac)_2$ has been used as catalyst. [e] After 2 days.

Table 6. 6a or 6b formation as a function of $[H^+]$, $[H_2O_2]$, and V catalysts (1f or $VO(acac)_2$).[a]

In order to prove catalyst **1f** stability under turnover conditions analogous reactions were performed with $VO(acac)_2$ (5% and 0.05%): in both cases slower reaction and lower conversions into products were obtained (54% *vs* 92% using 5% of catalyst and 30% *vs* 63% using 0.05%, Table 6 entries 4, 5, 8 and 9). Reaction performed without catalyst afforded **6a** in low yields (11%) after much longer reaction time (Table 6, entry 6).

Reactions were also carried out in presence of Cl⁻ ions. Slow chlorination of **5** could be achieved (**1f**=5%) obtaining **6b** in 40% yields after 2 days (Table 4, entry 10). Increasing acid and oxidant to a **5**:H_2O_2:$HClO_4$=1:2:1 ratio (Table 6, entry 11) did not increase the system performances: similar substrate conversions were obtained (1.1 mM) indicating that the system cannot perform more than one catalytic cycle. Cl⁻ oxidation can be observed in these reaction conditions because of the partial protonation of the active vanadium peroxo complex even in the presence of a large excess of chloride ions.[3c]

4.5 Conclusions

In the present work the V(V)-catalytic oxidation of sulfides and halides using hydrogen peroxide as primary oxidant has been described and investigated in detail. Mononuclear C_3-symmetric V(V) amine triphenolate complex **1f** is particularly stable and proved to be highly efficient catalyst for these oxidations and it can be defined as a structural and also a functional model for VHPOs.

The complex adopts a trigonal bypiramidal geometry (TBP) and the coordination environment of vanadium is characterized by an oxo group, phenolate moieties and one nitrogen donor unit.

Sufoxidations proceed in high yields, without oxidant decomposition, with catalyst loading down to 0.015, TONs up to 9900 and TOFs up to 8000 h^{-1}: the system **1f**/H_2O_2 reported here seems to be the most active VHPOs model so far reported, as far as TONs (9900 in 4 h) and TOFs (up to 8000) are concerned. Moreover, bromide oxidation can be performed efficiently, leading to the halogenation of **5** and confirming that this complex can emulate the reactivity of VHPOs.

4.6 Experimental

General remarks

All chemicals and dry solvent have been purchased from Aldrich or Fluka and used as provided, without further purifications. 70 % aqueous hydrogen peroxide was purchased from Ausimont. 70 % aqueous $HClO_4$ was purchased from Erba. Triphenolamines were synthesized as previously reported.[32]

Flash chromatographies have been performed with Macherey-Nagel silica gel 60 (0.04-0.063 mm, 230-400 mesh). The NMR spectra have been recorded on a Bruker AC 250 (^{1}H: 250.13 MHz; ^{13}C: 62.9 MHz) or a Bruker AV 300 (^{1}H: 300.13 MHz; ^{13}C: 75.5 MHz) spectrometer. Chemical shift (δ) have been reported in parts per million (ppm) relative to the residual undeuterated solvent as an internal reference ($CDCl_3$: 7.26 ppm for ^{1}H NMR and 77.0 ppm for ^{13}C NMR; CD_3OD: 4.84 ppm for ^{1}H NMR and 49.05 ppm for ^{13}C NMR). The following abbreviations have been used to explain the multiplicities: s = singlet, d = doublet, t =triplet, dd = double doublet, m = multiplet, br = broad. ^{13}C NMR spectra have been recorded with complete proton decoupling. ^{51}V NMR spectra have been recorded at 301K with 10000 scans at 78.28 MHz with a broadband probe, using $VO(O_2)$ picolinate (5 10^{-3} M, water, pH = 1) as external standard. Analytical gas chromatography analysis has been carried out on a Shimadzu GC-2010 gas chromatograph with a FID detector and a capillary column EQUITY™-5 using decane as internal standard. Injector temperature has been 250 °C, detector temperature has been 280 °C and the carrier gas has been He (1 mL/min) with a HP-5MS column. APCI-MS spectra have been obtained on a LC/MS Agilent series 1100 spectrometer in positive mode, by direct flow injection using methanol as mobile phase, with ESI-ion trap mass detector. High-resolution mass spectra have been obtained with ESI-TOF Mariner™ Biospectrometry™ Workstation of Applied Biosystem by flow injection analysis; exact mass measurements have been obtained by external calibration with two appropriate lock mass compounds.

IR spectra have been recorded on a Nicolet 5700 FT-IR, with range 4000-400 cm^{-1} and resolution 4 cm^{-1}, using KBr pellets.

Melting points are uncorrected and have been determined with a Leitz-Laboroux 12.

---

[32] For the synthetic procedure of the ligands and their characterizations see Prins, L. J.; Mba, M.; Kolarović, A.; Licini, G. *Tetrahedron Letters* **2006**, *47*, 2735.

All oxygen or moisture sensitive compounds have been handled under controlled atmosphere (nitrogen) in a glovebox Mbraun MB 200MOD, equipped with a MB 150 G-I recycling system. V(V) complexes were always prepared, handled and stored in glovebox, with exception of complex **1f** which could be handled in open air.

General procedure for preparation of oxovanadatrane complexes

Complexes **1d-f** were prepared in glovebox by slowly addition of a solution of VO(O*i*-Pr)$_3$ (0.615 mmol) in dry THF (1mL) to a solution of the corresponding ligand[32] (0.610 mmol) in dry THF (5 mL). An immediate change in colour of the solution was observed (from colourless to dark-red). The solution was stirred for 1 hr at rt and then the solvent was evaporated under vacuum leading to a dark-red solid, which was repeatedly washed with small volumes of hexane and dried in vacuum. Yield: 92- 94%.

VO/*tris*-(2-hydroxy-benzyl) amine (1d)

^{1}H-NMR (300 MHz, CDCl$_3$): δ 3.61 (12H, *bs*) 7.08-6.80 (12H, *m*), 7.47-7.08 (13H, *m*), 7.82 (1H, *d*, J = *8.4* Hz),. ^{51}V-NMR (78.28 MHz, CDCl$_3$): δ -396.83, -428.78. IR (KBr, cm^{-1}): 754, 960, 1072, 1119, 1265, 1457, 1726, 2957.

VO/ *tris*-(2-hydroxy-3-methylbenzyl) amine (1e)

^{1}H-NMR (300 MHz, CDCl$_3$): δ 2.45 (9H, *s*), 2.90 (3H, *bs*), 3.77 (3H, *bs*), 6.97 (3H, *d*, J = *7.1* Hz), 7.10 (3H, *d*, J = *7.1* Hz). ^{13}C-NMR (50 MHz, CDCl$_3$): δ 16.8 (*CH$_3$*), 57.62 (*CH$_2$*), 123.4 (*CH*), 124.8 (*C*), 125.7 (*CH*), 127.6 (*CH*), 129.7 (*CH*), 167.2 (*C*). ^{51}V-NMR (78.28 MHz, CDCl$_3$): δ -381.9, (78.28 MHz, CD$_3$OD): δ -387.9. IR (KBr, cm^{-1}): 776, 890, 960, 1079, 1231, 1461, 2923, 3058. Anal. Calcd. for C$_{24}$H$_{24}$NO$_4$V: C 65.39, H 5.48, N 3.17. Found: C 65.02, H 5.52, N 3.08.

VO/*tris*-(2-hydroxy-3-*tert*-butylbenzyl) amine (1f)

^{1}H-NMR (300 MHz, CDCl$_3$): δ 1.53 (27H, *s*), 2.87 (3H, *bs*), 3.77 (3H, *bs*), 6.89 (3H, *t*, J= *7.5* Hz), 7.03 (3H, *d*, J = *7.3* Hz), 7.24 (3H, *d*, J = *7.3* Hz). ^{13}C-NMR (50 MHz, CDCl$_3$): δ 29.9 (*CH$_3$*), 35.3 (*C*), 57.6 (*CH$_2$*), 123.3 (*CH*), 125.7 (*CH*), 126.8 (*C*), 128.1 (*CH*), 136.5 (*C*), 143.9 (*C*). ^{51}V-NMR (78.28 MHz, CDCl$_3$): δ -389.07 , (78.28 MHz, CD$_3$OD): δ -396.2. IR (KBr, cm^{-1}): 752, 891, 945, 1080, 1188, 1236, 1426, 2952, 3081. APCI-MS: 568.25 [M + H]$^+$, calc. 568.26. Anal. Calcd. for C$_{33}$H$_{42}$NO$_4$V: C 69.83, H 7.46, N 2.47. Found: C 69.38, H 7.51, N 2.35.

X-ray crystallographic data collection and structure refinement for 1f

In order to obtain crystals suitable of crystallographic analysis, in a screw capped vial 30 mg of **1f** were dissolved in 2.0 mL of dichloromethane and 5.0 mL of hexane were layered on the top of the solution. After standing for a week, dark red crystals of **1f** were collected.

Crystallographic parameters are given in Table 7.

Empirical Formula	$C_{33}H_{42}NO_4V$
Formula Weight	567.7 g/mol
Crystal System	Triclinic
Space Group	P $\overline{1}$
Unit Cell Dimensions: lengths,Å	a = 8.8248(6), b =9.8319 (7), c= 17.6222(12)
angles, deg	a= 93.345(8), β= 90.242(8), γ= 92.825(8)°.
Volume, Å³	1524.5(18)
Z	2
Density d_x, g·cm⁻³	1.237
Absorption Coefficient μ, mm⁻¹	0.360
Crystal Size, mm³	0.128 x 0.205 x 0.234
Température	150 K
Scanning mode	φ-scan
$Mo_{k\alpha}$ radiation: λ(Å)	0.71073
φ min, max	0- 300.3 (°)
Index Ranges	-10 < h < 10 ; -12 < k < 12 ; -21< l < 21
Angular range	4.3° < 2θ < 51.2°
Reflections Measured at 150 K	16203
Unique reflections	5554 (R_{int}= 0.039)
Reflections with $\|Fo\| > 3\square(Fo)$	3997
Refinement Method	Full-matrix least-squares based on F using weights of $1/[\sigma^2(Fo) +0.00015 (Fo^2)$
Resolution	Direct methods (SIR97)
Minimized function	$\Sigma (\omega (Fo\text{-}Fc)^2)$
Function of weight	$\omega = 1/[\sigma^2(Fo)+0.00015(Fo^2)]$
Goodness-of-fit (S)	1.30 (1)
Final R Indices [I>2σ(I)]	R= 0.034, ωR= 0.032
Largest Diff. Peaks and Holes, eÅ⁻³	0.88 and -0.63

Table 7. Crystallographic experimental details for **1f**.

General procedure for monitoring thioanisole 2a oxidation catalyzed by 1d-f using aqueous H₂O₂ as oxidant (Table 3).

A screw-cap NMR tube was charged with a solution of complex **1d-f** (0.0054 mmol) in CDCl₃, solvent was removed under vacuum and then CD₃OD, the internal standard (1,2-dichloroethane, DCE), 35% aqueous H₂O₂ (0.0540 mmol) and thioanisole (0.0540 mmol) were added, to a final volume of 0.6 mL. Concentrations of sulfide **2a**, sulfoxide **3a** and sulfone **4a** were determinated by integration of the methyl group signals: Ph-S-*Me* (2.4 ppm), Ph-SO-*Me* (2.8 ppm) and Ph-SO₂-*Me* (3.1 ppm) in respect of the internal standard, DCE (3.78 ppm).

General procedure for monitoring thioanisole 2a oxidation catalyzed by 1f using aqueous H₂O₂ as oxidant (Table 4).

A screw-cap NMR tube was charged with a solution of the complex **1f** in CDCl₃, solvent was removed under vacuum and then CD₃OD followed by the internal standard (1,2-dichloroethane), aqueous H₂O₂ (35% or 70% in water as indicated in Table 4) and thioanisole **2a** were added to a final volume of 0.6 mL, with final concentrations as reported in Table 4.

The monitoring of the concentration of sulfide, sulfoxide and sulfone was made by integration of the methyl group signals: Ph-S-*Me* (2.4 ppm), Ph-SO-*Me* (2.8 ppm) and Ph-SO$_2$-*Me* (3.1 ppm). Final yields were determined by ^{1}H-NMR after complete H$_2$O$_2$ consumption (iodimetric test) in respect of the internal standard DCE (3.78 ppm).

General procedure for sulfoxidation reactions catalyzed by 1f using aqueous H$_2$O$_2$ as oxidant (Table 5).

To a solution of the corresponding thioethers **2a-g** (0.8 mmol) and catalyst **1f** (0.008 mmol) in MeOH, was added 35% aqueous H$_2$O$_2$ (0.8 mmol), to a final volume of 1.6 mL. The reaction mixture was stirred at rt until all oxidant consumption (iodometric test). The reaction mixture was washed with 5% sodium metabisulfite aqueous solution, the layers were separated and the aqueous one extracted with chloroform. The organic layers were washed with brine, dried over MgSO$_4$ and the solvent was removed under reduced pressure. The crude was purified by column chromatography on silica gel (petroleum ether/ ethyl acetate 1:1) obtaining the products with isolated yields reported on Table 5. Ratios sulfoxide:sulfone were determined by quantitative GC analysis and by ^{1}H NMR (CDCl$_3$, 300 MHz). Yields were determined by quantitative GC analysis. The sulfoxides **3a-g** and sulfones **4a-g** ^{1}H NMR spectra match those already reported in the literature.[33]

Procedure for the monitoring of the effect of the addition of 35% hydrogen peroxide to complex 1f.

A screw cap NMR tube was charged with a solution of complex **1f** (0.003 mmol) in CDCl$_3$. The solvent was removed under vacuum and then CD$_3$OD (0.5 mL) was added. Increasing amount of 35% aqueous H$_2$O$_2$ were added corresponding to 0.5, 1, 2 or 3 equivalents as indicated in Figure 11 and 12, recording the corresponding ^{1}H- and ^{51}V-NMR. After 3 equivalents of thioanisole were added and after total oxidant consumption (iodometric test), ^{1}H- and ^{51}V-NMR spectra were recorded.

General procedure for monitoring the bromination and chlorination reactions catalyzed by 1f using aqueous H$_2$O$_2$ as oxidant (Table 6).

A screw-cap NMR tube was charged with a solution of the complex **1f** in DMF-*d$_7$* (0.0006 mmol), 1,3,5-trimethoxybenzene (0.012 mmol), TBABr or TBACl (0.06 mmol) and DCE as internal standard. An appropriate volume of 35% aqueous H$_2$O$_2$ and 70% aqueous HClO$_4$ were added, as reported in Table 6, to a final volume of 0.6 mL. reactions were performed at rt and monitored via ^{1}H-NMR (concentrations of TMB and halogenated product were detected by integration of the aromatic CH: **5** (6.11 ppm), BrTMB **6a** (6.38 ppm) and ClTMb **6b** (6.40 ppm). Final yields were determined by ^{1}H-NMR after complete H$_2$O$_2$ consumption (iodimetric test) in respect of the internal standard DCE (3.78 ppm). Mono halogenation of

[33] (a) Brunel, J.M.; Diter, P.; Duetsch, M.; Kagan, H. B. *J Org. Chem.* **1995**, *60*, 8086. (b) Rebiere, F.; Samuel, O.; Ricard, L.; Kagan, H. B. *J. Org. Chem.* **1991**, *56*, 5991. (c) Pitchen, P.; Dunach, E.; Dshmukh, M. N.; Kagan, H. B. *J Am. Chem. Soc.* **1984**, *106*, 8188.

the substrate has been confirmed via ^{1}H-NMR and GC-MS analysis that match those already reported in the literature.[34]

[34] For compound **6a**: de La Rosa, R; Claque, M.J.; Butler, A. *J. Am. Chem. Soc.* **1992**, *114*, 760. Mondal, M.; Vedavati, G. Puranik, V.G.; Argade, N. P. *J. Org. Chem.* **2006**, *71*, 4992.
For compound **6b**: Masao, H.; Shigetaka, Y.; Hirohuki, M.; Takashi, M. *Can. J. Chem.* **1997**, *75*, 1905.

Chapter 5

Synthesis of a New Fluorinated Polyhedral Oligomeric Silsesquioxane Ligand
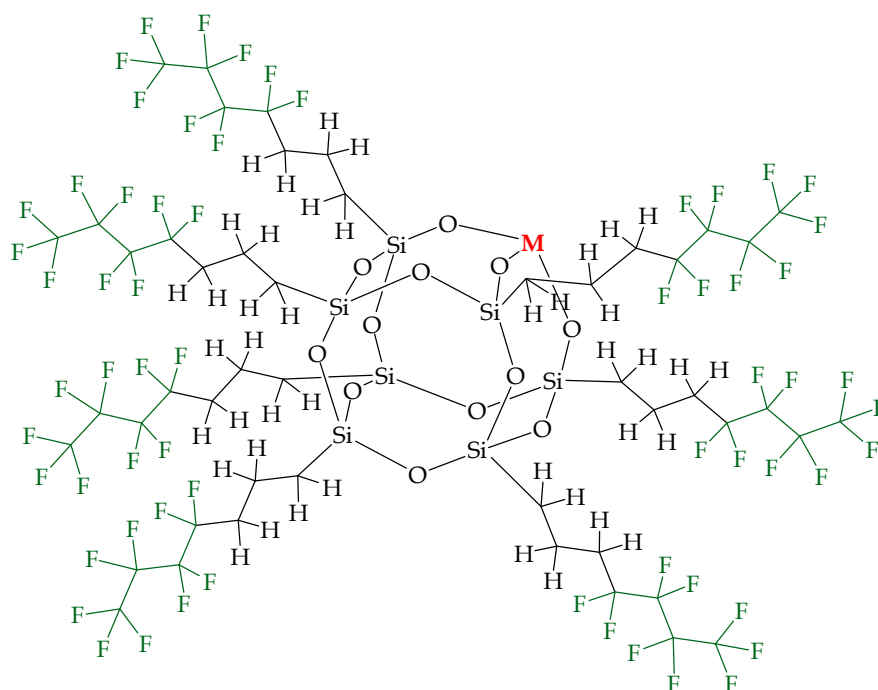
The polyhedral oligomeric silsesquioxane are an interesting class of ligands for both main group and transition-metal elements. This metal-containing silsesquioxane derivatives are proved to be efficient catalysts both in homogeneous and heterogeneous catalysis. Recently, the synthesis of a higly hydrophobic completely condensed polyhedral oligomeric silsesquioxane providied with long fluoroalkil chains was reported. This result inspired us to synthesized a new fluorinated incompletely condensed polyhedral oligomeric silsesquioxane suitable to be immobilized on polymeric fluorous membranes or in addition able to be dissolved in fluorous solvents. A series of sinthetic strategy to obtain this interesting product have been explored in our laboratory.

5.1 Introduction

Silasesquioxane is the official IUPAC[1] name for (polycyclic) compounds consisting of silicon and oxygen. Nevertheless, *silsesquioxane* is also commonly used to refer to this class of molecules. In these structures each silicon atom is bound to an average of one and a half (*sesqui*) oxygen atoms and to one hydrocarbon group (*ane*). They have the general formula $(RSiO_{1.5})$ where R is hydrogen or any alkyl, alkylene, aryl, arylene, or organofunctional derivative of alkyl, alkylene, aryl, or arylene groups.

The silsesquioxanes include random structures, ladder structures, cage structures, and partial cage structures (Figure 1). In spite of the widespread applicability of various ladder-like silsesquioxane polymers in numerous areas ranging from the development of new materials to medical fields, much more attention has attracted the silsesquioxanes with specific cage structures (structures **c-f**, Figure 1).[2]
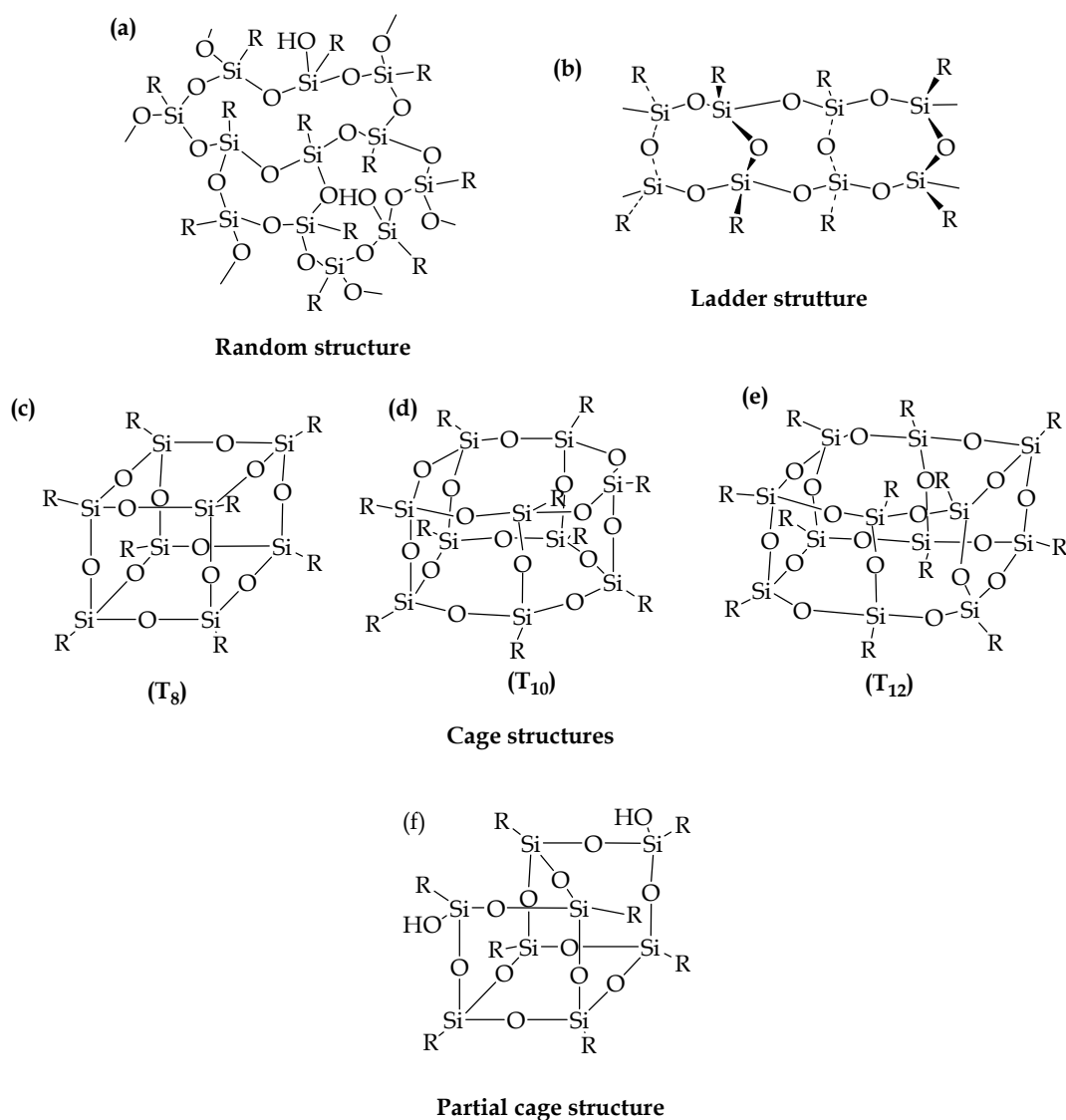

Figure 1. Structures of silsesquioxanes.

---

[1] IUPAC-rule D-6.6

[2] Baney, R. H.; Itoh, M.; Sakakibara, A.; Suxuki, T. *Chem. Rev.* **1995**, 95, 1409-1430.

These polyhedral oligomeric silsesquioxanes have been designated by the abbreviation POSS. POSS compounds, with sizes of from 1 to 3 nm in diameter, can be thought of as the smallest possible particles of silica. They may be viewed as molecular silicas. However, unlike silica, silicones, or fillers, each POSS molecule contains organic substituents on its outer surface that make the POSS nanostructure compatible with polymers, biological systems or surfaces. Furthermore, these groups can be specially designed to be nonreactive or reactive.[3]

A variety of POSS nanostructured chemicals has been prepared which contain one, or more, covalently bonded reactive functionalities that are suitable for polymerization, grafting, surface bonding or other transformations. The incorporation of POSS derivatives into polymeric materials can lead to dramatic improvements in polymer properties which include, but are not limited, to: increases in use temperature, oxidation resistance, surface hardening, and improved mechanical properties, as well as reductions in flammability, heat evolution and viscosity during processing. POSS nanostructures have also shown significant promises for use in catalyst supports, biomedical applications as scaffolds for drug delivery, imaging reagents, and combinatorial drug development.[2]

More recently, these scaffolds have attracted particular interest for the preparation of superhydrophic surfaces. Mabry et al. prepared fully fluorinated polyhedral POSS molecules (FH and FD in Figure 2), in which the low surface energy of the fluorinated compounds are accompanied by the increased roughness of the material surface induced by the structural features of the polyhedral molecules.[4]
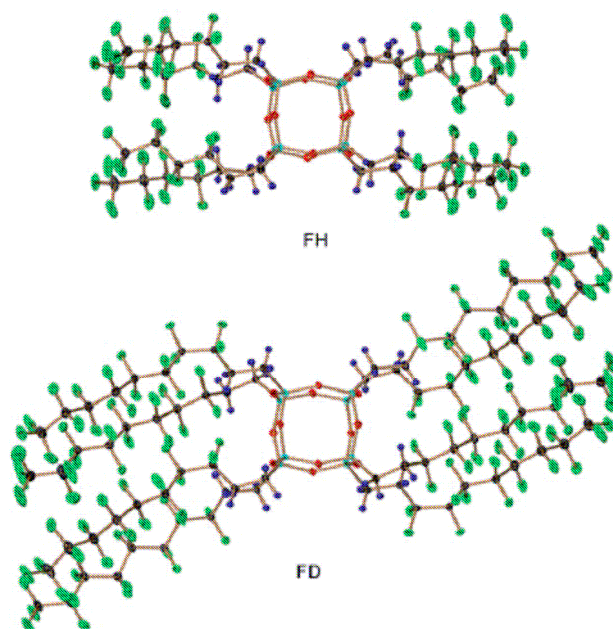

Figure 2. X-Ray structures of F-POSS compounds synthesized by Mabry. Crystals were obtained dissolving the molecules in fluorinated solvents and using solvent evaporation/vapour diffusion techniques.

[3] Li, G.; Wang, L.; Ni, H.; Pittmann, C. U. *J. of Inorg. and Organomet. Pol.* **2002**, 11, 123-154.
[4] Mabry, J. M.; Vij, A.; Iacono, S. T.; Viers, B. D. *Angew. Chem. Int. Ed.* **2008**, 47, 4137-4140.

Both the low surface energy, and the increased roughness contribute to enhance the hydrophobic character of these materials. Crystals suitable for X-Ray analysis of F-POSS compounds were obtained dissolving the molecules in fluorinated solvents and using solvent evaporation/vapour diffusion techniques. The representations of FH and FD are shown in Figure 2.

The packing of FD results in the POSS cores resting at an angle, with respect to the linear fluoroalkyl groups. This results in a rougher packing surface than FH, as seen in the electrostatic potential surfaces (Figure 3). As written by the authors in their paper "To our knowledge, FD is the most hydrophobic crystalline solid material known."[21]
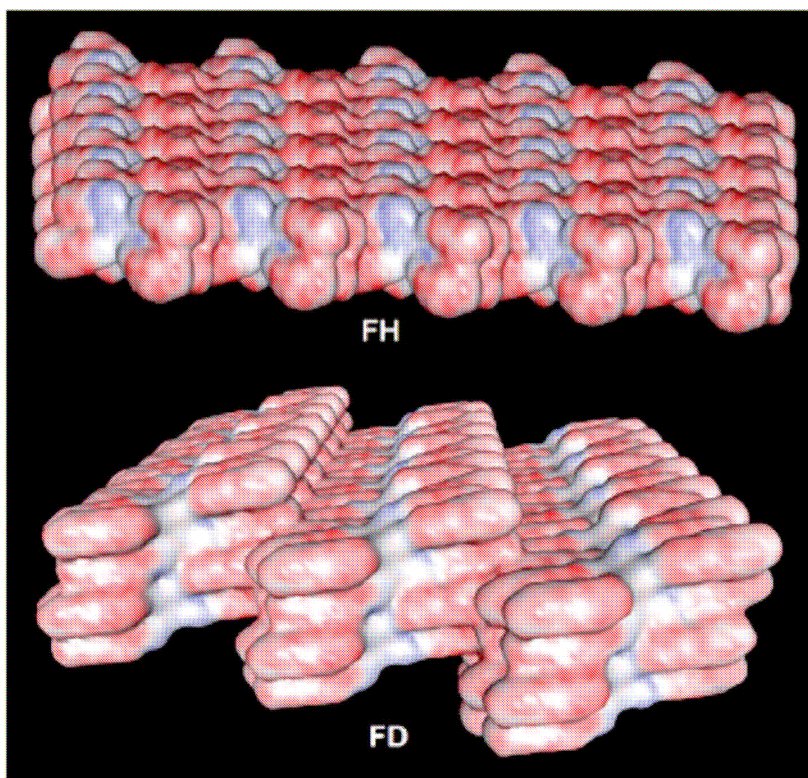

Figure 3. Electrostatic potential surfaces of FH and FD POSS.

Besides fully condensed POSS structures, open-corner POSS compounds with incompletely condensed silanol groups (with general formula $R_7Si_7O_9(OH)_3$ are far more interesting due to the possibility of further functionalization both with specific organosilanes and with heteroelements. Moreover, these compounds are suitable for reaction with a variety of transition metal complexes to form completely condensed metal-silsesquioxanes (**M-POSS**).[5] Numerous strategies were developed for the synthesis of POSS metal complexes. In particular three techniques have been mostly utilized:[6] i) the direct metathetic reaction between silanols and less acidic alkyl, amide or alkoxide ligands, ii) amine-assisted metathesis of metal-halide complexes and iii) metathetic replacement of M-halide bonds by

---

[5] a) Hanssen, R. W. J. M.; van Santen, R. A.; Abbenhuis, H. C. L. *Eur. J. Inorg. Chem.* **2004**, 675. b) Feher, F. J.; Walzer, J. F. *Inorg. Chem.* **1991**, 30, 1689. c) Wada, K.; Nakashita, M.; Yamamoto, A.; Mitsudo, T. *Chem. Comm.* **1998**, 133. d) Maschmeyer, T.; Klunduk, M. C.; Martin, C. M.; Shephard, D. S.; Thomas, J. M.; Johnson, B. F. G. *Chem. Commun.* **1997**, 1847. e) Smet, P.; Devreese, B.; Verpoort, F.; Pauwels, T.; Svoboda, I.; Foro, S.; van Beeumen, J.; Verdonck, L. *Inorg. Chem.* **1998**, 37, 6583.

[6] Feher, F. J.; Budzichowski, T. A. *Polyhedron* **1995**, 14, 3239-3252.

silasesquioxide anion "equivalents". These are shown in Scheme 1 (equations **a-c** respectively).
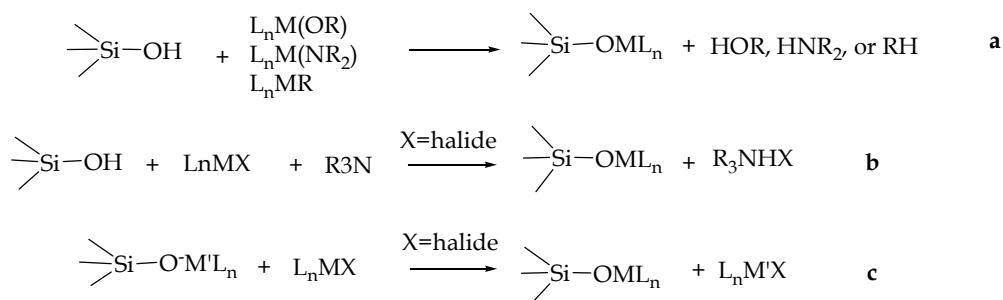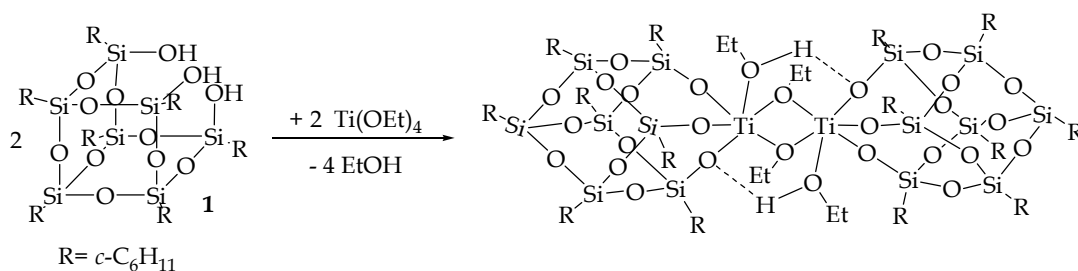

Scheme 1

The amine-assisted metathesis of SiO-H for LnM-X bonds is quite convenient and has proven to be the most effective method for the synthesis of POSS complexes. This procedure, exemplified in Scheme 2[7] for the synthesis of a zirconium complex, can be applied to a variety of other reagent including: $O=VCl_3$,[5b] $CpTiCl_3$, $TiCl_3(Nme_3)_2$,[8] $VCl_3(Nme_3)_2$,[9] $CrCl_3(Nme_3)_2$,[9] $RsiCl_3$ (R= H, aryl, alkyl, Cl),[10] $MeGeCl_3$,[10] PCl_3,[11] $AsCl_3$,[11] $SbCl_3$,[11] BI_3.[12]
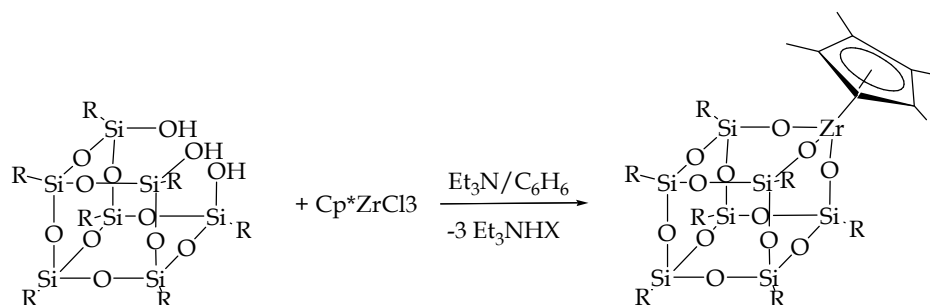
Scheme 2. Synthesis of a zirconium complex via amine-assisted metathesis of metal-halide complexes

The direct reaction between silanols and alkoxides ligands are largely used and studied especially with early transition metals. For example, in the presence of titanium tetraethoxide, trisilanol **1** forms a dimeric complex (Scheme 3).[13]

$R= c\text{-}C_6H_{11}$

Scheme 3. Synthesis of the Ti(IV) complex. In this complex two titanium-capped silsesquioxane cages are connected through alkoxide bridges.[13]

[7] Feher, F.J. *J. Am. Chem. Soc.* **1986**, 108, 3805.
[8] Feher, F.J., Gonzales, S. L.; Ziller, J. W. *Inorg. Chem.* **1988**, 27, 3440.
[9] Feher, F.J., Walzer, J. F. *Inorg. Chem.* **1990**, 29, 1604.
[10] Feher, F.J., Newman, D. N.; Walzer, J. F. *J. Am. Chem. Soc.* **1989**, 111, 1741.
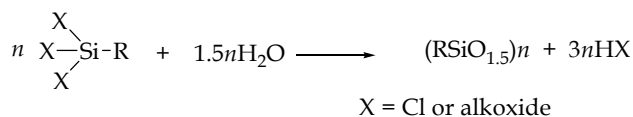[11] Feher, F.J., Budzichowski, T. A. *Organometallics* **1991**, 10, 812.
[12] Feher, F. J.; Budzichowski, T. A., Ziller, J. W. *Inorg. Chem.* **1992**, 31, 5100.
[13] Crocker, M.; Herold, R. H. M.; Orpen, A. G.; Overgaag, M. T. A. *J. Chem. Soc. Dalton. Trans.* **1999**, 3791.

These particular structures provide an important tool in understanding the processes occurring at the active sites of heterogeneous silica supported catalysts and the nature of the active species involved in catalysis. Indeed, as on silica surfaces, the incompletely condensed silsesquioxanes present a variety of silanol groups ready to react with transition metals, in such a way they constitute valid homogeneous models for heterogeneous catalysts. These metal-containing cage structures have also proved to be promising as homogeneous catalysts especially in alkene polymerisation, alkene methatesis and alkene epoxidations.[5a,14]
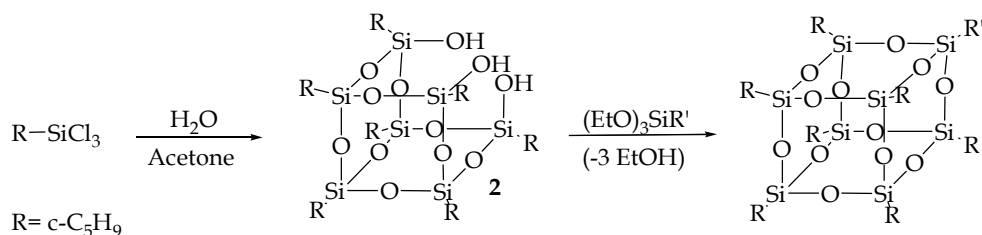
5.2 Synthesis of incompletely-Condensed POSS Frameworks

Since their discovery and isolation in 1946,[15] many stoichiometrically well-defined polyhedral oligomeric silsesquioxanes frameworks have been reported with synthetically useful functional groups.[16] Synthetic methodologies for their preparation are well documented. The general route consists in hydrolitic condensation of $RSiCl_3$ or $RSi(OR^I)_3$ precursors (Scheme 4).

$$n \; X-\underset{\underset{X}{|}}{\overset{\overset{X}{|}}{Si}}-R \;\; + \;\; 1.5n H_2O \longrightarrow (RSiO_{1.5})n \; + \; 3nHX$$

X = Cl or alkoxide

Scheme 4

The structure of the species formed in the reaction is highly dependent on the reaction conditions, especially the concentration of reactants (particularly the silane monomers), solvent, pH, temperature, availability of water, acid or base catalysis and the solubility of the product. For the synthesis of fully-condensed silsesquioxanes, $RSiX_3$ (X= Cl or OR^I) a wide variety of hydrocarbon substituent R can be used. T_8 cages are often formed preferentially due to lower solubility in common organic solvent than the corresponding T_{10} or T_6 analogues. Fully condensed silsesquioxanes can also be prepared by corner-capping reactions of the incompletely condensed $R_7Si_7O_9(OH)_3$ molecule (Scheme 5, structure **2**).

Scheme 5

As mentioned earlier, besides fully condensed POSS structures, the so-called incompletely condensed silanol POSS structure exist. Unfortunately, for many years, the pool of incompletely condensed silsesquioxanes available in synthetically useful quantities was limited to a small number of compounds synthesized via hydrolitic condensation of

[14] For review about the activity of M-POSS as homogeneous catalysts see: a) Abbenhuis, H. C. L. *Chem. Eur. J.* **2000**, 6, 25. b) Duchateau, R. *Chem. Rev.* **2002**, 102, 3525.

[15] Scott, D. W. *J. Am. Chem. Soc.* **1946**, 68, 356.

[16] a) Baney, R. H.; Itoh, M.; Sakakibara, A.; Suzuki, T. *Chem. Rev.* **1995**, 95, 1409. b) Voronkov, M. G.; Lavrent'yev, V. I. *Top. Curr. Chem.* **1982**, 102, 199. c) Sellinger, A.; Laine, R. M. *Macromolecules*, **1996**, 29, 2327.

trifunctional silanes possessing relatively bulky organic groups. We have called this synthetic strategy *direct synthesis.*

In the *direct synthesis* the trifunctional organosilicon monomers $RSiCl_3$ or $RSi(OCH_3)_3$ mixed with water in an appropriate solvent give the open corner POSS that precipitate out of the solution.

However, in the literature is present a different synthetic strategy to obtain silanol POSS structures. We have named it *corner cleavage procedure.* In the *corner cleavage procedure*, the T_8 compound is previously prepared and successively hydrolyzed in acid or base conditions. This two synthetic routes, presented schematically in Scheme 6 (Equations **a** and **b**), will be explained in more details in the following.

Scheme 6

5.2.1 Direct Synthesis

For the preparation of partly-condensed silsesquioxanes via *direct synthesis*, alkyl trichlorosilanes $RSiCl_3$, are generally required and, interestingly, the choice of hydrocarbon substituent is restricted to cyclopenthyl, cyclohexyl, cycloheptyl or *iso*-buthyl group. A drawback of the synthesis of incompletely-condensed silsesquioxanes is that often gestation periods of several months are required.

$R= c\text{-}C_5H_9 \text{ or } c\text{-}C_6H_{11}$

Scheme 7. The first synthesis of multigram quantities of incompletely condensed silsesquioxanes in a short period of time.[17]

Most attempts to speed up these reactions have failed. For the hydrolysis of $RSiCl_3$ to $R_7Si_7O_9(OH)_3$ where R= c-C_5H_9 or c-C_6H_{11} the gestation time can be shortened considerably by heating the reaction mixture to reflux (Scheme 7).[17] However, the yield of products is lower since variable amounts of resins are also formed, which require additional purification steps. In all of these cases, the outcome of the reaction is strongly driven by the low solubility of the desired product in the solvent used which subtract to the equilibria the $T_7(OH)_3$ compound. However, as for T_8 POSS, this is strongly dependent on the R-substituents and to the experimental conditions.

More recently a successful strategy have been developed for the synthesis of **3** (Scheme 8) having 3,3,3-trifluoropropyl substituents. This methodology is based on the low solubility of the trisodium salt $Na_3(3,3,3$-trifluoropropyl$)_7Si_7O_{12}$ which is formed when the exact stoichiometric conditions reported in Scheme 8 are adopted.[18]

$RSi(OMe)_3$: H_2O: NaOH= 7:12:3
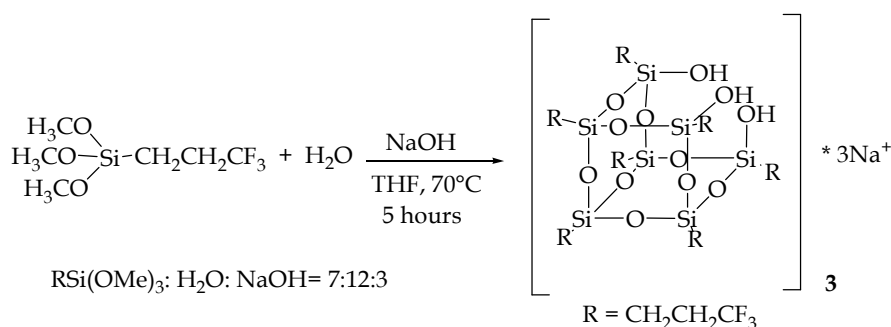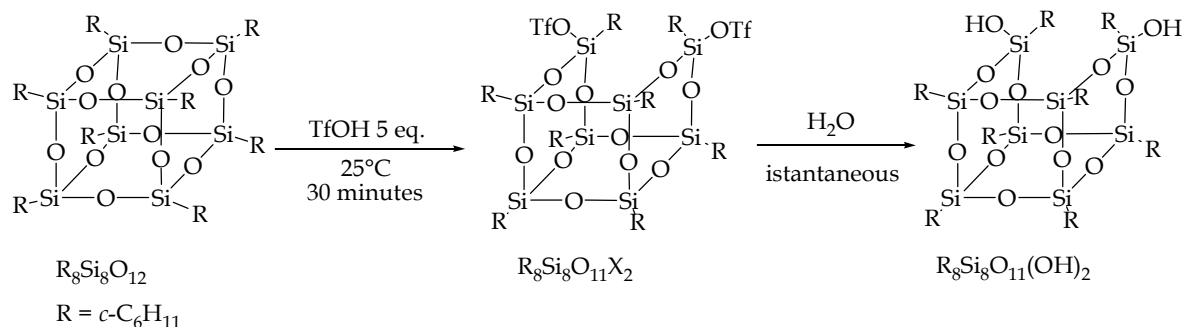
Scheme 8

5.2.2 Corner Cleavage

Feher and co-workers have carried out impressive work on both improving the existing, as well as developing new, silsesquioxanes synthesis. In particular, they reported an interesting route to incompletely condensed silsesquioxanes by either acid- or base-mediated splitting of the Si-O-Si edges of the fully condensed silsesquioxanes $R_6Si_6O_9$ or $R_8Si_8O_{12}$. In principle incompletely-condensed silsesquioxanes with a wide variety of substituents are available by this synthetic route overcoming the limit imposed by the solubility of several POSS compounds, characteristic that is essential for the selectivity of the product formation.

The first reported controlled cleavage of a cube-octamer silsesquioxane ($R_8Si_8O_{12}$) dates 1998.[19] Feher noted that $R_8Si_8O_{12}$ react with strong acids such as CF_3SO_3H (TfOH= triflic acid) or HBF_4/BF_3 to produce $R_8Si_8O_{11}X_2$ (X= F, OTf) frameworks resulting from selective cleavage of one Si-O-Si linkage; subsequent hydrolisis affords the $R_8Si_8O_{11}(OH)_2$ molecules derived from the net hydrolisis of one Si-O-Si linkage in $R_8Si_8O_{12}$ (Scheme 10).

---

[17] Feher, J. F.; Budzichowski, T. A.; Blanski, R. L.; Weller, K. J.; Ziller, J. W. *Organometallics* **1991**, 10, 2526-2528.

[18] Koh, K.; Sugiyama, S.; Morinaga, T.; Ohno, K.; Tsujii, Y.; Fukuda, T.; Yamahiro, M.; Iijima, T.; Oikawa, H.; Watanabe, K.; Miyashita, T. *Macromolecules* **2005**, 38, 1264-1270.

[19] Feher, F. J.; Soulivong, D.; Eklund, A. G. *Chem. Comm.* **1998**, 399-400.

$R_8Si_8O_{12}$

$R = c\text{-}C_6H_{11}$

$R_8Si_8O_{11}X_2$

$R_8Si_8O_{11}(OH)_2$

Scheme 9

These results have demonstrated for the first time that readily available $R_8Si_8O_{12}$ frameworks can be used as precursors for incompletely condensed Si/O frameworks. Later Feher reported that $R_8Si_8O_{12}$ frameworks react selectively with aqueous Et_4NOH to afford incompletely condensed POSS. The product obtained (**4** or **5** in Scheme 10) is dependent on the reaction conditions (in particular temperature and reaction time).


$R = c\text{-}C_6H_{11}$
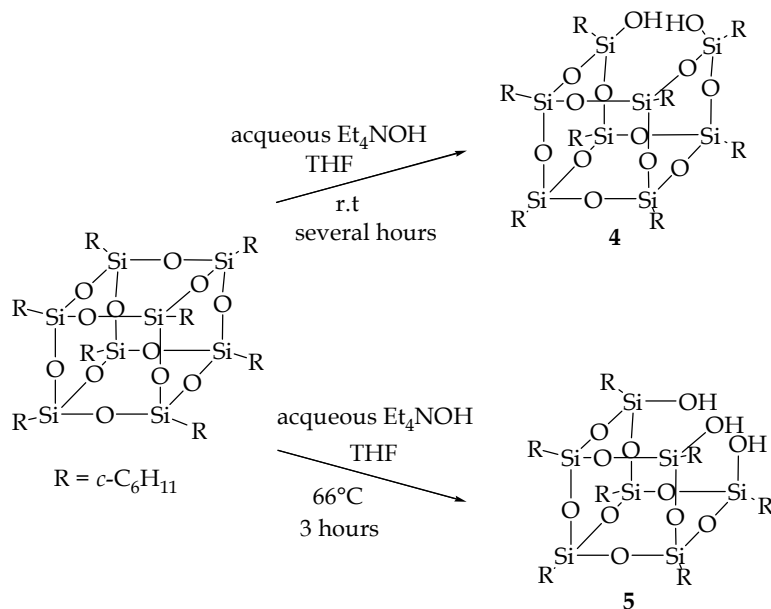
Scheme 10

5.2.3 Synthesis of incompletely condensed Fluoropropyl POSS

As emerged from the studies described in detail in chapter 2, the vanadium silsesquioxane complex **6** show high efficiency and selectivity as catalyst in oxygen transfer reactions. As described, sulfoxidation reactions carried out in CHCl₃, using cumylhydroperoxide as oxidant, displays high reactivities and selectivities. Furthermore, this compound is also capable to catalyze *N*-oxidations and epoxidations.[20]

---

[20] Unpublished data.

6   R= *i*-butyl
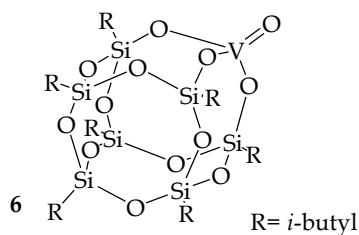
The high reactivity of vanadium POSS complex **6** in oxidation reactions led us to explore the possibility to utilize a fluorinated POSS analog able to be immobilized on polymeric fluorous membranes or in addition able to be dissolved in fluorous solvents. In this way the catalyst could be recycled. Furthermore, the fluoroalkyl substituents ensure an hydrophobic environment surrounding the active site of the catalyst, preventing in this way both the hydrolysis of the catalyst and the leaching of the metal.


7
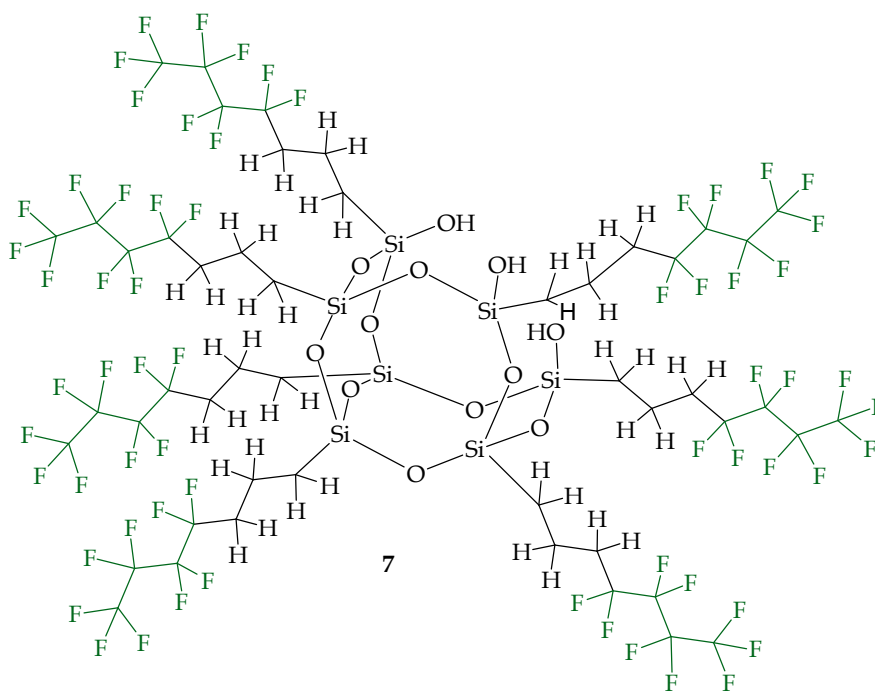
For the synthesis of the fluoroalkyl POSS ligand **7** (T_7 F-POSS) we have followed three different strategies: (*i*) the synthesis of the T_8 F-POSS compounds reported by Mabry *et al.*[21], and its hydrolytic corner cleavage under basic environment, (*ii*) the direct synthesis of the T_7 F-POSS starting from appropriate quantities of a base, water and the monomer **8** (*iii*) the preparation of the trisodium salt of the corresponding perfluoralkilated ethoxymolecules.

The synthesis of the T_8 F-POSS compound was carried out following the procedure reported by Mabry (Scheme 11) [21] : to a solution of **8** (4.1 g) in ethanol (10 mL) was added KOH (2 mg) and deionized water (270 mg) at room temperature. After continuous stirring for 24 hours, a white precipitate was filtered and washed several times with ethanol and water obtaining 3.56 g of product **9**. The product was analyzed by ^{1}H NMR (Figure 4) and ^{19}F NMR spectroscopy.

[21] Mabry, J. M.; Vij, A.; Iacono, S. T.; Viers, B. D. *Angew. Chem. Int. Ed.* **2008**, 47, 1-5.
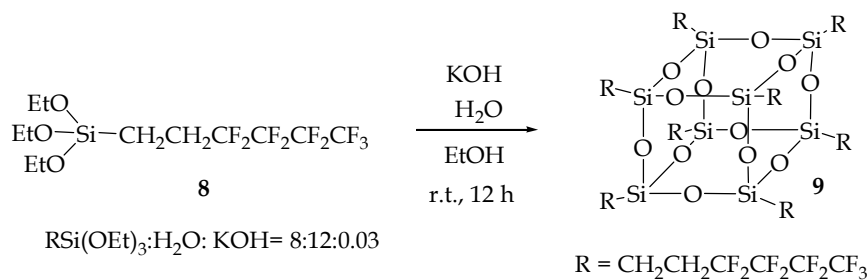
Scheme 11
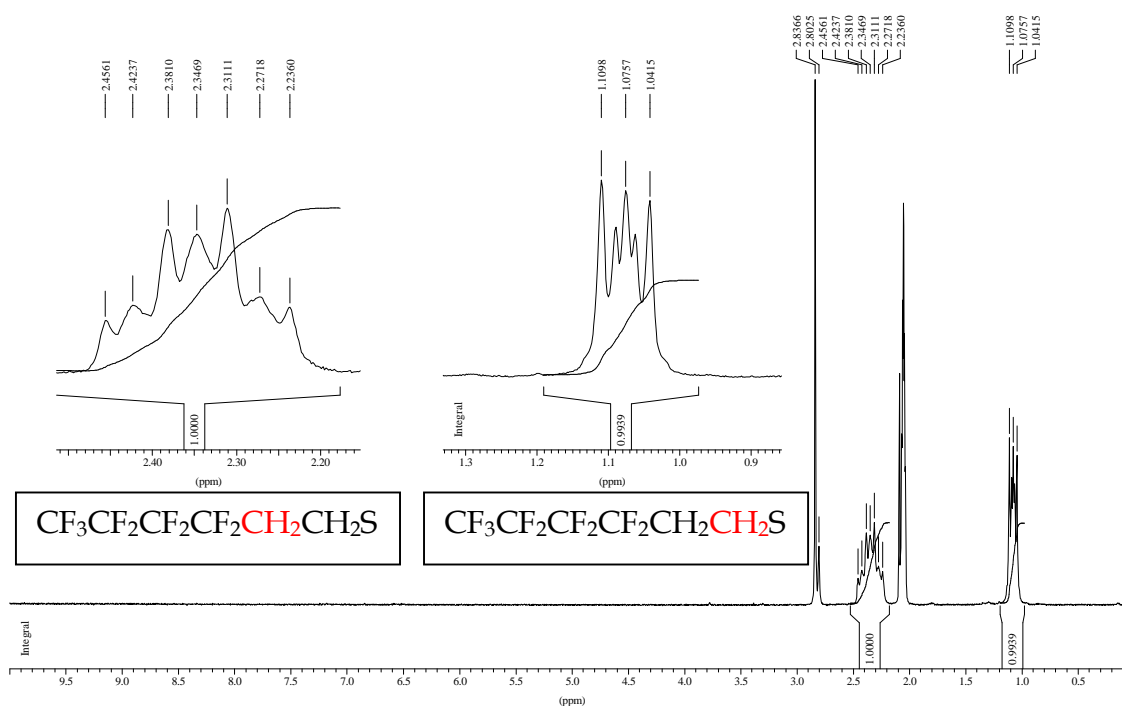
Figure 4. ^{1}H NMR spectrum of the product T_8 F-POSS **9**.

At first, we examined the possibility to obtain a fluorinated POSS ligand **7** via a base mediated selective cleavage of the corresponding T_8 F-POSS (Scheme 12). An overview of the experimental conditions applied for the cleavage is provided in Table 1.
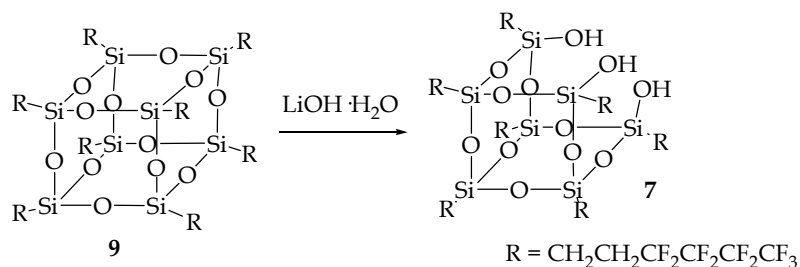
Scheme 12

Entry	LiOH (equiv) [a]	H_2O (equiv)[a]	Time(h)	Solvent	T (°C)	Product
1	6.9	7.9	12	EtOH	r.t.	No
2	6.9	7.9	48	EtOH	r.t.	No
3	6.9	7.9	18	EtOH	60	Traces
4	10	10	18	EtOH	60	Traces
5	20	20	18	EtOH	60	Traces
6	10	10	60	EtOH	60	Yes
7	10	10	19	THF	66	No

Table 1. [a] LiOH and H_2O equivalents with respect to **8** (T_8 F-POSS).

In order to obtain the desired trisilanol POSS **7**, octameric F-POSS compound **9**, distilled water, LiOH·H_2O and the appropriate dry solvent were used under an argon atmosphere. The mixtures were magnetically stirred under the conditions reported in Table 1. Acidification of the reaction mixture with 1N HCl(aq), gives a sticky oil when ethanol was used as solvent (entries 1-6). These oils, slightly soluble in common organic solvents, were analyzed by mean of ^{1}H NMR, ^{19}F NMR and IR spectroscopy.

The reactions carried out at room temperature (Entries 1-2) yielded a mixture of products, as far as ^{1}H NMR analysis is concerned, but no evidence of the desired products could be observed by ^{19}F NMR spectroscopy. However, rising the temperature to 60°C (Entries 3-5), the complex reaction mixture showed the presence of new signals in ^{19}F NMR spectrum, compatible with the desire product formation, however a more complex ^{1}H NMR spectrum was obtained.

The extension of the reaction time (60 hours, Entry 6) allowed to obtain a white powder, even if in low amount. The crude product, washed several times with water and dried under vacuum for many hours, was analyzed by IR and ^{19}F NMR spectroscopy. IR spectrum revealed a characteristic –OH absorpition band at 3376.9 cm^1 (Figure 5), while ^{19}F NMR spectrum showed the presence of a new product (Figure 6). The peaks at –83.11 ppm and –82.29 ppm are present in a 4:3 ratio, consistent with the formation of the trisilanol x. Unfortunately the amount of compound oftained was not sufficient for further characterisations and any attempts to scale up the reaction or obtaining the same compound have been so far unsuccesful.
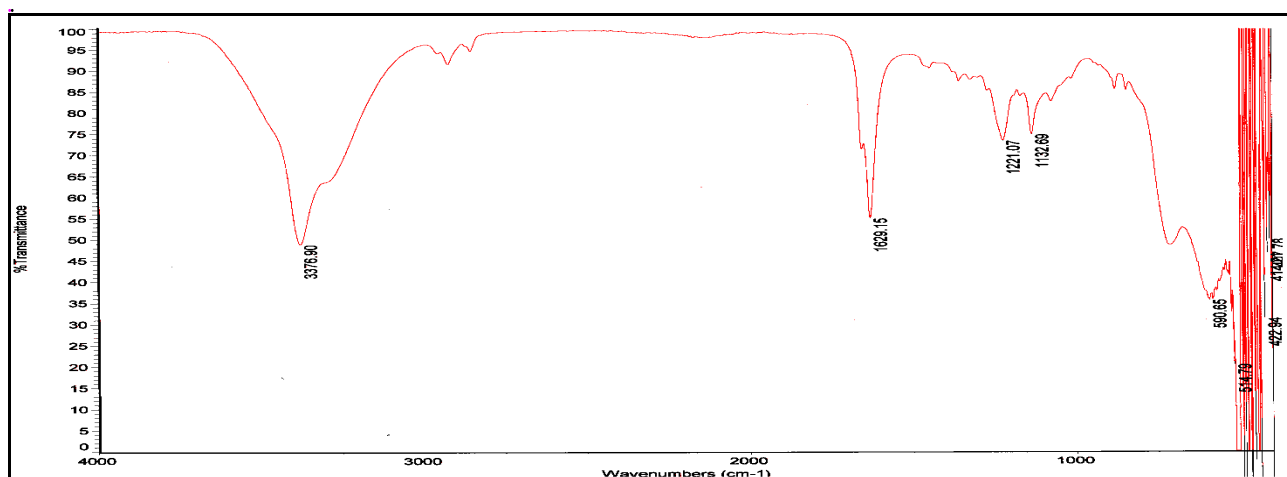
Figure 5. IR spectrum of product obtained under experimental conditions as shown in entry 6 (Table 1).
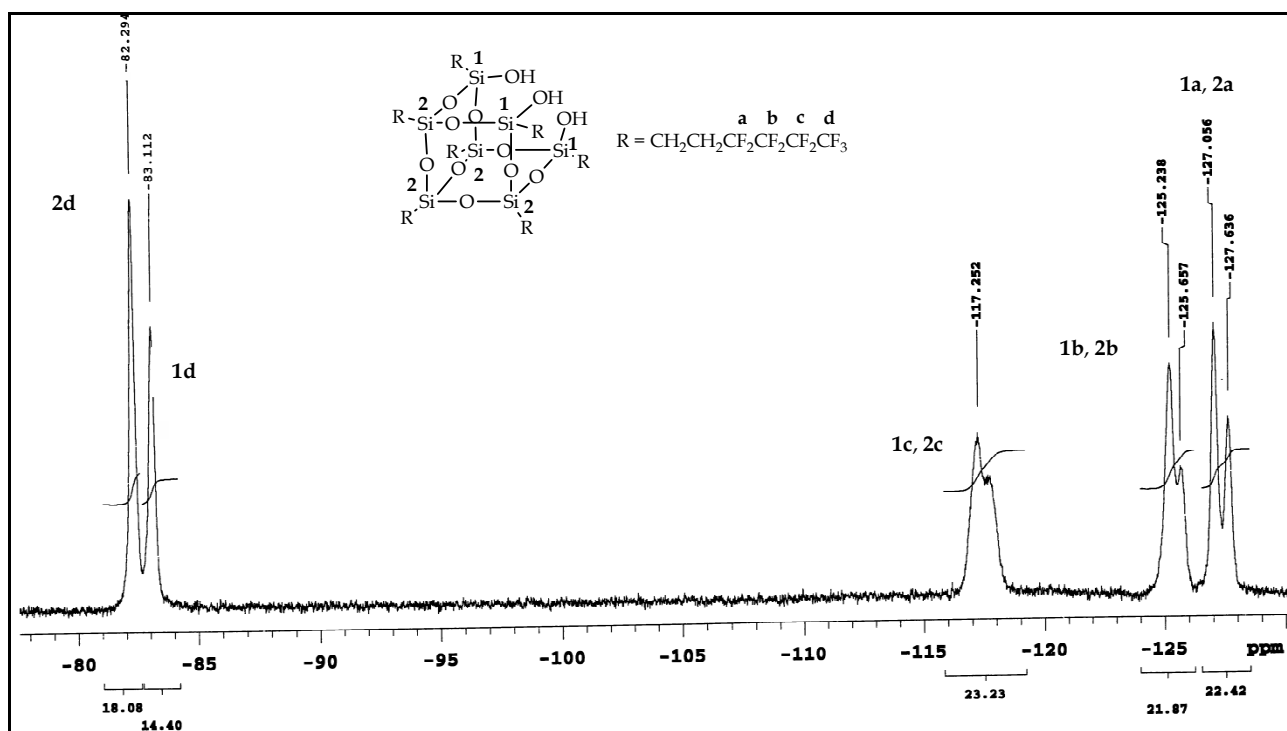

Figure 6. ^{19}F NMR (200 MHz, Acetone) of product obtained under experimental conditions as shown in entry 6 (Table 1).

Another synthetic route was also investigated. This strategy follows the so called *direct synthesis.* 1H,1H,2H-nonafluorohexyltriethoxysilane **8** was hydrolytically condensed in the presence of KOH as base. As shown in **Eqs 14**, the reaction with KOH, carried out in ethanol, was performed at room temperature for 12 hours. Acidification with 1N HCl(aq) and solvent removal in vacuo, led to the formation of a white solid. ^{1}H NMR spectrum displayed the presence of the fully condensed product **9** (T_8 F-POSS). Working with NaOH as a base, a colourless sticky oil precipitate was obtined after acidification. However no significative ^{1}H and ^{19}F NMR signals were detected.
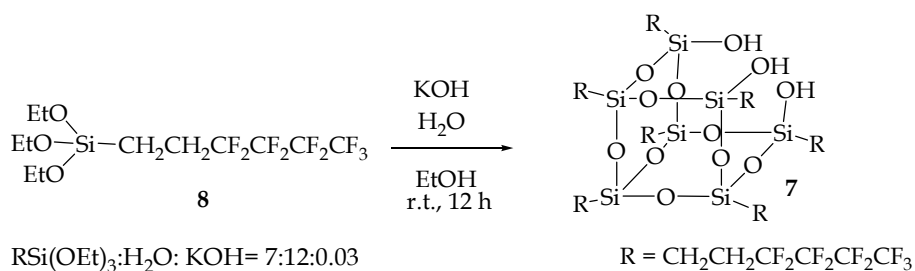
Scheme 13

The third strategy consisted in the hydrolitic condensation of 1H,1H,2H-nonafluorohexyltriethoxysilane **8** in the presence of NaOH and water (Scheme 14). Unfortunately the trisodium salts did not precipitate from the reaction mixture even after 12 hours of reaction. After acidification with HCl, a colourless sticky oil was obtained and also in this case, no significative ^{1}H and ^{19}F NMR signals could be detected.
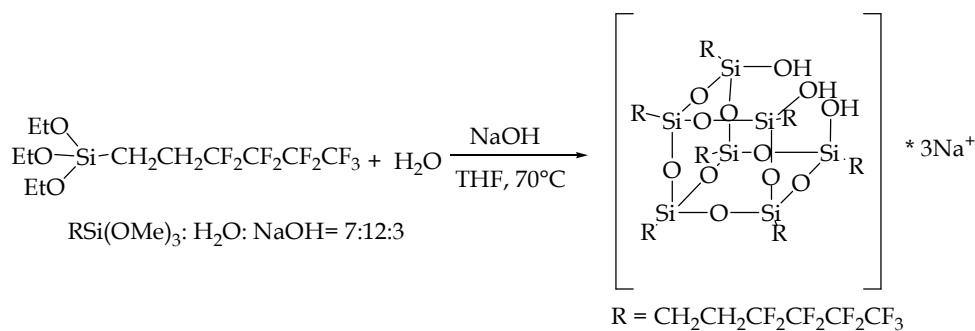
Scheme 14

The crude product, obtained via this route, was anyhow purified via gel permeation chromatography (GPC) in tetrahydrofuran (THF). The GPC chromatograms of T_8 F-POSS **9** (Scheme 11) and the crude product (Scheme 14) are reported in Figure 7. The chromatograms show the presence of a new specie in the crude product in Scheme 14 with a different eluition time for the T_8 F-POSS compound (T_8 F-POSS **9** 13.5 min, the new compound T_7 F-POSS 14 min). However T_8 can be present in the reaction mixture. Attempts to purify the reaction mixture via GPC has been so far unsuccesful.
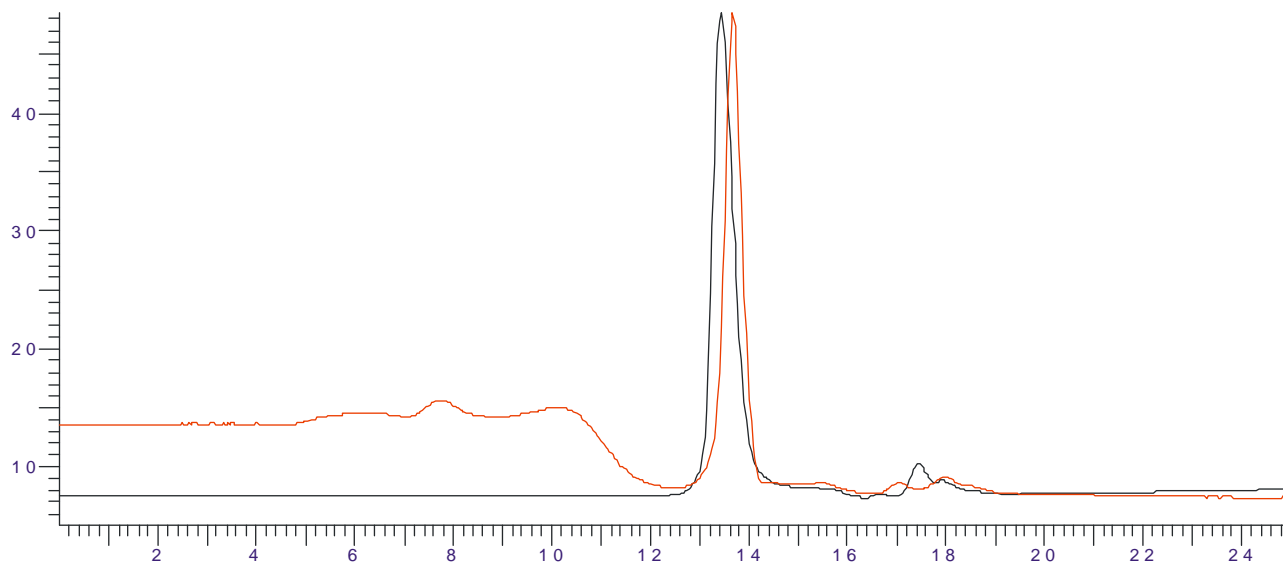
Figure 7. GPC chromatograms obtained for T_8 F-POSS (retention time 13.5 min.) and T_7 F-POSS (retention time 14 min.).

5.3 Conclusions

Initial attempts to obtain the $T_7(OH)_3$ F-POSS ligand **7** following three different synthetic procedures have been carried out.

Results so far obtained by this work, which is still in progress, may be summarized as follows:

1. the base mediated corner cleavage of T_8 F-POSS **9** has been carried out in various reaction conditions: solvents, concentrations of reactants and reaction temperatures. The best results was observed in the reaction conditions shown in entry 6, Table 1 (10 equivalents of LiOH and 10 equivalents of water added to a suspension of T_8 F-POSS in EtOH, heated at 60°C for 60 hours). Unfortunately, a reproducible procedure could not be developed. The direct synthesis of $T_7(OH)_3$ F-POSS **7** resulted to be ineffective, because a too much complex mixture of products have been obtained.

2. The synthetic method occurring through the formation of the trisodium salt, even did not allow so far the obtainment of the desired product, seems to be promising. GPC analysis shows the prevalent presence of a single product, different from the T_8.

Further studies will be carried out in the next future in order to obtain this new class of very promising fluorinated ligands.

5.4 Experimental

General remarks

All chemicals and dry solvent have been purchased from Aldrich or Fluka and used as provided, without further purifications. (1H,1H,2H-nonafluorohexyl)triethixysilane was purchesed from Gelest Inc. The NMR spectra have been recorded on a Bruker AC 250 (^{1}H: 250.13 MHz; ^{13}C: 62.9 MHz) or a Bruker AV 300 (^{1}H: 300.13 MHz; ^{13}C: 75.5 MHz) spectrometer. The ^{19}F NMR spectra were recorded on Varian Mercury 200 MHz spectrometer. IR spectra have been recorded on a Nicolet 5700 FT-IR, with range 4000-400 cm^{-1} and resolution 4 cm^{-1}, using KBr pellets. The GPC consists of a high pressure liquid chromatography pump (HPLC), two size exclusion columns (Phenogel 5 x 10^3 Å and 5 x 10^{-4} Å) connected in series, a differential refractometer (ERC-7512, Erma Tokyo) to monitor the refractive index continuously and a data acquiasition system to store the data. The samples were injected through a valve of capacity 20 µl. Tetrahydrofuran (THF) was used as the eluent at a flow rate of 1 mL/min.

Synthesis of the T$_8$ F-POSS 9:

To a solution of 1*H*,1*H*,2*H*-nonafluorohexyl)triethixysilane **8** (4.1 g, 0.01 mol) in ethanol (10 mL) was added KOH (2 mg, 0.035 mmol) dissolved in deionized water (270 mg, 0.015 mol) at room temperature. After continuous stirring for 24 hours a white precipitate was filtered and washed repeatedly with ethanol and water obtaining 2.7 g (80% yield) of product.

Synthesis of the trisilanol F-POSS 7 by hydrolytic corner cleavage (Table 1, entry 6):

To a suspension in ethanol (10 mL) of T$_8$ F-POSS **9** (0.5 g, 0.209 mmol), LiOH·H2O (90 mg, 2.09 mmol) and water (20 mg, 1.045 mmol) were added. The reaction mixture was heated at 60°C under nitrogen. After 30 minutes of stiring, a complete dissolution of **9** was observed. After the dissolution, the reaction was continued for 60 hours at the same conditions. The reaction mixture was quenched with HCl 1M obtaining a white gel-like precipitate that was washed several times with water. The crude product was leave in a vacuo oven for a night obtaining a white powder that was analized by ^{19}F NMR and IR spectroscopy.
^{19}F NMR (200 MHz, Acetone): δ -82.29 (12 F), -83.112 (9 F), -117.25 (14 F), -125.23 and –125.657 (14 F), -127.056 and –127.636 (14 F).
IR v (cm^{-1}): 3376.60, 1629.15, 1221.07, 1132.69.

Synthesis of the trisilanol F-POSS via direct synthesis (Eqs 15):

(1*H*,1*H*,2*H*-nonafluorohexyl)triethixysilane **8** (5 g, 0.0136 mol), THF dry (20 mL), distilled water (0.315 g, 0.0174 mol), and sodium hydroxide (0.233 g, 0.0058 mol) were charged into a four-necked flask equipped with a reflux condenser. The mixture was refluxed in an oil bath thermostated at 70°C for 5 h with magnetically stirring and under nitrogen. The system was allowed to get cool to room temperature and left for a night. The reaction mixture was added dropwise and under vigorous stirring to a 1M solution of HCl obtaining a yellowish oil that was washed several times with water and dried under vacuo for a night. The product was analyzed by GPC technique.

Abbreviations

Acac   Acetylacetonate

AE   asymmetric epoxidation

AD   asymmetric dihydroxylation

Alk   Alkyl

APCI-MS   Atmospheric Pressure Chemical Ionization Mass Spectroscopy

Btp   Trigonal-bipyramidal geometry

CHP   Cumene hydroperoxide

DCE   1,2-Dichloroethane

DET   Diethyl tartrate

DIPET   Diisopropyltartrate

DMENO   Dimethylhexyl-*N*-oxide

DHQ   Dihydroquinine

DHQD   Dihydroquinidine esters

DMF   *N,N*-Dimethylformamide

e.e.   enantiomeric excess

ESI-MS   Electron Spray Ionization Mass Spectrometry

Etpy   ethyl pyruvate

GPC   Gel Permeation Chromatography

HMPT   Hexamethylphosphorous triamide

*i***-Bu**   Isobutyl

*i***-Pr**   Isopropyl

Oct   Octahedral

O*i*-Pr   Isopropoxide

O*t*-Bu   Terzbutoxide

O*n*-Et   Normalethoxide

O*n*-Bu   Normalbutoxide

LAC   ligand accelerated catalysis

M.S.   molecular sieves

PhIO   Iodosylbenzene

POSS   Polyhedral Oligomeric Silsesquioxane

PPh$_3$ Triphenylphosphine

PyO   Piridine *N*-oxide

Ph$_3$PO   Triphenylphosphine oxide

RT　　　　room temperature

TBHP　　　*terz*-buthyl hydroperoxide

TOF　　　Turn Over Frequency

TON　　　Turn Over Number

Summary

Oxidative transformation is one of the fundamental reactions occurring in organic chemistry and is the basis of many synthetic processes. This ia an area of an ongoing research work addressed both to the synthetic application and to the understanding of the mechanism involved in these processes, whose interest include reactions occurring in biological system also. In enzymes, as in artificial catalysts, the presence of metals in high oxidation state allow the activation of hydrogen peroxide (H_2O_2) and alkyl hydroperoxides (RO_2H) and the subsequent oxidation of different organic substrates. Both in enzymes and in artificial systems the sourranding environment of the peroxidic reactive species is of great importance. The ligands bounded to a metal center, such as proteins or molecules from synthesis, are able to increase not only the stability and reactivity, but also the stereoselectivity of the metal. However, there are numerous examples in the literature of how the reactivity, stability and stereoselectivity of cataytic synthetic processes catalyzed by polidentate catalysts may be largely influenced by the presence of additives or monodentate ligands able to bind to the metal center. The influence that polidentate ligands or monodentate ligands may exsert on the reactivity of several catalytic systems is part of the topics covered in the first chapter of this thesis. In particular, we have addressed our attention to catalytic oxidative processes which are accelerated after the bind of ligands both poly- and monodentate. Numerous examples from recent literature have been reported. They are divided into two classes of phenomena: the "ligand accelerated catalysis (LAC) and the co-ligand accelerated catalysis (LAC-CO). In LAC, as defined by Sharpless, the addition of a polydentate chiral ligand induces the genaration, towards ligand exchange, of a new chiral metallic complex characterized by an increased reactivity. In CO-LAC, the addition of a chiral or achiral monodentate ligand allows the modification of the reactivity of the original metal complex without the occurrency of a ligand exchange.

In *Chapter 2* we have focused our attention on the reactivity of a polyhedral oligomeric silsesquioxane trisilanolate vanadium(V) complex towards oxidation reactions. This catalyst, at room temeperature and in the presence of cumyl hydroperoxide as the terminal oxidant is efficient in oxygen transfer processes towards sulfides, tertiary amine and secondary amine. Sulfoxidations and *N*-oxidations have been carried out yielding the corrisponding products in good yields. The addition of a Lewis base as a co-ligand can markedly affect reactivity, stability, chemo- and stereo-selectivity. A proposal for the intermolecular activation, using Gutmann analysis supported by MP2/TZVP calculations, has been presented.

In *Chapter 3* catalytic sulfoxidations, using cumylhydroperoxide as primary oxidant, has been tested in a series of eight aminotriphenolate d_0 metals complexes [Sc(III), Ti(IV), Zr(IV), Hf(IV), V(V), Nb(V), Ta(V), Mo(VI)]. The reactivity and selectivity properties ,both in presence and in absence of a strong Lewis Base (dimethylhexyl-*N*-oxide) as co-ligand, has been determined experimentally. The experimental values have been correlated with the Sanderson value of electronegativity. MP2/LANL2DZ theoretical calculations on model complexes have furnished more insights on the characteristics of the reactive peroxo specie.

The experimentals combined with the theoretical calculations have offered the possibility to propose a general mechanism for the peroxide activation and reactivity.

The study described in *Chapter 4* pertains to V(V)-oxo amine triphenolate complexes as functional and structural model of vanadium haloperoxidases: their trigonal bypiramidal geometry emulates the one found in the enzymes and their ability to catalyse efficiently sulfoxidations as well as chlorination and bromination of trimethoxybenzene reflects the properties of the enzyme. In particular, sulfoxidations using hydrogen peroxide as terminal oxidant are performaed in quantitative yields and high selectivities (catalyst loading down to 0.01%, TONs up to 9900, TOF up to 8000 h^{-1}), while in the second case TONs up to 1260 and TOF up to 220 h^{-1} are achieved with a acatlyst loading down to 0.05%.

In *Chapter 5* some synthtic method for the preparation of a new fluorinated incompletely condensed polyhedral oligomeric silsesquioxane suitable to be immobilized on polymeric fluorous membranes or in addition able to be dissolved in fluorous solvents have been reported.

Riassunto

La trasformazione ossidativa di gruppi funzionali costituisce una delle reazioni fondamentali della chimica organica ed è alla base di moltissimi processi sintetici. Si tratta di un settore che è oggetto di un continuo lavoro di ricerca, indirizzato sia alla risoluzione di problemi sintetico-applicativi che alla comprensione dei meccanismi che operano in tali processi il cui interesse è così vasto da includere reazioni che avvengono anche in sistemi biologici. Negli enzimi, così come nei catalizzatori artificiali, la presenza di metalli in elevato stato di ossidazione permette l'attivazione di acqua ossigenata (H_2O_2) e di idroperossidi alchilici (RO_2H) consentendo l'ossidazione di diversi substrati organici. Sia negli enzimi che nei sistemi artificiali particolare importanza riveste l'intorno chimico della specie reattiva metalloperossidica responsabile del trasferimento di ossigeno. I leganti al centro metallico, siano essi di natura proteica o costituiti da molecole di sintesi, sono in grado di aumentare non solo la stabilità e la reattività ma anche la capacità di stereoselezione del centro reattivo. Tuttavia, si trovano in letteratura numerosi esempi di come la reattività, la stabilità e la stereoselezione di processi sintetici catalizzati da complessi con leganti polidentati vengano ampiamente influenzati anche dalla presenza di additivi, o leganti monodentati per lo più basici, in seguito alla loro interazione con il metallo.

L'influenza che leganti polidentati e co-leganti monodentati possono avere sulla reattività di numerosi sistemi catalitici è parte degli argomenti trattati nel primo capitolo di questa tesi di dottorato. In particolare abbiamo voluto indirizzare la nostra attenzione verso processi reattivi, soprattutto di tipo ossidativo, che vengono accelerati in seguito all'azione sia di leganti polidentati che di co-leganti monodentati. I numerosi esempi che sono stati riportati su questo argomento, tratti dalla recente letteratura, sono stati suddivisi all'interno di due classi di fenomeni: la "*ligand accelerated catalysis*" (LAC) e la "*co-ligand accelerated catalysis*" (CO-LAC). Nella LAC, secondo la definizione di Sharpless, l'aggiunta di un legante chirale polidentato induce la formazione, tramite scambio di legante, di un nuovo complesso metallico dotato di una aumentata reattività che spesso si accompagna anche ad una aumentata stereoselettività. Nella CO-LAC invece, l'aggiunta di un legante monodentato chirale o achirale, induce una modificazione della reattività del complesso metallico senza che vi sia scambio di legante. Numerosi esempi di CO-LAC prevedono l'utilizzo di leganti monodentati basici. Durante questo dottorato, abbiamo potuto constatare che il processo di trasferimento di ossigeno verso il metil *p*-tolil solfuro catalizzato da un complesso polisilosanico di V(V) recanti sostituenti *iso*-butilici in presenza di CHP come ossidante primario viene accelerato, anche di 24 volte, a seguito dell'aggiunta di basi di Lewis in quantità confrontabili con quelle del catalizzatore. Nel *Capitolo 2* i dati sperimentali riportati evidenziano l'esistenza di una corrispondenza tra accelerazione osservata del processo e natura elettron donatrice della base di Lewis usata. Più elettron ricca è la base di Lewis maggiore è la reattività del sistema e, probabilmente a causa delle migliori capacità coordinanti del co-legante, minore è la quantità di base di Lewis necessaria per avere l'effetto massimo. Calcoli computazionali condotti hanno dimostrato come la coordinazione di basi di Lewis al vanadio inducano variazioni di distribuzione elettronica con aumento di densità

elettronica all'ossigeno della specie reattiva metalloperossidica coinvolto nel trasferimento di ossigeno e contemporanea diminuzione della stessa a livello del centro metallico con conseguente stabilizzazione dell'intermedio reattivo.

Lo studio sugli effetti delle basi di Lewis in processi di trasferimento di ossigeno a solfuri organici è stato esteso anche verso un'altra classe di leganti ossia le trifenolammine. Nel *Capitolo 3* sono stati investigati processi catalitici di ossidazione del metil *p*-tolil solfuro per mezzo di cumilidroperossido come ossidante primario in presenza di otto complessi ammino *tri*-fenolati di metalli d_0 [Sc(III), Ti(IV), Zr(IV), Hf(IV), V(V), Nb(V), Ta(V), Mo(VI)]. La reattività e la selettività di questi processi, sia in assenza che in presenza di una base di Lewis forte come il dimetilsil-*N*-ossido è stata determinata sperimentalmente. I dati sperimentali ottenuti sono stati correlati con i valori di elettronegatività di Sanderson e tramite studi teorici sono state tratte delle delucidazioni sulle caratteristiche della specie reattiva metalloperossidica. I dati sperimentali raccolti e i calcoli teorici ci hanno permesso di proporre un meccanismo generale per spiegare l'attivazione della specie perossidica e la sua reattività.

Nel *Capitolo 4* sono descritti i complessi ammino tri-fenolati di ossovanadio(V) come modelli funzionali e strutturali di aloperossidasi, grazie alla loro geometria trigonale bipiramidale e alla loro abilità nel catalizzare efficacemente sia le solfossidazioni così come la bromurazione e la clorurazione del trimetossibenzene. In particolare, nell'ossidazione di solfuri, usando perossido d'idrogeno come ossidante primario, sono state ottenute con rese quantitative in prodotto con alta chemoselettività, anche in presenza dello 0.01% di catalizzatore, con TON fino a 9900 e TOF fino a 8000 h^{-1}. Nel caso della bromurazione si sono ottenuti TON pari a 1260 e TOF fino a 220 h^{-1} usando fino allo 0.05% di catalizzatore.

Nel *Capitolo 5* viene riportata una serie di strategie di sintesi per la formazione di un nuovo legante trisilanolico polisilossanico recante lunghe catene perfluorurate come sostituenti.

Ringraziamenti